ASPECTS OF CYCLIC SEDIMENTATION IN THE UPPER MISSISSIPPIAN, MAUCH CHUNK GROUP, SOUTHERN WEST VIRGINIA AND SOUTHWEST VIRGINIA

Ty Bradford Buller

Thesis submitted to the faculty of the Virginia Polytechnic Institute and State University in partial fulfillment of the requirements for the degree of

Masters of Science
In
Geosciences

Kenneth A. Eriksson
Benjamin C. Gill
Brian W. Romans

May 5th, 2014
Blacksburg, Virginia

Keywords: Appalachian Basin, Mississippian, Incised-valley, Carbon

ASPECTS OF CYCLIC SEDIMENTATION IN THE UPPER MISSISSIPPIAN, MAUCH CHUNK GROUP, SOUTHERN WEST VIRGINIA AND SOUTHWEST VIRGINIA

Ty B. Buller

ABSTRACT

Late Mississippian, Mauch Chunk Group strata constitute a westward-thinning clastic wedge of strata up to 1000m thick that developed in the Central Appalachian Basin over a ~ 7 million year time interval. Included within the Mauch Chunk Group are multiple incised-valley fills and a distinctive prodeltaic succession of laminated sandstones and mudstones.

Calculated estimates of drainage basin areas for incised-valley fills in the Mauch Chunk Group range from > 1,000,000 km^2 for the Stony Gap Sandstone to < 100,000 km^2 for the Princeton Formation. Drainage area estimates are consistent with detrital zircon geochronology and petrographic data and suggest that the Stony Gap and Ravencliff incised-valley fills were derived from distal, northern and northwestern cratonic sources that dispersed sediment into NE-SW-oriented, longitudinal incised-valley drainages and that the Princeton Formation was derived from proximal tectonic highland sources along the eastern margin of the Appalachian Basin which dispersed sediment into a transverse incised-valley.

The Pride Shale overlies the Princeton incised valley fill and records a hierarchy of tidal periodicities is preserved in the Pride Shale. Microlaminated, semi-diurnal sandstone-siltstone/shale couplets record the dominant ebb tide of the day. Up to 17 semi-diurnal couplets are stacked into neap-spring (fortnightly) tidal cycles. Neap-spring cycles are arranged in thickening and thinning that record seasonal cycles driven by the annual monsoon. Total organic carbon (TOC) values are a proxy for annual climatic cycles. TOC contents are higher within intermonsoonal and lower within monsoonal components of annual cycles reflecting, respectively, lesser and greater dilution by terrestrial flux.

ACKNOWLEDGEMENTS

My foremost thanks go to my thesis adviser Dr. Kenneth A. Eriksson. Without his support, attention to detail, hard work, and persistent patience this thesis would not have been possible. I hope to become half the Geologist that Dr. Eriksson is one day.

I thank the rest of my thesis committee members: Dr. Benjamin Gill and Dr. Brian Romans. Their valuable feedback helped me to improve the thesis in many ways. Student Program Coordinator, Connie Lowe deserves all the thanks I can give for her unwavering support while helping me wade through administrative details. I am also grateful to my former undergraduate adviser Dr. Diane Kamola, who greatly influenced my research tract and encouraged me to pursue a graduate degree in Geology. Her energetic working style influenced me greatly as a geologist. Many thanks go to my closest group of friends Neal Auchter, Patrick Boyle, Angela Gerhardt, Cody Mason and Theodore Them. Because of them, I look at graduate school as one of the best times of my life so far.

Last but not least, I thank my parents Kenton and Barbara Buller and my siblings Tony, Monica and Cody, for always being there when I needed them most, and for supporting me through all these years.

TABLE OF CONTENTS

FIGURES:

CHAPTER 1

CHAPTER 2

Chapter One:

INCISED VALLEY FILLS IN THE UPPER MISSISSIPPIAN MAUCH CHUNK GROUP, CENTRAL APPALACHIAN BASIN: UPSTREAM CONTROLS ON PALEOVALLEY DIMENSIONS AND FILL

Ty B. Buller

Department of Geosciences, Virginia Polytechnic Institute and State University, Blacksburg, Virginia 24061, U.S.A

ABSTRACT

Subsurface mapping of the Mauch Chunk Group, combined with facies and architectural element analysis on outcrop, detrital zircon geochronology and petrographic characterization of percentages of framework grains in fluvial sandstones are used to reconstruct the total source to sink system of the Stony Gap, Ravencliff, and Princeton incised-valley fills.

The Stony Gap and Ravencliff are both relatively broad incised-valleys infilled with quartzarenite fluvial facies and consist of downstream accreting elements that range from 6 to 9 m in thickness. The Princeton incised-valley occupies a relatively smaller incised valley infilled with sublitharenite fluvial facies and consists of channel elements that range in thicknesses from .25 to 3.6m. Detrital zircon data from the Stony Gap Sandstone display prominent Acadian and Taconic peaks (350-500 Ma), broad Grenvillian peaks (0.95-1.5 Ga) and lesser Yavapai-Mazatal (1.6-1.8 Ga) and Archean-age clusters (2.5-3.0 Ga), whereas data from the Princeton Formation display prominent Acadian and Taconic peaks (350-500 Ma), and broad Grenvillian peaks (0.95-1.5 Ga) but lack the older age populations.

Calculated estimates of drainage basin areas for incised-valley fills in the Mauch Chunk Group range from > 1,000,000 km^2 for the Stony Gap Sandstone to < 100,000 km^2 for the Princeton Formation. Drainage areas are consistent with detrital zircon geochronology and

petrographic data and suggest that the Stony Gap and Ravencliff incised-valley fills were derived from distal, northern and northwestern, cratonic sources that dispersed sediment into NE-SW-oriented, longitudinal incised-valley drainages and with the Princeton Formation having been derived from proximal tectonic highland sources to the northeast along the eastern margin of the Appalachian Basin which dispersed sediment into a transverse incised-valley.

1. Introduction

Extensive research has been conducted on both modern and ancient incised-valley systems because of their potential to record complex sedimentary responses to changes in relative sea level and climate, and because of their economic potential (e.g. Schumm, 1993; Ashley & Sheridan, 1994; Dalrymple, *et al*., 1994; Van Wagoner, 1995; Anderson *et al*., 1996; Blum & Price, 1998; Talling, 1998; Miall & Arush, 2001). Incised-valleys have long been considered as a product of fluvial incision and sediment by-pass associated with base-level fall (e.g. Van Wagoner *et al*., 1990; Schumm & Ethridge, 1994) whereas other workers have demonstrated that modern and ancient incised-valleys are more complex in origin and can be the product of multiple incision events alternating with periods of deposition (e.g. Blum & Price, 1994; Korus *et al*., 2008). Regardless of their origin, the base of incised-valleys along with their correlative 'interfluve' surfaces, define regionally correlatable, sequence-bounding unconformities (McCarthy & Plint, 1998; Korus *et al*., 2008). The dimensions of incised-valleys and the scale of fluvial architectural elements developed in the valleys are controlled by a number of factors, including the size of the drainage basin and climate and, in particular, the existence of greenhouse versus icehouse conditions (Gibling, 2006; Mattheus *et al*., 2007; Davidson & North, 2009). In the Central Appalachian Basin, Upper Mississippian to Early

Pennsylvanian incised-valley fill successions have been well documented (e.g. Englund, 1974; Rice & Schwietering, 1988; Rice & Wier, 1984; Beuthin, 1994; Blake *et al*., 2000; Miller & Eriksson, 2000; Beuthin & Blake, 2001; Smith, 2010; Grimm *et al*., 2013) but none of these studies have investigated the influence of upstream controls on paleovalley dimensions and fill.

This study focuses on incised-valley deposits from the Upper Mississippian Hinton and Princeton Formations of the Mauch Chunk Group of southern West Virginia and southwestern Virginia (Fig. 1.1) that developed in response to high-frequency, high- amplitude eustatic changes related to Gondwanan glacial-interglacial episodes (Miller & Eriksson, 2000). Based on outcrop and subsurface mapping integrated with previously published petrographic data and detrital zircon age spectra, we investigate the effect of upstream controls on the dimensions and fill of the Stony Gap Sandstone, Ravencliff sandstone and Princeton Formation incised-valleys (Fig. 1.2). Specifically, this investigation will: 1) allow for the discrimination of incised-valley fills related to different provenances; 2) provide insight on how dimensions of incised valleys are a product of drainage basin size; and 3) permit comparison of Late Mississippian with Early Pennsylvanian paleovalley fills with a view to understanding drainage pattern evolution in relation to the Alleghanian orogeny and paleoclimate change across the Mississippian-Pennsylvanian boundary.

2. General Geologic Setting

2.1 Tectonics

The Appalachian Basin extends ~1800 km from Alabama to New York, ranges from 100-500 km in width, and is partitioned into a series of sub-basins, including the Central

Appalachian Basin in West Virginia, southwest Virginia, eastern Kentucky, and southern Tennessee (Kelafant *et al.,* 1988; Grimm *et al*., 2013). In the Central Appalachian Foreland Basin, the craton responded to initial crustal shortening and loading associated with the onset of the Alleghanian orogeny in the Late Mississippian producing a foredeep flanked to the northwest by a forebulge (Ettensohn, 1994). Strata of the Upper Mississippian Mauch Chunk Group developed in this foreland basin as a clastic wedge that is up to 1000m thick (Fig. 1.3; Miller & Eriksson, 2000). Basin infilling was coincident with the northward paleolatitudinal drift through subequatorial latitudes during the collisional assembly of Pangea (Cecil, 1990; Golonka *et al*., 1994). During the middle and Late Chesterian, Mauch Chunk sediments prograded from eastern tectonic highland sources, into the narrow embayment and represent approximately seven million years of deposition (DeWitt & McGrew, 1979, Englund & Thomas, 1990, Miller & Eriksson, 2000).

2.2 Late Mississippian Stratigraphy

Correlation of biostratigraphic data to standard North American stages of Gradstein (2012), combined with geochronological ages, constrains the age of the Mauch Chunk Group to between 323.2 and 330.9 Ma (Fig. 1.4). Conodonts in the basal portion of the Bluestone Formation are designated as lower Serpukhovian (Fig. 1.4; Repetski & Stamm, 2009). Stamm (1997) demonstrated that fauna in the Bramwell Member at the top of the Bluestone Formation can be assigned to the latest Chesterian *Gnathodus postbilneatus* conodont zone (Fig. 1.4). These are the youngest Mississippian conodonts found in the Appalachian Basin.

Thus, the top of the Bramwell Member is designated as latest Serpukhovian (Repetski & Stamm, 2009).

Based on outcrop and subsurface studies, the Mauch Chunk Group has been subdivided into three, third-order composite sequences (Fig. 1.2; Miller & Eriksson, 2000; Maynard *et al*., 2006). Third-order composite sequences consist of fourth-order sequences that are stacked into retrogradational - aggradational and progradational sequence sets (Miller & Eriksson, 2000; Maynard *et al*., 2006). Fourth-order sequences are of ca. ~400 kyr duration and are inferred to reflect high-frequency, high-amplitude glacioeustatic changes related to waxing and waning of the Gondwanan glaciation (Miller & Eriksson, 2000; Maynard *et al*., 2006). Third-order composite sequences are of ca. 2.5 Myr. duration and are considered to be of tectonoeustatic origin (Miller & Eriksson, 1997), in common with the conclusions of the Grimm *et al*. (2013) for Early Pennsylvanian third-order composite sequences in the Central Appalachian Basin.

The Bluefield Formation represents the lowermost, third-order, composite sequence (Fig. 1.2) and is subdivided into a lower carbonate-dominated interval and an upper siliciclastic-dominated interval. In general, the lower Bluefield Formation is dominated by skeletal carbonates rocks, carbonaceous mudstones, and black shales whereas the upper Bluefield Formation is dominated by cyclic siliciclastics (Maynard *et al*., 2006). The top of the Bluefield Formation is recognized as a sharp contact with the overlying Stony Gap Sandstone Member of the Hinton Formation (Fig. 1.3).

The Hinton Formation represents the middle, third-order composite sequence and is dominated by siliciclastic facies (Miller & Eriksson, 2000). The Stony Gap Sandstone Member at the base of the Hinton Formation consists of white, cross-bedded quartzose sandstone overlain by heterolithic facies (Miller & Eriksson, 2000). The remainder of the Hinton Formation in southern West Virginia is dominated by red beds and subordinate marine facies (Smith, 2009). The Little Stone Gap Limestone Member in the middle of the Hinton Formation consists of a widespread carbonate up to 18 m thick that is easily distinguished in the subsurface and represents a third-order maximum flood deposit (Figs. 1.2 and 1.3; Miller & Eriksson, 2000). A number of thin, tan-colored sandstone bodies, the Neal, Tallery and Fall Mills sandstones, are developed in the upper Hinton Formation (Fig. 1.2 and 1.3; Miller & Eriksson, 2000). Based on subsurface mapping, Yang (1998) identified a prominent regional unconformity at the top of the Little Stone Gap Limestone. The informal Ravencliff sandstone, as it is commonly referred to by drillers, overlies the unconformity in Mingo, McDowell, Mercer and Wyoming Counties in southern West Virginia and extends further north into central West Virginia (Yang, 1998). Presley (1977) reported a sandstone body at a similar stratigraphic level in the Mauch Chunk Group in western Marion and Monongalia counties in northern West Virginia named the Goodhope sandstone. Based on its stratigraphic position, Yang (1998) suggests that the Goodhope sandstone is the equivalent of the Ravencliff sandstone of southern West Virginia.

The Princeton-Bluestone interval represents the uppermost, third-order, composite sequence, part of which is truncated at the Mississippian-Pennsylvanian unconformity (Figs. 1.2 and 1.3). The Princeton Formation defines the base of this composite sequence and consists of polymictic conglomerates and lithic sandstone overlain by heterolithic facies (Miller & Eriksson,

2000). The base of the overlying Bluestone Formation is easily recognized in the subsurface by a high gamma-ray kick at the base of the Pride Shale Member (Fig. 1.3; Miller & Eriksson, 2000). Overall, the Bluestone Formation consist of black to dark-gray shales, siltstone and sandstones of the Pride Shale Member overlain by grey, red, and green shales with lesser amounts of sandstone, siltstone and limestone (Yang, 1998; Miller & Eriksson, 2000). The fossiliferous Bramwell Member is interpreted as the maximum flood deposit of the uppermost, composite sequence (Miller & Eriksson, 2000).

Englund & Thomas (1990) documented an unconformity at the base of the Princeton Formation in outcrop in Tazewell County, Virginia. Yang (1998) observed the same unconformity surface below the Ravencliff sandstone in outcrops in eastern McDowell and Mercer Counties, West Virginia. Even though Yang (1998) observed the Princeton Formation to be stratigraphically higher than the Ravencliff sandstone, he proposed that the Ravencliff sandstone and the Princeton Formation developed concurrently in western and eastern incised-valleys, respectively. He inferred that two valleys had separate drainage basins and converged downstream in southern West Virginia or possibly southwestern Virginia (Fig. 1.5). With this hypothesis, Yang (1998) proposed that the informal Ravencliff sandstone of the Hinton Formation be recognized as a formal lithostratigraphic unit which he called the “Ravencliff Formation”. The proposed “Ravencliff Formation” would encompass all strata from the top of the Little Stone Gap Limestone Member of the Hinton Formation to the base of the Pride Shale Member of the Bluestone Formation. Within this definition, the formal Princeton Formation would be included in the “Ravencliff Formation” as one of several incised-valley deposits of the

"Ravencliff Formation" (Yang, 1998). This proposed nomenclature is yet to be recognized or used.

3. Methods

Subsurface mapping of the Stony Gap, Ravencliff and Princeton incised-valleys utilized 195 digitized, unnormalized gamma-ray wireline logs from natural gas development wells to construct a series of cross-sections through the study area. More modern logs contain a suite of log curves including not only gamma-ray but also bulk density, neutron density, neutron porosity and photoelectric index that aided in correlation. In particular, photoelectric index logs were used to identify and correlate the Little Stone Gap Limestone (Fig. 1.2). Of the 195 available wireline logs, 111 logs were used to construct seven NW-SE dip-oriented cross-sections (Fig. 1.1). Cross-sections are hung from the base of Pride Shale Member, characterized by a high gamma ray spike (Fig. 1.3).

Stratigraphic sections were measured at isolated exposures throughout the study area. Facies were described with regard to color, lithology, fossil content, and sedimentary structures. Paleocurrent observations from the Stony Gap Sandstone and the Princeton Formation supplemented data were from previously published work of Miller & Eriksson (2000). Architectural elements were mapped using photomosaics and field observations based on the architectural element and bounding surface framework developed by Miall (1985 & 1988).

Petrographic point count data and detrital zircon age data from previous studies on the Mauch Chunk Group were integrated to compare and contrast provenances of incised-valley fill

sandstones. Petrographic data from Kamm (1981), Pinnix (1993) and Reed *et al*. (2005) are plotted on QFL and QmFLt ternary diagrams of Dickinson *et al.,* (1983) whereas detrital zircon ages from Park *et al*. (2010) are plotted as histograms. Drainage basin areas were estimated using the approach of Davidson and North (2009) that utilize published empirical relationships based on thicknesses of erosionally based architectural elements corrected for paleo-bankfull channel depths.

4. Major Incised-Valley Fills in the Mauch Chunk Group

Based on a combination of subsurface mapping (Fig. 1.6), facies and architectural element analysis on outcrop (Figs. 1.7 and 1.10) and petrographic characterization of percentages of framework grains in sandstones (Fig. 1.8), three major incised-valley fills are recognized and characterized in terms of their geometry, stratigraphy, facies, paleocurrents, and depositional processes and environments. The Stony Gap Sandstone, Ravencliff sandstone and Princeton Formation are interpreted as incised-valley fills and consist of basal fluvial facies overlain by estuarine facies (Pinnix, 1993; Yang, 1998; Miller & Eriksson, 2000). The Stony Gap Sandstone and Princeton Formation are exposed at numerous locations in southern West Virginia and are thus amenable to detailed facies analysis. In contrast, the Ravencliff sandstone is exposed only locally and observations are mainly from the subsurface.

4.1 Stony Gap Sandstone Member

The Stony Gap Sandstone Member occupies a broad valley up to 70 km wide and ranges in thickness from 3 to 60 m (Fig. 1.6). Fluvial facies of Stony Gap Sandstone range in thickness from 3 to 50 m and consist predominantly of fine-to-medium grained, cross-bedded sandstone.

Petrographic analysis characterizes these sandstones as quartzarenites (Figs. 1.8 and 1.9a; Read *et al*., 2005) with mean QFL% = 92.3/1.9/5.8% and mean QmFLt% = 82.2/1.9/15.9% (Fig. 1.8). Lithic grain types are primarily sedimentary and metamorphic rock fragments, replacement illite, muscovite, chlorite and polycrystalline quartz (Read *et al*., 2005). Fluvial facies in the Stony Gap Sandstone contain sparse conglomerate beds between 2 and 10 cm thick that consist of well-rounded quartz pebbles and intrabasinal siltstone and shale clasts up to 10 cm in length (Kirkpatrick, 1994; Miller & Eriksson, 2000). Using the architectural element and bounding surface framework developed by Miall (1985 & 1988), the primary architectural elements within the Stony Gap Sandstone are downstream accreting elements interpreted as macroforms within major channel fills. Individual downstream accreting elements range 7 to 9 m in thickness and are bounded by fourth-order surfaces (Fig 1.7a).

Paleocurrent data for the fluvial facies indicate that the Stony Gap incised-valley was oriented NE-SW (Miller & Eriksson, 2000). Internal characteristics of downstream accreting macroforms can vary, but a predictable facies assemblage is illustrated on Figure 1.7a. Individual downstream accreting macroforms consist of, from bottom to top: 1) basal erosional surface, ideally defined by thin conglomeratic sandstones; 2) large-scale (0.13- 1.1 m thick) planar-tabular cross-beds (Fig. 1.10a); 3) compound cross-bed cosets consisting of gently inclined, downstream accretionary surfaces containing tabular-tangential cross-bed sets. Overlying fourth-order bounding surfaces, the thin conglomeratic sandstone represent channel floor deposits. Large-scale planner tabular cross-beds represent platforms built into deep reaches of the channel in front of the macroform and are deposits of straight- to sinuous-crested dunes migrating along the channel floor (Bluck, 1976; Haszeldine, 1983a, b). Inclined

surfaces containing tabular-tangential cross-bed sets represent slightly sinuous-crested dunes descending down the lee face of a macroform (Wizevich, 1992).

The upper Stony Gap incised-valley fill consists of tidal channel, point-bar deposits that sharply overlie the quartzose fluvial facies and consist of large-scale (up to 10 m) inclined strata (Fig. 1.10b). The inclined strata represent lateral-accretion deposits and internally consist of heterolithic strata of millimeter- to meter-thick, interlayered, fine-grained and rippled sandstone and mudstone. Heterolithic facies grade upwards into dark silty mudstones overlain by a regionally extensive, gray calcareous paleosol.

4.2 Ravencliff sandstone

The Ravencliff sandstone occupies a broad valley up to 60 km wide and ranges in thickness from 3 to 55 m (Fig. 1.6). This interval is mapped in the subsurface as a sandstone-dominated unit with interbedded siltstones, shales, and red beds up to 40 m thick (Yang, 1998). Based on core studies, Kamm & Heald (1983) described the Ravencliff sandstone as a clean, white to tan colored, fine- to coarse-grained quartzarenite with mean QFL% = 94.85/0.8/4.35% and mean QmFLt% = 92.57/0.8/6.63% (Fig. 1.8). Grains are well-rounded with a high degree of sphericity. Lithic grain types are primarily sedimentary rock fragments including shale and limestone, metamorphic rock fragments, feldspar replaced by diagenetic kaolinite, and polycrystalline quartz (Kamm, 1981). Quartz pebbles up to two centimeters in diameter are present at the base of the Ravencliff interval with intrabasinal shale and limestone clasts present throughout the interval (Kamm & Heald, 1983). Observations from core (Kamm, 1981) reveal that the Ravencliff sandstone has a sharp and erosional basal contact overlain by steeply

dipping unidirectional cross-beds, displays an upward decrease in grain and bed thickness, a slight increase in quartz content and a lack of distinct marine indicators. In a singular, poor exposure at Camp Creek, WV, the Ravencliff sandstone appears to consist of similar downstream accretionary elements to the Stony Gap Sandstone.

All of the above criteria lead to a braided alluvial fluvial interpretation of depositional environment for the Ravencliff sandstone (Kamm, 1981; Kamm & Heald, 1983; Wrightstone, 1985). In common with the Stony Gap Sandstone, the Ravencliff interval contains estuarine deposits overlying quartzose fluvial sandstones and conglomerates. The estuarine deposits do not outcrop and are described from core as dark-gray, sparsely rooted, shale and silty shales up to 10 m thick (Yang, 1998). Coeval with deposits of the Ravencliff incised valley, thin sandstone bodies (3 – 20 m thick) (Miller and Eriksson, 2000), observed in both outcrop and the subsurface east of the mapped extent of the Ravencliff incised-valley fill, may represent tributary fluvial systems (Fig. 1.2). These sandstone bodies have been interpreted by Miller & Eriksson (2000) as minor incised-valley fill deposits with southwesterly paleoflow directions. Minor incised-valley tributary systems would likely have sourced the proximal tectonic highlands along the eastern margin of the Appalachian Basin and merged downstream with the main Ravencliff incised-valley trunk channel.

4.3 Princeton Formation

The Princeton Formation occupies a valley up to 35 km wide and ranges in thickness from 1 to 40 m (Fig. 1.6). Fluvial lithofacies of the Princeton Formation range in thickness from 1 to 25 m and consist of polymictic conglomerates and sandstones. Sandstones are lithic-to-

sublitharenites with mean QFL% = 88/1.8/10.2% and mean QmFLt% = 85.2/1.6/13.4% (Fig. 1.8). Lithic grain types are dominantly sedimentary and metamorphic rock fragments, replacement Illite, muscovite, and abundant polycrystalline quartz (Fig. 1.9b-c). Sedimentary rock fragments include limestone, siltstone, and shale clasts (Fig. 1.10c; Pinnix, 1993; Read *et al*., 2005). Conglomerates are between 1 and 20 cm thick and contain pebble-to-cobble-size clasts of vein quartz and lesser amounts of sandstone, limestone, chert and shale as well as nodules of caliche and siderite (Miller & Eriksson, 2000). Princeton Formation fluvial facies fill a series of erosionally based, lenticular, multistory-multichannel, architectural elements (Fig. 1.7b and 1.10d; Miall, 1985). Architectural elements range in thickness of from 0.25 to 3.6 m, are upward fining and consist of basal conglomeratic intervals that are typically horizontally stratified, overlain by cosets of trough and less common planar cross-bedded sandstone. Cosets range in thickness from 0.6 - 3.6 m

Architectural elements are interpreted as the product of fluvial sand bars and channel fills. Erosional surfaces separating channel elements are attributed to lateral switching (combing) of active channels across the floodplain. Basal, coarse-grained sandstones and conglomerates represent channel lags. Overlying, trough and planar cross-beds are the product of in-channel dune migration and aggradation (Holbrook, 2001). Paleocurrent data indicate southwest paleoflow (Pinnix, 1993; Miller & Eriksson, 2000).

Estuarine deposits in the Princeton Formation overlie the conglomeratic and lithic sandstone fluvial deposits and consist of dark mudstones containing plant fossils and siderite nodules. Mudstones enclose lenses of fine-to medium-grained, flat-laminated to ripple-bedded

sandstone units up to 5 m thick. Locally, inclined heterolithic strata consisting of interlaminated fine-grained sandstone and mudstone occupy shallow (<2 m deep) and narrow (2-5 m wide) channels (Miller & Eriksson, 2000). Some heterolithic units are characterized by systematic thickness variations of millimeter-to-centimeter-scale sandstone/mudstone couplets that represent fortnightly, neap-spring cycles (Figs. 1.11 and 1.12). Also apparent are thick-thin pairs of laminae representing the deposits of diurnal dominant and subordinate tides. A depositional model for the Princeton incised valley fill is illustrated in Figure 1.13.

5. Detrital Zircon Geochronology

Published detrital zircon ages (Park *et al.,* 2010) from the Stony Gap Sandstone and the Princeton Formation are used in this study to compare their age spectra (Fig. 1.14). No zircon analyses are available for the Ravencliff sandstone. Detrital zircons from the Stony Gap Sandstone quartzarenite fluvial facies display prominent Acadian and Taconic peaks (350-500 Ma) as well as broad Grenvillian peaks (0.95-1.5 Ga). Lesser Yavapai-Mazatal (1.6-1.8 Ga) and Archeane clusters (2.5-3.0 Ga) are also present (Fig 1.14a). Detrital zircons from the Princeton Formation fluvial facies also display prominent Acadian and Taconic peaks (350-500 Ma), and broad Grenvillian peaks (0.95-1.5 Ga). No older Yavapai-Mazatal (1.6-1.8 Ga) or Archean zircons were observed (Fig. 1.14b; Park *et al*., 2010)

6. Upstream Controls on Characteristics of Incised-Valleys and their fills

Understanding and linking scales of incised-valley fluvial deposits to upstream controls such as drainage basin characteristics can provide a potential link between incised-valleys and their fills, and other components of sediment-dispersal systems. A wide variety of scaling

relationships between fluvial systems and their drainage basin areas have been recognized (e.g. Milliman & Syvitski, 1992; Schumm & Winkley, 1994; Mattheus *et al*., 2007; Blum *et al*., 2013). Foremost among these is the relationship between incised-valley drainage area and the dimensions of incised-valleys and the architectural elements of their fill. By integrating estimates of drainage sizes with other data such as sandstone petrography and detrital zircon geochronology, insights can be gained on how incised-valleys and their internal architectural element dimensions are products of upstream controls such as drainage basin area (e.g. Mattheus *et al*., 2007; Davidson & North, 2009; Blum *et al*., 2013).

Studies from modern river systems have shown that river channels scale to discharge (Leopold & Maddock, 1953; Best & Ashworth, 1997; Knighton, 1998). Channel width and depth increase downstream with discharge because of the cumulatively increasing drainage area (Leopold *et al*., 1964). Several studies have applied these concepts to preserved channel-fill deposits to estimate paleohydrological characteristics in particular, bankfull discharge. Bankfull discharge is considered to be the dominant, or channel-forming, discharge because it corresponds to the flow that transports most bed-material load in the long term (e.g. Wolman & Miller, 1960; Gibling, 2006; Davidson & North, 2009).

6.1 Regional Curves for Estimating Drainage Areas

To estimate paleo-drainage basin areas for the Stony Gap, Ravencliff and Princeton incised-valleys, the method of Davidson & North (2009) is employed. This method relates bankfull depth (d) to drainage basin area (DA) [$d = a(DA)^b$] where (a) and (b) are region specific variables dependent on climate, geographic location and lithology, and that represent a

"regional hydraulic geometry curve" obtained from modern catchment surveys (Davidson & North, 2009). Ideally, the selected regional curve mimics the characteristics of the example from the rock-record, notably, similar location and climate.

6.2 Bankfull Depth Estimates

Preserved thicknesses of channel-fills and downstream accreting elements are used to estimate bankfull depth, an approximation that has been used numerous times in interpreting fluvial deposits (Allen, 1965; Miall, 1993; Willis, 1993). We employ the method of Paola & Borgman (1991), based on statistical analysis, that the average ratio of preserved element thickness to mean bankfull depth is roughly 0.6. Thickness of macroforms provides a safe minimum value for bankfull depth (Davidson & North, 2009).

Deposits of inferred downstream accreting elements of the Stony Gap Sandstone range from 7 to 9 meters in thickness, suggesting bankfull depth range of 11.2 to 14.4 meters (Fig. 1.7a, Table 1.1). Cross-bed set thicknesses also can be used to estimate bankfull depth (Adams & Bhattacharya, 2005). Results from cross-beds in the Stony Gap Sandstone that range in thickness from 0.13 to 1.2 m (Fig. 1.10a) give a comparable ranges for bankfull depth of 10.71 to 17.85 m. From the single exposure of the Ravencliff sandstone, a bankfull depth of 9.6 m can be inferred from the 6 m-thick deposit of a downstream accreting element. Thicknesses of interpreted channel-fill elements of the Princeton Formation range 0.25 to 3.6 m in thickness resulting in bankfull depth estimates range of 0.4 to 5.7 m (Figs. 1.7b and 1.10d, Table 1.1).

6.3 Selection of Regional Curves

Late Mississippian paleogeographic reconstructions place the Central Appalachian Basin at near equatorial-latitudes (15° to 5° S) during the time of assembly of Pangea (cf. Golonka *et al*., 1994). Climatic conditions during the Late Mississippian in the Central Appalachian Basin were characterized by predominantly semi- arid, monsoonal conditions, as reflected by the presence of ubiquitous vertisols identified by their shrink-swell features, alternating with more humid conditions, as reflected by the presence of leached paleosols and coals immediately beneath incised valley fills (Miller & Eriksson, 1999). Shifts from seasonal, semi-arid to humid climatic conditions are attributed to systematic variations in monsoonal circulation, whereby seasonal moisture was restricted to the equatorial belt during lowstands of each ~400 k.y. Milankovitch glacial-interglacial cycle (Cecil *et al*., 1997; Miller & Eriksson, 1999). Using the CIA-K proxy, mean annual precipitation estimates range from 519 to 1361 mm/yr (Kahmann & Driese, 2008). By Pennsylvanian time, the Central Appalachian Basin had drifted into the equatorial belt resulting in more humid conditions (Read & Eriksson, 2012).

A regional hydraulic geometry curve that ideally matches conditions in the Late Mississippian, Central Appalachian Basin is not available. However, an example from the Western Cordillera of the US Pacific Northwest coast compares favorably. The climate for this regional curve is characterized by an amalgamation of dry summer continental climates, with seasonal precipitation, to humid continental climates with no dry season (Castro & Jackson, 2001). While this case example does not exactly mimic the paleoclimate or the paleolatitude of the Late Mississippian, Central Appalachian Basin, the application of the Davidson & North (2009) to the rock record is in its infancy and a complete set of regional curves do not yet exist.

6.4 Results of Drainage Area Estimation

Table 1.1 shows the calculated drainage area estimates for the Stony Gap, Ravencliff and Princeton incised-valleys using the regional curve for Western Cordillera of the US Pacific Northwest coast. The Stony Gap Sandstone incised-valley has an estimated maximum drainage basin area of ~1,373,000 km^2. Drainage basin area for the Ravencliff sandstone incised-valley is estimated at ~402,000 km^2. Because of the limited exposures of the Ravencliff sandstone, estimated bankfull depths and thus calculated drainage basin area likely do not reflect the true metrics of this incised-valley fill. The estimated maximum drainage basin area for the Princeton Formation incised-valley computes to ~85,500 km^2. It must be emphasized that these values are no more than estimates but do suggest that the Stony Gap Sandstone drainage basin area was an order-of magnitude greater than that for the Princeton Formation.

7. Discussion

7.1 Icehouse vs Greenhouse Controls on Incised-Valley Dimensions

The Upper Mississippian time period during which the Stony Gap, Ravencliff and Princeton incised-valleys formed is widely considered to coincide with the onset of the Permo-Carboniferous, Gondwana glaciation (Gordon & Henry, 1981; Sutherland, 1988; Golonka *et al*., 1994). Gibling (2006) plotted width vs. thickness measurements of 22 published paleoincised-valleys ranging in age from Carboniferous to Cretaceous. Carboniferous (icehouse) incised-valleys had mean thicknesses and widths of 31.0 m and 10 km, respectively, whereas Cretaceous-age (greenhouse) incised-valleys had mean thicknesses and widths of 21.2 m and 5.6 km, respectively (Fig. 1.15). The dimensions of the Stony Gap, Ravencliff and Princeton

incised-valleys are comparable in scale to other documented Carboniferous-age incised-valleys (Fig. 1.15). These results provide support that high-magnitude Carboniferous glacioeustatic fluctuations were capable of producing incised-valleys of comparable dimensions to the Stony Gap, Ravencliff and Princeton incised-valleys.

7.2 Carboniferous Sediment Routing Systems of the Appalachian Basin

Results from subsurface mapping and architectural element analysis combined with petrographic data and detrital zircon geochronology are consistent with the Stony Gap and Ravencliff incised-valley fills having been derived from distal, northern and northwestern, cratonic sources that dispersed sediment into NE-SW-oriented, longitudinal incised-valley drainages; and with the Princeton Formation having been derived from proximal tectonic highland sources to the northeast along the eastern margin of the Appalachian Basin which dispersed sediment into transverse oriented incised-valleys. We propose that by constraining the drainage basin areas of the three Upper Mississippian incised-valleys and their fills it is possible to reconstruct the total source to sink system.

7.2.1 Longitudinal Drainage Systems

The occurrence of Archean- and Paleoproterozoic zircons in the Stony Gap Sandstone suggest a linkage to Penokean, Yavapai-Mazatzal, and Superior provinces (Hoffman, 1989; Stott, 1997) but interpretations vary as to the source of Archean zircons in Carboniferous sandstones. Some studies interpret Archean-age zircons in the three synorogenic clastic wedges of the Central Appalachian Basin as a product of recycling of older sedimentary units in the Appalachian Basin (e.g. Gray & Zeitler, 1997; McLennan *et al*., 2001; Park *et al.,* 2010) whereas

other workers propose that the Archean zircons are first-cycle and were derived directly from distant cratonic sources of the Canadian Shield and transported in longitudinal (axial) drainage systems in the foreland basin (Robinson & Prave, 1995; Eriksson *et al*., 2004; Thomas *et al.,* 2004; Becker *et al*., 2005). The Early Pennsylvanian, quartz-rich Warren Point Formation and upper Raleigh Sandstone (Sewanee) in the Appalachian Basin contain significant populations of Archean detrital zircons whereas more lithic Alleghanian foreland basin sandstones are devoid of Archean zircons (Eriksson *et al*., 2004; Thomas *et al*., 2004; Becker *et al*., 2005; Park *et al*., 2010). The composition, detrital zircon age peaks and paleocurrent data for the Stony Gap Sandstone (Figs. 1.8 and 1.14a) coupled with the absence of Archean zircons in older Mississippian sandstones (Park *et al*., 2010) are compatible with a northern, distal cratonic source most likely the Superior Province. Grenvillian and Paleozoic zircons in the Stony Gap Sandstone are interpreted to have been recycled from older Paleozoic strata in the fold-and-thrust belt to the southeast and supplied to the longitudinal drainage system by small, transverse fluvial systems. The likely source for the Paleoproterozoic zircons is the large tract of mid-continent igneous rocks of the Penokean and Yavapai-Mazatzal provinces to the north and west (Fig. 1.16; Karlstrom *et al*., 2001).

Minimum distances of ~850 km northwest and ~1000 km north of the study are required to source the Penokean and Yavapai-Mazatzal and Superior Provinces (Fig. 1.16). Tectonic highlands uplifted during the waning stages of the Late Devonian-Mississippian Acadian orogeny and the early stages of the Allegheny orogeny to the east set the limit of the eastern extent of drainage configurations. The estimated 1, 373,000 km^2 drainage area of the Stony Gap incised-valley (Table 1.1) is of appropriate scale to explain the detrital zircon age

spectrum. Using a length ~2350 km and a width of ~590 km (2:1 ratio) for the Stony Gap incised-valley drainage basin results in adequate headward reaches for sourcing Penokean, Yavapai-Mazatzal and Superior Provinces (Fig. 1.16). The framework petrology of the Stony Gap quartzarenites suggests derivation from mature sources. Given the inferred 15°S paleolatitude for the Mauch Chunk depocenter in the study area (Englund & Thomas, 1990; Cecil, 1990; Witzke, 1990; cf. Golonka *et al*., 1994) the northern Superior Province headwaters of the Stony Gap drainage system are likely to have experienced more humid climatic conditions based on proximity to the equator. Exposure to the more tropical, humid climate would have resulted in intense chemical weathering to produce quartz-rich detritus from the northern extent of the drainage system (Wizevich, 1993). Detrital zircon age spectra in the Stony Gap Sandstone also support recycling of older Paleozoic strata uplifted in the fold-and-thrust belt to the southeast. The loss of less durable lithic grains downstream through transport and chemical weathering is interpreted to be responsible for the compositional and textural maturity exhibited in Stony Gap fluvial quartzarenites. A combination detrital zircon ages from the Stony Gap Sandstone with petrography and paleocurrent analysis supports the interpretation that quartzarenites were deposited within a NE-SW oriented longitudinal incised-valley.

Estimates of drainage area for the Ravencliff sandstone are based on one interpreted downstream accretionary element. Ideally, multiple measurements are made to minimize the risk of mistaking tributary or delta distributary channels for the primary trunk channel (Bhattacharya & Tye, 2004). Therefore, the estimated drainage area of 402,000 km^2 is unlikely to reflect the true scale of the Ravencliff incised-valley. Comparing sandstone petrology and incised-valley dimensions of the Ravencliff sandstone with the Stony Gap incised-valley helps to

provide constraints on the origin of the Ravencliff incised-valley. Like the Stony Gap Sandstone, the mature composition of the Ravencliff sandstone implies a mature source with sediment transport distances capable of producing quartz rich detritus. The estimated drainage area of ~402,000 km^2 does allow for relatively distal reaches of headwaters to extend into northern, equatorial paleolatitudes where the more humid, tropical climate would promote more intense chemical weathering (Fig. 1.16).

When compared to the Stony Gap incised-valley, the Ravencliff incised-valley is relatively shallow (Table 1.1). Depths of incised-valleys have been shown to be largely influenced by the magnitude and duration of the sea-level lowstand (Schumm & Ethridge, 1994; Van Heijst & Postma, 2001). Substrate lithology has also been interpreted to exert a strong control on incision depths (Van Heijst & Postma, 2001; Wohl & Achyuthan, 2002; Ardies *et al*., 2002; Tooth *et al*., 2004, Mattheus *et al*., 2007; Blum *et al*., 2013). The resistant Little Stone Gap Limestone commonly underlies the Ravencliff sandstone and likely slowed and even inhibited incision. Where incision depths do not reach the Little Stone Gap Limestone, substrate lithologies consist of shale and siltstone. The mature composition of the Ravencliff sandstone and the architectural element thickness coupled with the relatively wide incised-valley is consistent with the Ravencliff sandstone having developed within a NE-SW oriented longitudinal incised-valley similar to the Stony Gap Sandstone.

7.2.2 Transverse Drainage Systems

Detrital zircon age spectra from Princeton Formation sandstones are dominated by Grenvillian-and Taconic- zircons and are attributed to recycling of older Neoproterozoic and

Paleozoic sedimentary successions uplifted in the proximal fold-thrust belts to the northeast (Figs. 1.14 and 1.16; Eriksson *et al*., 2004; Beck*er et al*., 2005; Park *et al*., 2010; Grimm *et al*., 2013). Similarly, subordinate Paleoproterozoic zircons in the Princeton Formation likely resulted from recycling of older successions (McLennan *et al*., 2001; Eriksson *et al*., 2004).

The estimate drainage area of 85,500 km^2 for the Princeton incised-valley (Table 1.1) is interpreted to be of appropriate scale for a transverse river system. Assuming a drainage basin area of ~300 by 300 km results in a drainage configuration capable of sourcing proximal tectonic highlands along the eastern margin of the Appalachian Basin and explains for the predominant Grenvillian zircon spectrum (Fig. 1.16). This drainage area infers shorter distances of sediment transport compared to the Stony Gap Sandstone and explains the lithic character of the Princeton sandstone. Cameron & Blatt (1971) demonstrated that most metamorphic rock fragments (schist and phyllite) are mechanically destroyed in less than 25 km of fluvial transport. This implies that the metamorphic rock fragments in Princeton Formation conglomerates were sourced from proximal sources. Detrital zircon ages along with petrographic, paleocurrent and drainage basin area analysis for the Princeton Formation suggest that sediments were derived from proximal tectonic highlands along the eastern margin of the Appalachian Basin and dispersed into the transverse Princeton incised-valley.

7.3 Incised Valley Scaling Relationships

Studies of modern river systems have shown that river channels scale to discharge (Leopold & Maddock, 1953; Best & Ashworth, 1987; Knighton, 1998). Channel width and depth increase downstream because of the cumulatively increasing drainage area (Leopold *et al*.,

1964). This relationship can be inferred for the Stony Gap and Princeton incised-valleys. Higher bankfull depths of the Stony Gap incised-valley are interpreted to be a product of the larger drainage basin area, resulting in the greater widths and thicknesses of both the incised-valley and the internal architectural elements than those of the Princeton incised-valley.

7.4 Comparison with Early Pennsylvanian Incised-Valleys

Fluvial systems similar to the Stony Gap, Ravencliff, and Princeton incised-valleys have been identified in Early Pennsylvanian strata of the Central Appalachian Basin (e.g. Englund, 1974; Rice & Schwietering, 1988; Rice & Weir, 1984; Beuthin, 1994; Blake *et al*., 2000; Miller & Eriksson, 2000; Beuthin & Blake, 2001; Smith, 2010; Grimm *et al*., 2013). Grimm *et al*. (2013) as well as Rice & Schwietering, (1988) developed a two end-member depositional model for Early Pennsylvanian alluvial deposits (Fig. 1.17) that consists of either: 1) clean quartzarenite sandstones and conglomerates ranging from 10 to 50 m in thickness and 17-100 km in width; these deposits contain a mixture of Grenvillian and Archean zircons with subordinate Yavapai-Mazatzal zircons and developed in longitudinal drainage systems; or 2) lithic sandstones and conglomerates that range from 5 to 25 m in thickness and 1-10 km in width; these deposits contain Grenvillian zircons and developed in transverse drainage systems (Eriksson *et al*., 2004; Grimm *et al.*, 2013).

Sandstones of the Lee Formation in eastern Kentucky belong to the longitudinal alluvial facies belt of Grimm *et al*. (2013) and were interpreted by Wizevich (1992) as fluvial incised-valley deposits. The incised-valleys are up to 100 km wide and their fills are up to 200 m thick. Fluvial facies in Corbin Member of the Lee Formation exhibit similar downstream accretion

elements to those of the Stony Gap Sandstone described above. Downstream accretion elements in the Corbin Member range from 5 to 10 m in thickness and are interpreted as macroforms within major channels. From bottom to top the downstream accretion elements consist of: 1) thin conglomeratic sandstones; 2) large-scale planar or tangential cross-beds; and 3) compound cross-beds (Wizevich, 1992).

Based on the thicknesses of the downstream accreting elements in the Corbin Member, a maximum bankfull depth computes to 16 m. Using the regional curve of Metclaf (2004) from Alabama and northwest Florida coastal plains, and the method for estimating drainage areas of Davidson & North (2009), the estimated drainage basin area for the Corbin Member incised-valley is ~2,718,500 km^2. Archer & Greb (1995) estimated drainage areas for Early Pennsylvanian incised-valleys of the Central Appalachian Basin to range from 1,337,100 km^2 to 2,854,300 km^2. The Corbin drainage area follows the same scaling relationship as the Stony Gap, Ravencliff and Princeton incised-valleys, where dimensions of incised-valleys and their internal fill elements scale to the size of their drainage basin area.

8. Conclusions

Integration of incised-valley metrics, architectural element analysis of incised-valley fills, sandstone petrology and detrital zircon geochronology supports the existence of two asynchronous paleodrainage courses consisting of longitudinal and transverse incised-valley systems during the Late Mississippian in Central Appalachian Basin. Results of this study suggest that:

- The Stony Gap and Ravencliff sandstones were derived from distal, northern and northwestern cratonic sources that dispersed sediment into NE-SW-oriented, longitudinal incised-valley drainage systems.
- The Princeton Formation was derived from the proximal fold-and-thrust belt along the eastern margin of the Appalachian Basin which dispersed sediment into the transverse oriented, Princeton incised-valley system.
- A relationship between appropriate drainage area estimates and dimensions of incised-valleys, specifically width and the internal architectural element thicknesses is apparent.
- Drainage basin area estimates based on the method of Davidson & North (2009) for the Stony Gap, Ravencliff and Princeton incised-valleys result in drainages that are size-appropriate for Upper Mississippian paleogeographic reconstructions and that explain the dimensions of the incised-valleys and their fills.
- The larger Stony Gap incised-valley, which contains the thickest architectural elements, is a product of a drainage basin area that is one-half to a whole order-of-magnitude larger than that of the Ravencliff sandstone and Princeton Formation.
- By constraining the drainage basin areas of the three Upper Mississippian incised-valleys and their fills, it is possible to reconstruct aspects of the total source to sink system.

The intent of this study was not to identify all controls on incised-valleys, but rather provide insight on how the dimensions of incised-valley and their internal architectural elements are a product of upstream controls, most of which are reflected in the drainage area size. Calculating drainage basin areas is not suggested to be the absolute explanation for

interpreting incised-valleys. Instead, suitable estimates of drainage basin areas can provide significant value when examining source to sink processes of fluvial deposits.

9. References

ADAMS, M.M. & BHATTACHARYA, J.P. (2005) No change in fluvial style across a sequence boundary, Cretaceous Blackhawk and Castlegate Formations of central Utah, USA. Journal of Sedimentary Research, 75, 1038-1051.

ALLEN, J.R.L. (1965) The sedimentation and paleogeography of the Old Red Sandstone of Anglesey, north Wales. In: Proceedings of the Yorkshire Geological and Polytechnic Society, 35, 139-185.

ANDERSON, J.B., ABDULAH, K., SARZALEJO, S., SIRINGIN, F. & THOMAS, M.A. (1996) Late Quaternary sedimentation and high-resolution sequence stratigraphy of the East Texas Shelf. Geological Society of London, Special Publication 117, 95-124.

ASHLEY, G.M. & SHERIDAN, R.E. (1994) Depositional model for valley fills on a passive continental margin. In: Incised Valley Systems - Origin and Sedimentary Sequences (Ed. by R. W. Dalrymple, R. Boyd and B. A. Zaitlin), SEPM Special Publication, 51, 285-301.

ARCHER, A.W. & GREB, S. F. (1995) An Amazon-scale drainage system in the Early Pennsylvanian of central North America. The Journal of Geology, 611-627.

ARDIES, G.W., DALRYMPLE, R.W. & ZAITLIN, B.A. (2002) Controls on the geometry of incised valleys in the Basal Quartz unit (Lower Cretaceous), Western Canada Sedimentary Basin. Journal of Sedimentary Research, 72, 602-618.

BECKER, T.P., THOMAS, W.A., SAMSON, S.D. & GEHRELS, G.E. (2005) Detrital zircon evidence of Laurentian crustal dominance in the lower Pennsylvanian deposits of the Alleghanian clastic wedge in eastern North America. Sedimentary Geology, 182, 59-86.

BEST, J.L. & ASHWORTH, P.J. (1997) Scour in large braided rivers and the recognition of sequence stratigraphic boundaries. Nature, 387, 275–277.

BEUTHIN, J.D. (1994) A sub-Pennsylvanian paleovalley system in the central Appalachians and its implications for tectonic and eustatic controls on the origin of the regional Mississippian–Pennsylvanian unconformity. In: Tectonic and Eustatic Controls on Sedimentary Cycles (Ed. by J. M. Dennison and F. R. Ettensohn), SEPM Special Publication, 4, 107–120.

BEUTHIN, J.D. & BLAKE, B.M. (2001) Bedrock geologic map of the Athens quadrangle, West Virginia, West Virginia Geological and Economic Survey Open File Publication OF- 0104.

BHATTACHARYA, J.P. & TYE, R.S. (2004) Searching for modern Ferron analogs and application to subsurface interpretation. Regional to wellbore analog for fluvial-deltaic reservoir modeling: The Ferroan Sandstone of Utah. AAPG Studies in Geology, 50, 39-57.

BLAKE, B.M., BEUTHIN, J.D. & RADER, E. (2000) Bedrock geologic map of the Princeton quadrangle, West Virginia-Virginia. West Virginia Geological and Economic Survey Open File Report, scale 1:24000.

BLUCK, B.J. (1976) Sedimentation in some Scottish rivers of sinuosity. Trans. R. Soc. Edinburgh, 69, 425- 456.

BLUM, M.D. & PRICE, D.M. (1994) Glacio-eustatic and climatic controls on Quaternary alluvial plain deposition, Texas coastal plain. Gulf Coast Association of Geological Societies, Transactions, 44, 85-92.

BLUM, M.D. & PRICE, D.M. (1998) Quaternary alluvial plain construction in response to glacio-eustatic and climatic controls, Texas Gulf Coast Coastal Plain. In: Relative Role of Eustasy, Climate, and Tectonism in Continental Rocks (Ed. by K. Shanley, and P. McCabe), SEPM Special Publication, 59, 31-48.

BLUM, M., MARTIN, J., MILLIKEN, K. & GARVIN, M. (2013) Paleovalley systems: Insights from Quaternary analogs and experiments. Earth-Science Reviews, 116, 128-169.

CAMERON, K.L. & BLATT, H. (1971) Durabilities of sand size schist and 'volcanic' rock fragments during fluvial transport, Elk Creek, Black Hills, South Dakota. Journal of Sedimentary Research, 41, 565-576.

CASTRO, J.M. & JACKSON, P.L. (2001) Bankfull discharge recurrence intervals and regional hydraulic geometry relationships: Patterns in the Pacific Northwest, USA. American Water Resources Association Journal, 37, 1249–1262.

CECIL, C.B. (1990) Paleoclimate controls on stratigraphic repetition of chemical and siliciclastic rocks. Geology, 18, 533-536.

CECIL, C.B., DULONG, F.T., EDGAR, N.T. & WEST, R. (1997) Climatic controls on Carboniferous cyclic sedimentation: U.S.A. American Association of Petroleum Geologists Annual Meeting, Abstract, 6, 19.

DALRYMPLE, R.W., BOYD, R. & ZAITLIN, B.A. (1994) History of research, valley types, and internal organization of incised-valley systems: Introduction to volume. In: Incised Valley Systems: Origin and Sedimentary Sequences (Eds. by R. W. Dalrymple, R. Boyd and B. A. Zaitlin), SEPM Special Publication 51, 3-9.

DAVIDSON, S.K. & NORTH, C.P. (2009) Geomorphological regional curves for prediction of drainage area and screening modern analogues for rivers in the rock record. Journal of Sedimentary Research, 79, 773-792.

DEWITT, J.R. & MCGREW, L.W. (1979) Appalachian basin region. In: Paleotectonic Investigation of the Mississippian System in the United States Part I: Introduction and Regional Analysis of the Mississippian System (Ed. by L. C. Craig and C.W. Connor), U.S. Geol. Surv. Prof., 1010, C12–C48.

DICKINSON, W.R., BEARD, L.S., BRAKENRIDGE, G.R., ERJAVEC, J.L., FERGUSON, R.C., INMAN, K.F. & RYBERG, P.T. (1983) Provenance of North American Phanerozoic sandstones in relation to tectonic setting. Geological Society of America Bulletin, 94, 222-235.

ENGLUND., K.J. (1974) Sandstone distribution patterns in the Pocahontas Formation of southwest Virginia and southern West Virginia. Geological Society of America Special Papers, 148, 31-46.

ENGLUND, K.J. & THOMAS, R.E. (1990) Late Paleozoic depositional trends in the Central Appalachian Basin. U.S. Geol. Surv. Bull., 1839, 19.

ERIKSSON, K.A., CAMPBELL, I.H., PALIN, J.M., ALLEN, C.M. & BOCK, B. (2004) Evidence for multiple recycling in Neoproterozoic through Pennsylvanian sedimentary rocks of the Central Appalachian Basin. Journal of Geology, 112, 261-276.

ETHRIDGE, F.G. & SCHUMM, S.A. (1977) Reconstructing paleochannel morphologic and flow characteristics: methodology, limitations, and assessment. In: Fluvial Sedimentology (Ed. by A. D. Miall), Canadian Society Petroleum Geology Memoir, 5, 703–721.

ETTENSOHN, F.R. (1994) Tectonic control on formation and cyclicity of major Appalachian unconformities and associated stratigraphic sequences. In: Tectonic and Eustatic Controls on Sedimentary Cycles: Concepts in Sedimentology and Paleontology (Ed. by J.M. Dennison and F. R. Ettensohn), SEPM Special Publication, 4, 217-242.

GIBLING, M.R. (2006) Width and thickness of fluvial channel bodies and valley fills in the geological record: a literature compilation and classification. Journal of Sedimentary Research, 76, 731-770.

GOLONKA, J., ROSS, M.I. & SCOTESE, C.R. (1994) Phanerozoic paleogeographic and paleoclimatic modeling maps: Pangea: global environments and resources. Canadian Society of Petroleum Geologists Memoir, 17, 1-47.

GORDON, M.J. & HENRY, T.W. (1981) Late Mississippian and Early Pennsylvanian invertebrate faunas, east-central Appalachians-a preliminary report. In: Geological Society of America Cincinnati '81 field trip guidebooks: volume 1, stratigraphy, sedimentology (Ed. by T. G. Robert), American Geological Institute, 165-171.

GRADSTEIN, F.M., JAMES, G.O. & SCHMITZ, M. (2012) The Geologic Time Scale 2012, 2-volume set. Elsevier, Amsterdam, 1176.

GRAY, M.B. & ZEITLER, P.K. (1997) Comparison of clastic wedge provenances in the Appalachian foreland using U-Pb ages of detrital zircons. Tectonics, 16, 151–160.

GRIMM, R.P., ERIKSSON, K.A. & CARBAUGH, J. (2013) Orogenic controls on the temporal and spatial distribution of longitudinal and transverse alluvial facies belts in an Early Pennsylvanian foreland basin, Virginia, USA. Basin Research, 25, 450–470.

HASZELDINE, R.S. (1983a) Descending tabular crossbed sets and bounding surfaces from a fluvial channel in the Upper Carboniferous coalfield of north-east England. In: Modern and Ancient Fluvial Systems (Ed. by J.D Collinson and J. Lewin), International Association Sedimentologists Special Publication 6, 449-456.

HASZELDINE, R.S. (1983b) Fluvial bars reconstructed from a deep straight channel, Upper Carboniferous coalfield of northeast England. Journal Sedimentary Petrology, 53, 1233-1247.

HOFFMAN, P.F. (1989) Precambrian geology and tectonic history of North America. In: The Geology of North America: An Overview (Eds. by A.W. Bally and A. R. Palmer), Geological Society of America, Geology of North America, Boulder, Colorado, 447–512.

HOLBROOK, J. (2001) Origin, genetic interrelationships, and stratigraphy over the continuum of fluvial channel-form bounding surfaces: an illustration from middle Cretaceous strata, southeastern Colorado. Sedimentary Geology, 144, 179-222.

KAHMANN, J.A. & DRIESE, S.G. (2008) Paleopedology and geochemistry of Late Mississippian (Chesterian) Pennington Formation paleosols at Pound Gap, Kentucky, USA: Implications for high-frequency climate variations. Palaeogeography, Palaeoclimatology, Palaeoecology, 259, 357-381.

KAMM, M.W. (1981) Petrology and diagenesis of the Ravencliff Sandstone. Unpublished thesis. West Virginia University Libraries, University of West Virginia, West Virginia, Morgantown, 111.

KAMM, M.W. & HEALD, M.T. (1983) Petrology and diagenesis of the Ravencliff Sandstone in West Virginia. Southeastern Geology, 24, 1-12.

KARLSTROM, K.E., ÅHÄLL, K.I., HARLAN, S.S., WILLIAMS, M.L., MCLELLAND, J. & GEISSMAN, J.W. (2001) Long-lived (1.8–1.0 Ga) convergent orogen in southern Laurentia, its extensions to Australia and Baltica, and implications for refining Rodinia. Precambrian Research, 111, 5-30.

KELAFANT, J.R., WICKS, D.E. & KUUSKRAA, V.A. (1988) A geologic assessment of natural gas from coal seams in the Northern Appalachian Coal Basin. Topical Report – Final Geologic Report.

KIRKPATRICK, J. (1994) Sedimentology of the Stony Gap (Upper Mississippian), Summers and Mercer Counties, West Virginia. Unpublished thesis. University Libraries, East Carolina University, North Carolina, Greenville, 129.

KNIGHTON., D. (1998) Fluvial Forms and Processes. New York, John Wiley & Sons Inc., 383.

KORUS, J.T. (2002) The lower Pennsylvanian New River Formation a nonmarine record of glacioeustasy in a foreland basin. University Libraries, Virginia Polytechnic Institute and State University, Blacksburg, 61.

KORUS, J.T., KVALE, E.P., ERIKSSON, K.A. & JOECKEL, R.M. (2008) Compound paleovalley fills in the Lower Pennsylvanian New River Formation, West Virginia, USA. Sedimentary Geology, 208, 15-26.

LEOPOLD, L.B. & MADDOCK, T.J. (1953) The hydraulic geometry of stream channels and some physiographic implications. U.S. Geological Survey, Professional Paper 252, 57.

LEOPOLD, L.B., WOLMAN, M.G. & MILLER, J.P. (1964) Fluvial Processes in Geomorphology: San Francisco., Freeman, 503.

MATTHEUS, C.R., RODRIGUEZ, A.B., GREENE, J.R., SIMMS, A.R. & ANDERSON, J.B. (2007) Control of upstream variables on incised-valley dimension. Journal of Sedimentary Research, 77, 213-224.

MAYNARD, J.P., ERIKSSON, K.A. & LAW, R.D. (2006) The Upper Mississippian Bluefield Formation in the central Appalachian basin: A hierarchical sequence stratigraphic record of a greenhouse to icehouse transition. Sedimentary Geology, 192, 99-122.

METCALF, C. (2004) Regional Channel Characteristics for Maintaining Natural Fluvial Geomorphology in Florida Streams. U.S. Fish and Wildlife Service, Panama City Fisheries Resource Office.

MCCARTHY, P.J. & PLINT, A.G. (1998) Recognition of interfluve sequence boundaries: integrating paleopedology and sequence stratigraphy. Geology, 26, 387-390.

MCLENNAN, S.M., BOCK, B., COMPSTON, W., HEMMING, S.R. & MCDANIEL, D.K. (2001) Detrital zircon geochronology of Taconian and Acadian foreland sedimentary rocks in New England. Journal of Sedimentary Research, 71, 305-317.

MIALL, A.D. (1985) Architectural-element analysis: a new method of facies analysis applied to fluvial deposits. Earth-Science Reviews, 22, 261-308.

MIALL., A.D. (1988) Facies architecture in clastic sedimentary basins. In: New perspectives in basin analysis Springer New York, 67-81.

MIALL, A.D. (1993) The architecture of fluvial-deltaic sequences in the upper Mesaverde Group (Upper Cretaceous), Book Cliffs, Utah. Geological Society London, Special Publications, 75, 305-332.

MIALL, A.D. & MOHAMUD, A. (2001) The Castlegate Sandstone of the Book Cliffs, Utah: sequence stratigraphy, paleogeography, and tectonic controls. Journal of Sedimentary Research, 71, 537-548.

MILLER, D.J. & ERIKSSON, K.A. (1997) Late Mississippian prodeltaic rhythmites in the Appalachian basin: a hierarchical record of tidal and climatic periodicities. Journal of Sedimentary Research, 67, 653-660.

MILLER, D.J. & ERIKSSON, K.A. (1999) Linked sequence development and global climate change: The Upper Mississippian record in the Appalachian basin. Geology, 27, 35-38.

MILLER, D.J. & ERIKSSON, K.A. (2000) Sequence stratigraphy of Upper Mississippian strata in the central Appalachians: A record of glacioeustasy and tectonoeustasy in a foreland basin setting. American Association of Petroleum Geologists Bulletin, 84, 210-233.

MILLIMAN, J.D. & SYVITSKI, J.P. (1992) Geomorphic/tectonic control of sediment discharge to the ocean: the importance of small mountainous rivers. Journal of Geology, 525-544.

PAOLA, C. & BORGMAN, L. (1991) Reconstructing random topography from preserved stratification. Sedimentology, 38, 553-565.

PARK, H., BARBEAU, D.L., RICKENBAKER, A., BACHMANN-KRUG, D. & GEHRELS, G. (2010) Application of foreland basin detrital-zircon geochronology to the reconstruction of the southern and central Appalachian Orogen. Journal of Geology, 118, 23–44.

PINNIX, A.J. (1993) Sedimentology of the Princeton Sandstone (Upper Mississippian) in southeastern West Virginia. Unpublished thesis. University Libraries, East Carolina University, North Carolina, Greensville, 133.

PRESLEY, M.W. (1977) A depositional systems analysis of the Upper Mauch Chunk aPottsville Groups in northern West Virginia. Unpublished dissertation. University of West Virginia Libraries, West Virginia University, West Virginia, Morgantown, 314.

READ, J.F. & ERIKSSON, K.A. (2012) Paleozoic Sedimentary Successions of the Virginia Valley & Ridge and Plateau. VTechWorks. http://hdl.handle.net/10919/19078.

REED, J.S. (2005) Thermal and Diagenetic Evolution of Carboniferous Sandstones, Central Appalachian Basin. Unpublished dissertation. Virginia Tech University Libraries, Virginia Polytechnic Institute and State University, Virginia, Blacksburg, 115.

REPETSKI, J.E. & STAMM, R.G. (2009) Mississippian conodonts of the Appalachian Basin. Kentucky Geological Survey, Carboniferous Geology and Biostratigraphy of the Appalachian Basin, 59-61.

RICE, C.L. & SCHWIETERING, J.F. (1988) Fluvial deposition in the central Appalachians during the Early Pennsylvanian. Evolution of Sedimentary Basins - Appalachian Basin. Washington, D.C. United States Geological Survey Bulletin 1839, B1-B10.

RICE, C.L. & WEIR, G.W. (1984) Sandstone units of the Lee Formation and related strata in eastern Kentucky. Kentucky Geological Survey, 1-50.

ROBINSON, R.A.J. & PRAVE, A.R. (1995) Cratonal contributions to a classic molasse - the Carboniferous Pottsville Formation of eastern Pennsylvania revisited. Geology, 23, 369-372.

SCHUMM., S.A. (1993) River response to base level change: implications for sequence stratigraphy. Journal of Geology, 101, 279-294.

SCHUMM, S.A. & ETHRIDGE, F.G. (1994) Origin, evolution and morphology of fluvial valleys. In: Incised-Valley Systems: Origin and Sedimentary Sequences (Ed. by R. W. Dalrymple, R. Boyd and B. A. Zaitlin), SEPM Special Publication 51, 11–27.

SCHUMM, S.A. & WINKLEY, B.R. (1994) The character of large alluvial rivers. In: The Variability of Large Alluvial Rivers (Ed. by S. A. Schumm and B. R. Winkley), Society of Civil Engineers, 1-9.

STOTT, G.M. (1997) The Superior Province, Canada. In: Greenstone Belts. (Ed. by M. de Witt and L. D. Ashwal), Oxford University Press, 480–507.

SMITH, T. (2009) Sequence stratigraphy and stratigraphic architecture of the upper Mississippian lower Hinton Formation Appalachian Basin, West Virginia, USA. Unpublished thesis. University Libraries, University of North Carolina at Chapel Hill, North Carolina, Chapel Hill, 100.

SMITH, L.B. & READ, J.F. (2000) Rapid onset of Late Paleozoic glaciation: evidence from Upper Mississippian strata of the Midcontinent, United States. Geology, 28, 279-282.

STAMM, R.G. (1997): Late Mississippian conodont biostratigraphy and lithostratigraphy of the Appalachian Basin; preliminary correlations to the Eastern Interior Basin and eustatic curves. Geological Society of America, Abstracts with Programs, 29, 48.

SUTHERLAND, P.K. (1988) Late Mississippian and Pennsylvanian depositional history in the Arkoma basin area, Oklahoma and Arkansas. Geological Society of America Bulletin, 100, 1787-1802.

TALLING, P.J. (1998) How and where do incised valleys form if sea level remains above the shelf edge? Geology 26, 87-90.

THOMAS, W.A., BECKER, T.P., SAMSON, S.D. & HAMILTON, M.A. (2004) Detrital zircon evidence of a recycled orogenic foreland provenance for Alleghanian clastic-wedge sandstones. Journal of Geology, 112, 23-37.

TOOTH, S., BRANDT, D., HANCOX, P.J. & MCCARTHY, T.S. (2004) Geological controls on alluvial river behavior: a comparative study of three rivers on the South African highveld. J. Afr. Earth Sci., 38, 79–97.

VAN HEIJST, M.W. & POSTMA, G. (2001) Fluvial response to sea-level changes: a quantitative analogue, experimental approach. Basin Research, 13, 269-292.

VAN WAGONER, J.C., MITCHUM, R.M., CAMPION K.M. & RAHMANIAN, V.D. (1990) Siliciclastic sequence stratigraphy in well logs, cores and outcrops. AAPG Methods in Exploration Series, 7, 55.

VAN WAGONER, J.C. (1995) Sequence stratigraphy and marine to nonmarine facies architecture of Foreland Basin Strata, Book Cliffs, Utah, USA. In: Sequence Stratigraphy of Foreland Basin Deposits (Ed. by J. C. Van Wagoner and G. T. Bertram), American Association of Petroleum Geologists Memoir, 45,137-224.

Volga River. (2012) In Encyclopedia Britannica. Retrieved from http://www.britannica.com/EBchecked/topic/632239/Volga-River

WILLIS, B. (1993) Ancient river systems in the Himalayan foredeep, Chinji Village area, northern Pakistan. Sedimentary Geology, 88, 1-76.

WITZKE, B.J. (1990) Palaeoclimates constrains for Palaeozoic Paleolatitudes of Laurentia and Euramerica. Geological Society London Memoir, 12, 57-73.

WIZEVICH, M.C. (1992) Sedimentology of Pennsylvanian quartzose sandstones of the Lee Formation, central Appalachian Basin: fluvial interpretation based on lateral profile analysis. Sedimentary Geology, 78, 1-47.

WIZEVICH, M.C. (1993) Depositional controls in a bedload-dominated fluvial system: internal architecture of the Lee Formation, Kentucky. Sedimentary Geology, 85, 537-556.

WOHL, E. & ACHYUTHAN, H. (2002) Substrate influences on incised-channel morphology. Journal of Geology, 110, 115-120.

WOLMAN, M.G. & MILLER, J.P. (1960) Magnitude and frequency of forces in geomorphic processes. Journal of Geology, 68, 54-74.

WRIGHTSTONE, G. (1985) The stratigraphy and depositional environment of the Ravencliff Formation in McDowell and Wyoming Counties, West Virginia. Unpublished thesis, University of West Virginia Libraries, University of West Virginia, West Virginia, Morgantown, 113.

YANG, C. (1998) Basin Analysis of the Carboniferous Strata in Central and Southern West Virginia Using Sequence Stratigraphic Principles. Unpublished thesis. University of West Virginia Libraries, University of West Virginia, West Virginia, Morgantown, 350.

Figure 1.1: Locality map showing locations of outcrops and cross-sections based on subsurface data.

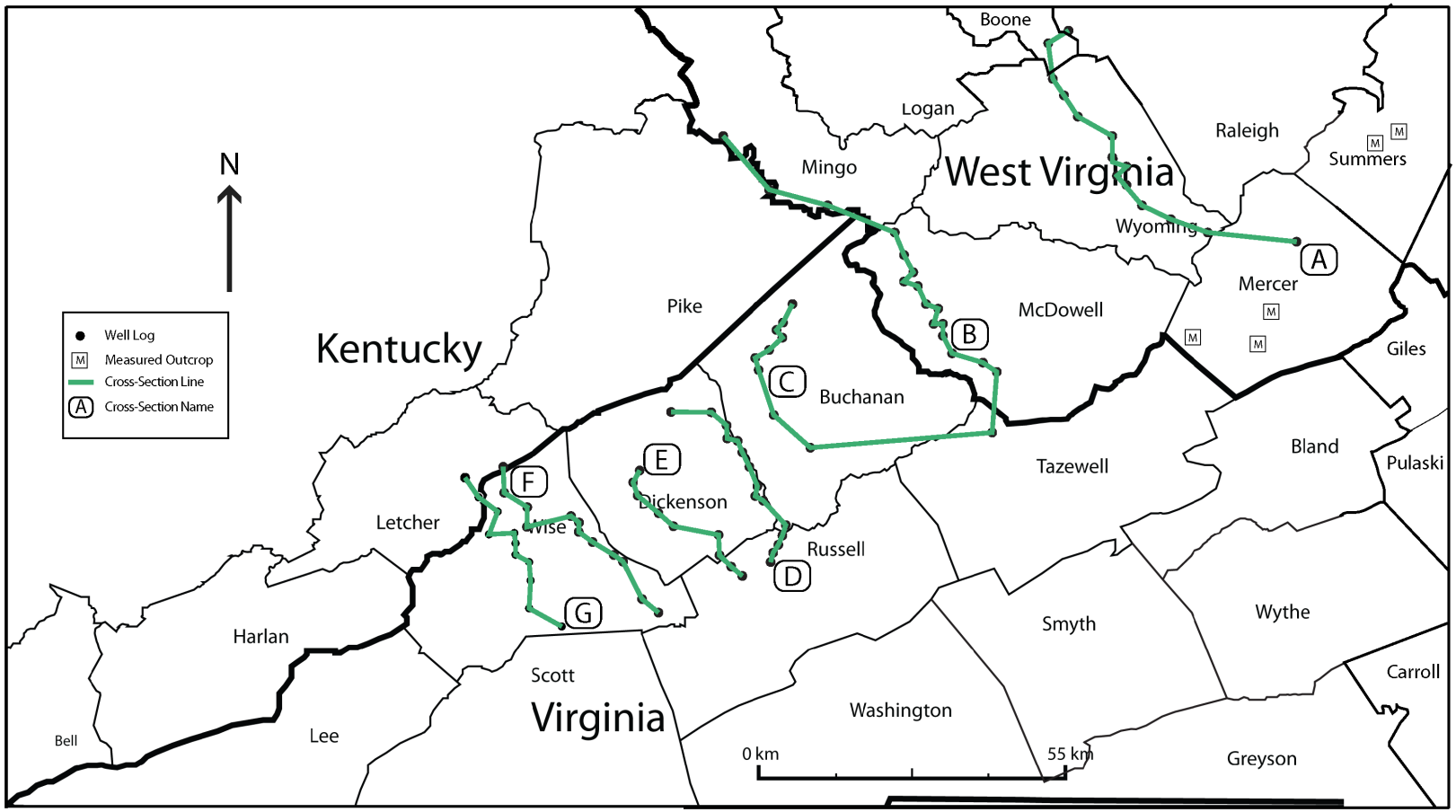
N
Well Log
Measured Outcrop
Cross-Section Line
Cross-Section Name
Kentucky
West Virginia
Virginia
Boone
Logan
Mingo
Raleigh
Summers
Wyoming
Mercer
McDowell
Pike
Buchanan
Giles
Tazewell
Bland
Pulaski
Dickenson
Russell
Wise
Letcher
Harlan
Bell
Lee
Scott
Smyth
Wythe
Carroll
Washington
Greyson
A
B
C
D
E
F
G
0 km
55 km

Figure 1.2: Stratigraphic column of the Mauch Chunk Group. Heavy black lines demarcate third-order sequence boundaries; blue highlights are third-order maximum flood deposits; red denotes incised-valley deposits investigated in this study and green defines the Pride Shale the base of which is used as a datum for constructing the cross-sections (Figs. 1.3, 1.6 and Appendix). See Fig. 1.4 for age constraints.

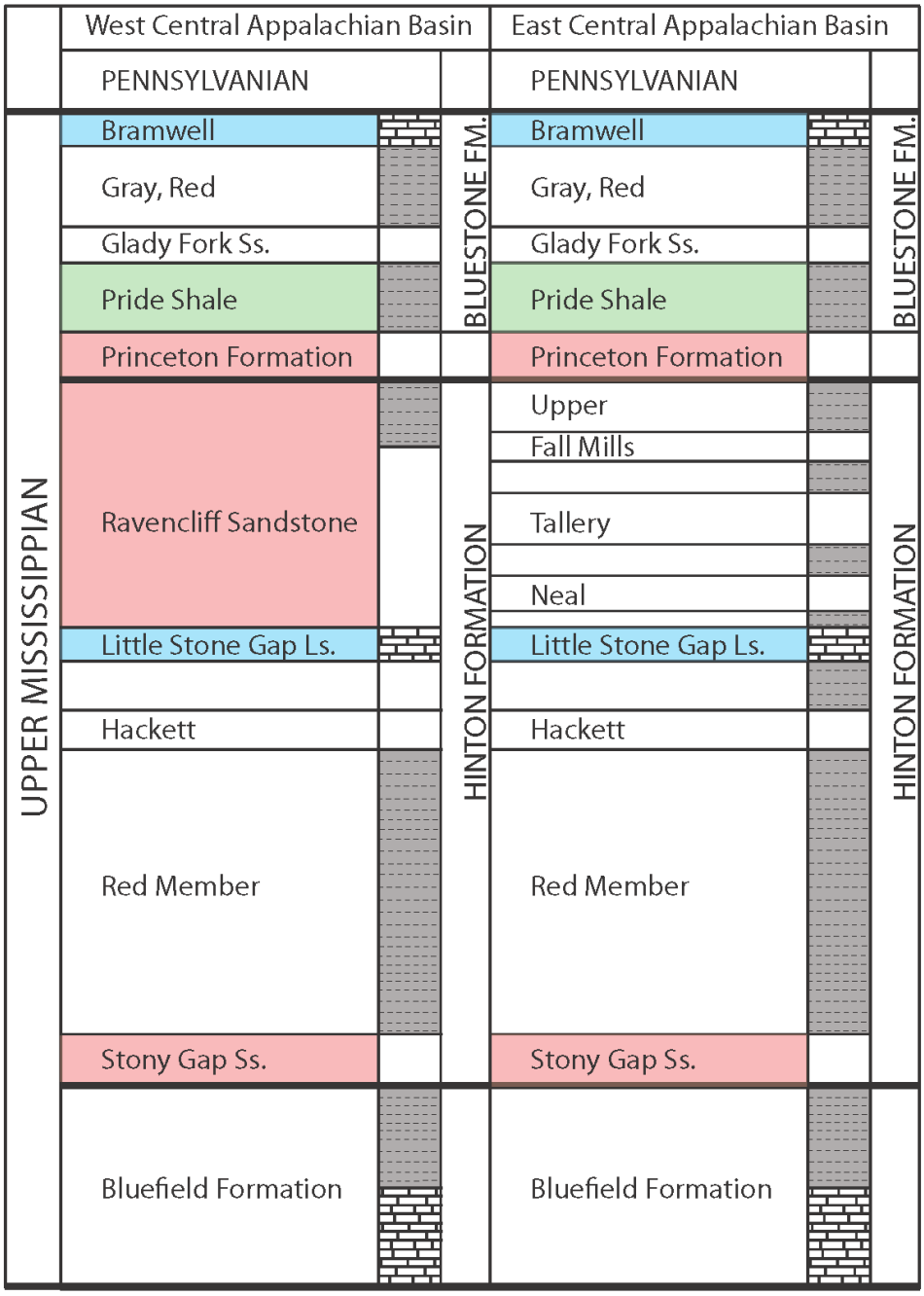
West Central Appalachian Basin
East Central Appalachian Basin
PENNSYLVANIAN
PENNSYLVANIAN
UPPER MISSISSIPPIAN
Bramwell
Gray, Red
Glady Fork Ss.
Pride Shale
Princeton Formation
BLUESTONE FM.
Bramwell
Gray, Red
Glady Fork Ss.
Pride Shale
Princeton Formation
BLUESTONE FM.
Ravencliff Sandstone
Little Stone Gap Ls.
Hackett
Red Member
Stony Gap Ss.
Bluefield Formation
HINTON FORMATION
Upper
Fall Mills
Tallery
Neal
Little Stone Gap Ls.
Hackett
Red Member
Stony Gap Ss.
Bluefield Formation
HINTON FORMATION

Figure 1.3: Regional NW-SE cross-section F-F' showing regional thinning of the Mauch Chunk Group. Refer to Figure 1.1 for location of cross-section.

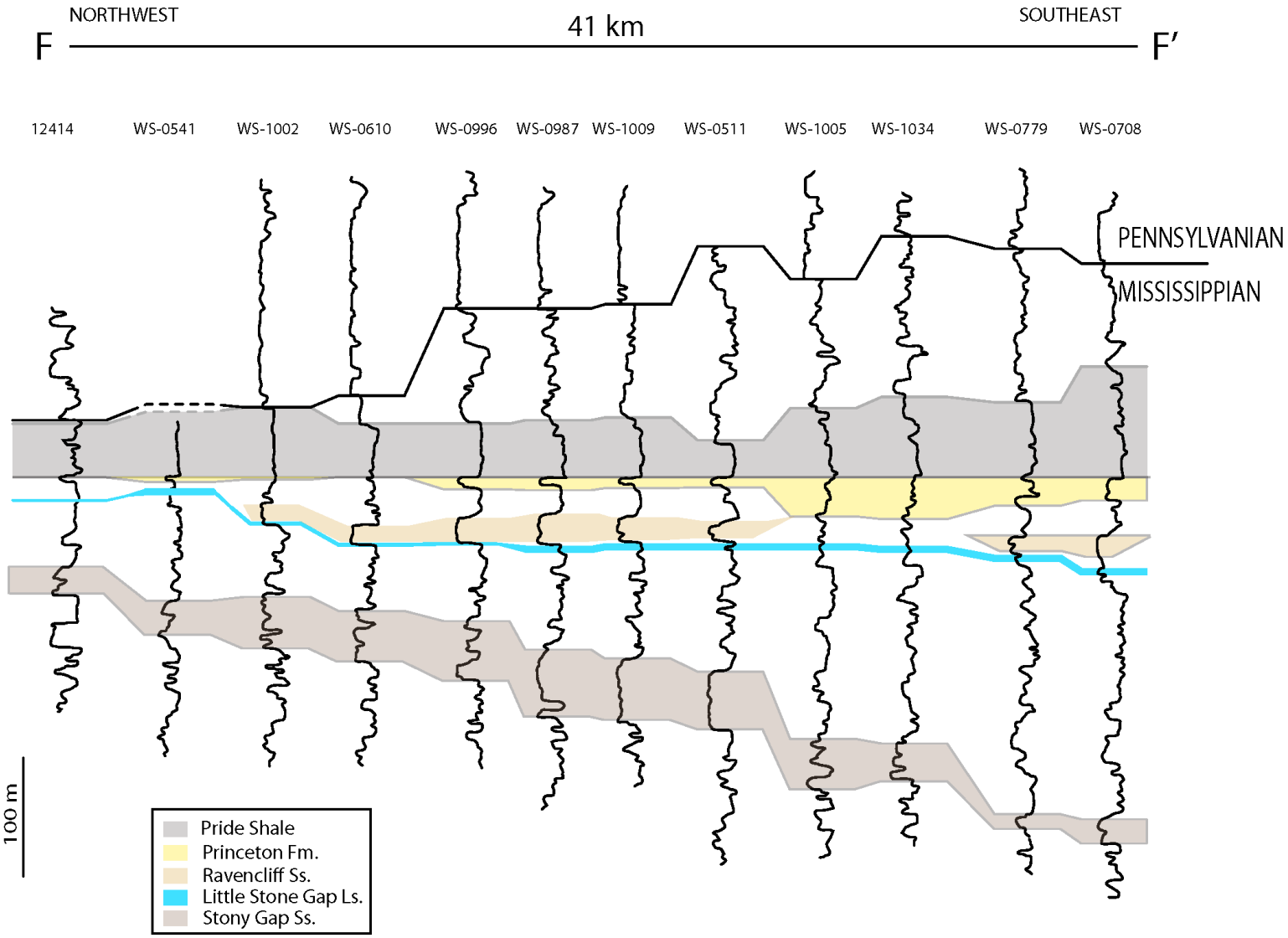
NORTHWEST
41 km
SOUTHEAST
F
F′
12414
WS-0541
WS-1002
WS-0610
WS-0996
WS-0987
WS-1009
WS-0511
WS-1005
WS-1034
WS-0779
WS-0708
PENNSYLVANIAN
MISSISSIPPIAN
100 m
Pride Shale
Princeton Fm.
Ravencliff Ss.
Little Stone Gap Ls.
Stony Gap Ss.

Figure 1.4: Lithostratigraphy and biostratigraphy of Upper Mississippian strata of the Appalachian Basin of southeastern West Virginia and southwestern Virginia (adapted from Repetski & Stamm, 2009; Gradstein & Ogg, 2012).

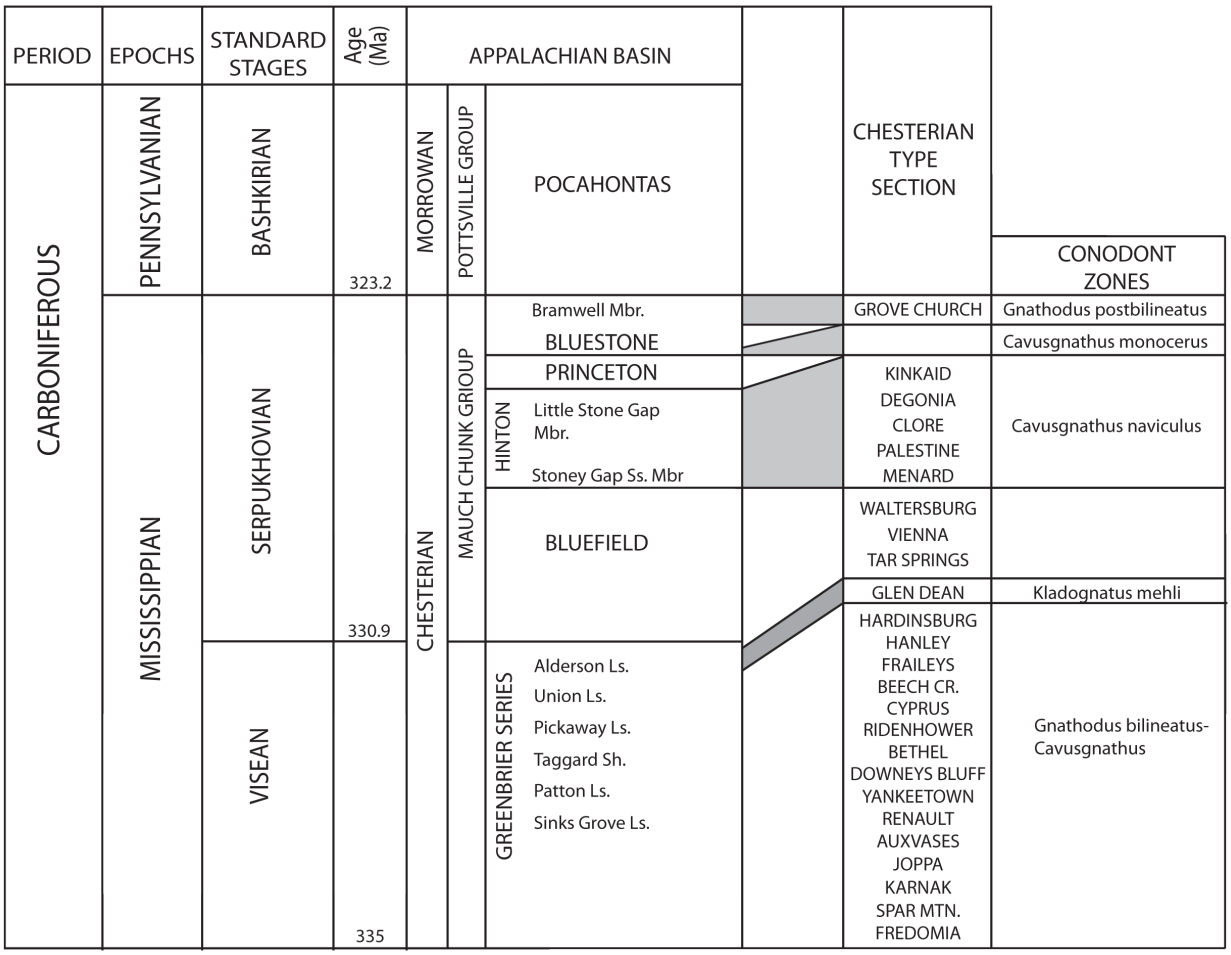
PERIOD
EPOCHS
STANDARD STAGES
Age (Ma)
APPALACHIAN BASIN
CHESTERIAN TYPE SECTION
CONODONT ZONES
CARBONIFEROUS
PENNSYLVANIAN
BASHKIRIAN
323.2
MORROWAN
POTTSVILLE GROUP
POCAHONTAS
MISSISSIPPIAN
SERPUKHOVIAN
330.9
CHESTERIAN
MAUCH CHUNK GRIOUP
Bramwell Mbr.
BLUESTONE
PRINCETON
HINTON
Little Stone Gap Mbr.
Stoney Gap Ss. Mbr
BLUEFIELD
VISEAN
335
GREENBRIER SERIES
Alderson Ls.
Union Ls.
Pickaway Ls.
Taggard Sh.
Patton Ls.
Sinks Grove Ls.
GROVE CHURCH
KINKAID
DEGONIA
CLORE
PALESTINE
MENARD
WALTERSBURG
VIENNA
TAR SPRINGS
GLEN DEAN
HARDINSBURG
HANLEY
FRAILEYS
BEECH CR.
CYPRUS
RIDENHOWER
BETHEL
DOWNEYS BLUFF
YANKEETOWN
RENAULT
AUXVASES
JOPPA
KARNAK
SPAR MTN.
FREDOMIA
Gnathodus postbilineatus
Cavusgnathus monocerus
Cavusgnathus naviculus
Kladognatus mehli
Gnathodus bilineatus-Cavusgnathus

Figure 1.5: Schematic diagram showing inferred paleogeography during the deposition of the Ravencliff sandstone and Princeton Formation as proposed by Yang (1998). Separate incised-valleys represent two different deposystems with their own provenance and drainage basin.

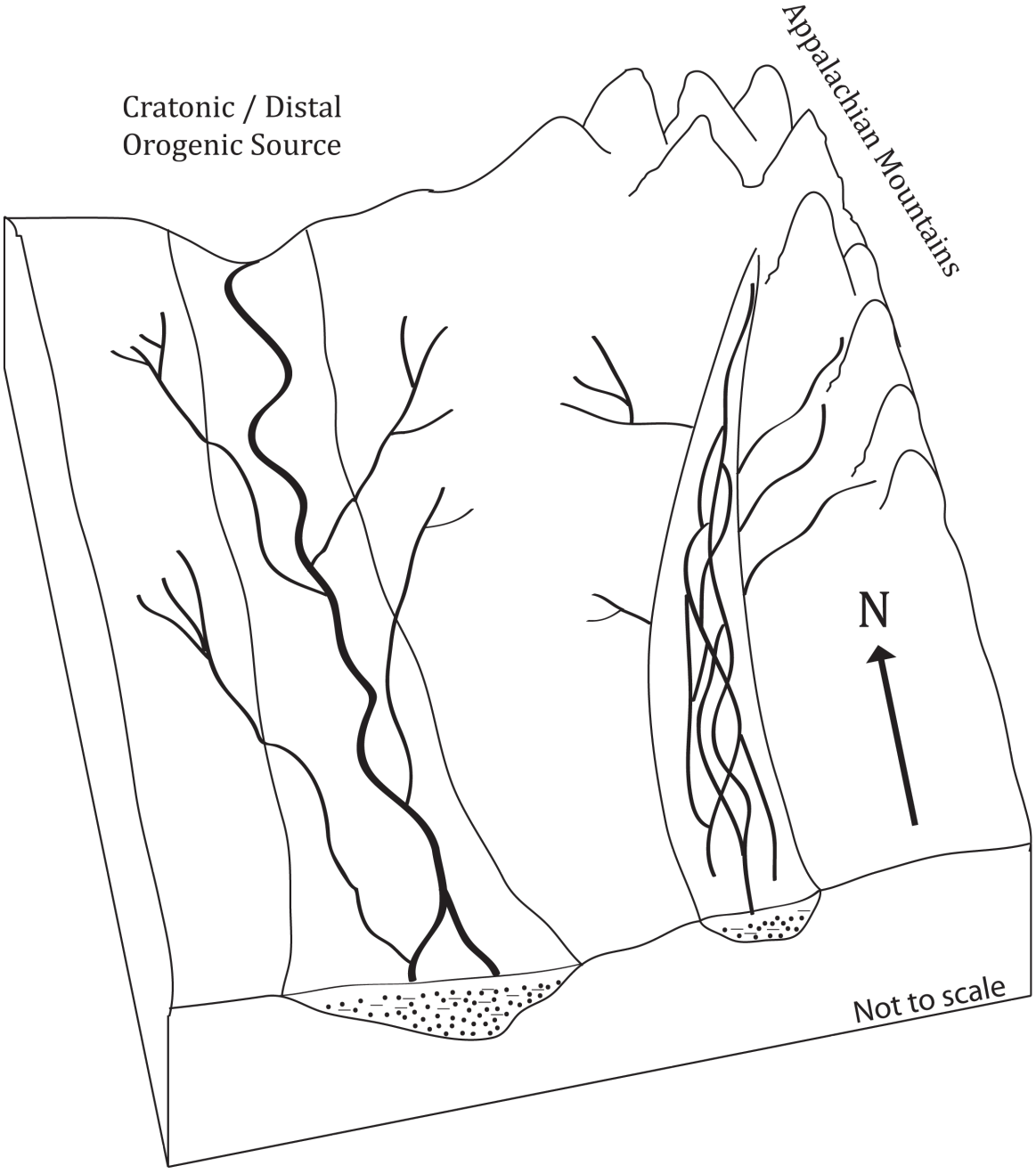
Cratonic / Distal
Orogenic Source
Appalachian Mountains
N
Not to scale

Figure 1.6: Cross-section B-B' showing the Stony Gap, Ravencliff and Princeton incised-valley fills. Note that the Stony Gap and Ravencliff incised-valleys are significantly wider than the Princeton incised-valley.

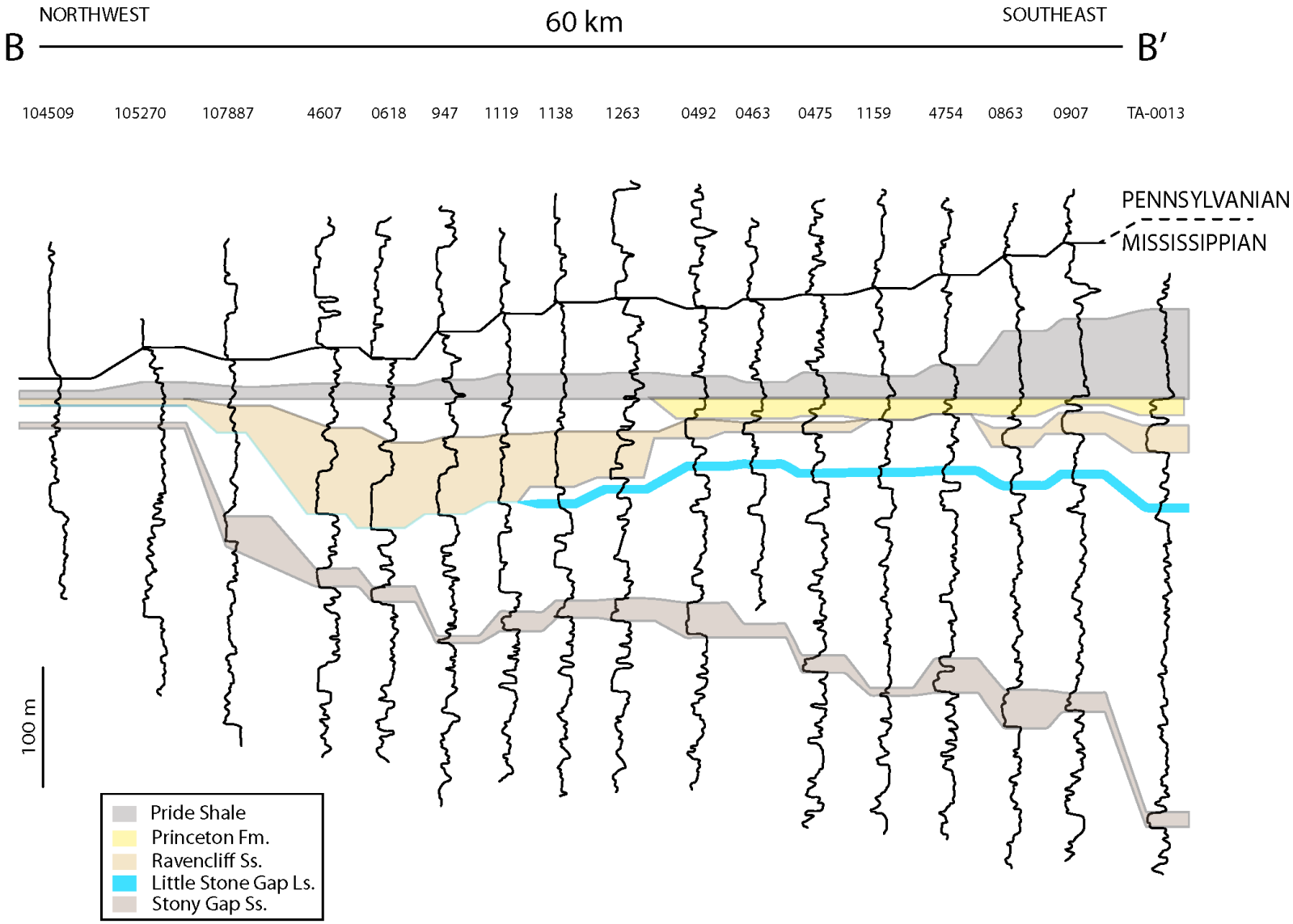
NORTHWEST
60 km
SOUTHEAST
B
B′
104509
105270
107887
4607
0618
947
1119
1138
1263
0492
0463
0475
1159
4754
0863
0907
TA-0013
PENNSYLVANIAN
MISSISSIPPIAN
100 m
Pride Shale
Princeton Fm.
Ravencliff Ss.
Little Stone Gap Ls.
Stony Gap Ss.

Figure 1.7: a) Interpreted Stony Gap downstream accreting architectural element from Sandstone, WV. This valley is erosional into the Bluefield Formation and overlies an inferred third-order sequence boundary; b) Multistory, multichannel architectural elements of the Princeton Formation at the Athens turnoff from I-77, WV. Person is shown for scale. This sandstone is erosional into the Hinton Formation and overlies an inferred third-order sequence boundary.

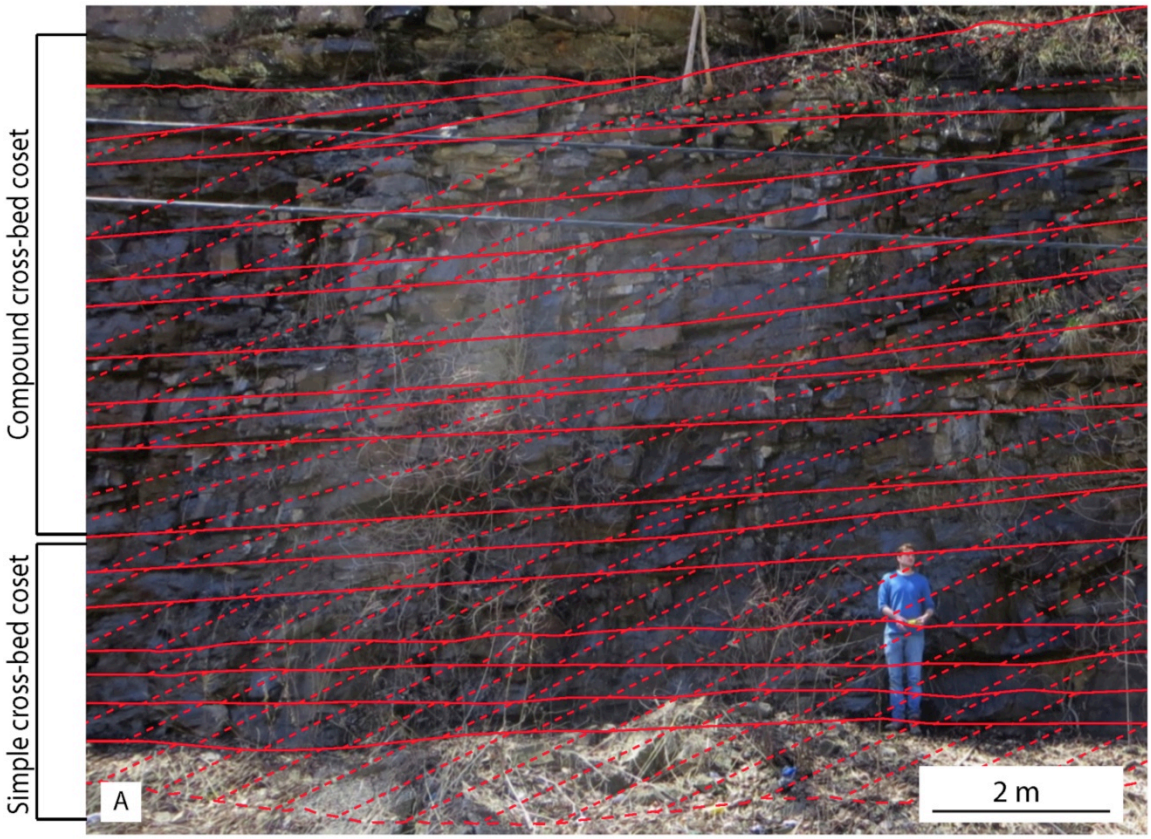
Compound cross-bed coset
Simple cross-bed coset
A
2 m


B

Figure 1.8: Ternary plots of point count data for Stony Gap, Ravencliff and Princeton sandstones (data from Kamm 1981; Pinnix, 1993; Reed *et al*., 2005).

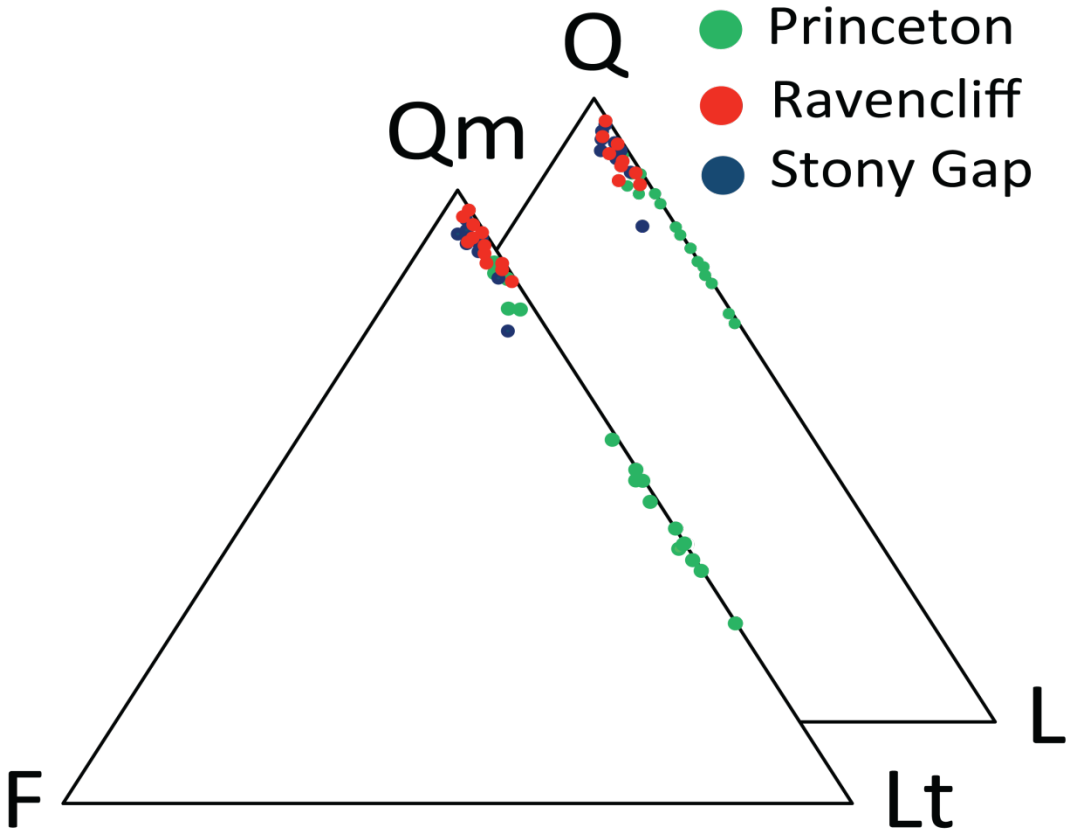
Q
Princeton
Ravencliff
Stony Gap
Qm
L
F
Lt

Figure 1.9: Photomicrographs of: a) Stony Gap fluvial quartzarenite consisting predominantly of monocrystalline quartz (field of view = 0.65 mm wide); b) Princeton fluvial sublitharenite consisting of quartz and lithic grains (field of view = 1.3 mm wide); c) Close-up image of metamorphic lithics in the Princeton fluvial sandstone (field of view = 0.65 mm wide); d) Close-up image of metamorphic lithics and kaolinitized feldspar in the Princeton fluvial sandstone (field of view = 0.65 mm wide).

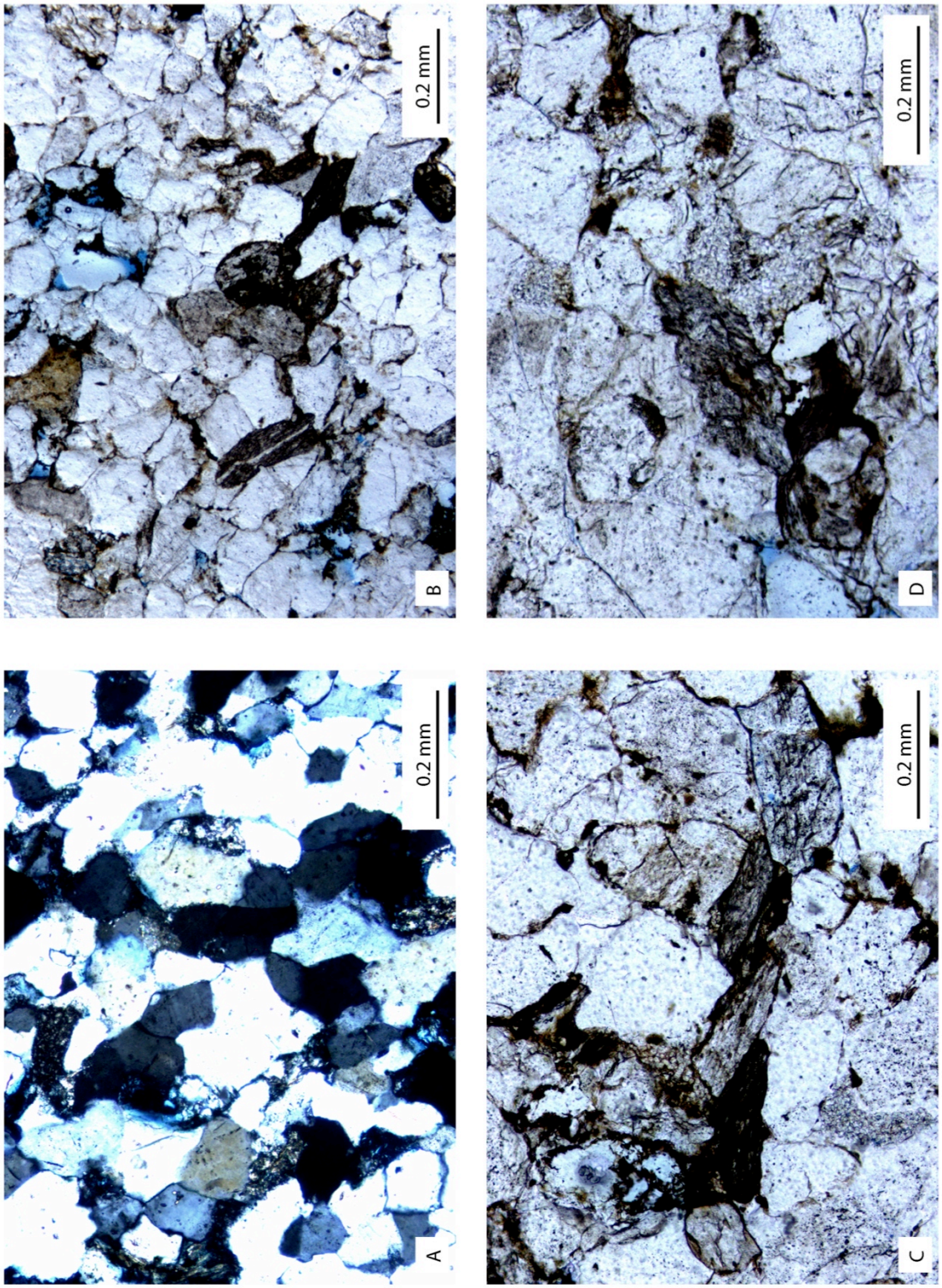
A
0.2 mm
B
0.2 mm
C
0.2 mm
D
0.2 mm

Figure 1.10: a) Tabular-planar cross-bed set from the Stony Gap Sandstone at Sandstone, WV; b) Large-scale lateral accretion architectural element from the upper Stony Gap Sandstone at Sandstone, WV; c) Conglomerate in basal Princeton Formation showing diversity of clast types. Rock hammer handle is 2.54 cm in width; d) Channel architectural element form Princeton Formation, Bluefield WV showing internal upward fining from trough cross-bedded pebbly sandstone overlain by sandstone. Person is shown for scale.


C

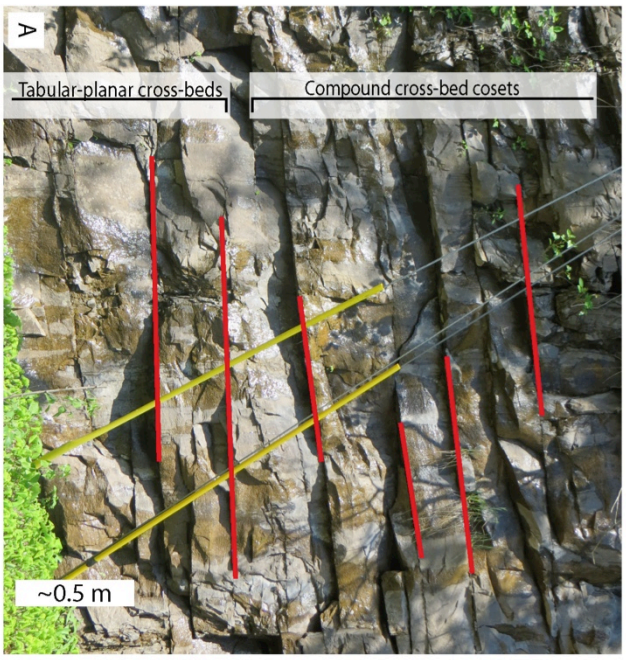
A
Tabular-planar cross-beds
Compound cross-bed cosets
~0.5 m


D


B
~5 m

Figure 1.11: Tidal creek rhythmites in estuarine deposits of the Princeton Formation. Each sandstone lamination represents a semi-diurnal deposit whereas thick-thin pairs of laminations represent the deposits of the dominant (D) and subordinate (S) tide of a single day. Diurnal laminations thicken and thin within fortnightly neap-spring cycles (Miller & Eriksson, 2000). Scale is 2.4 cm in diameter.

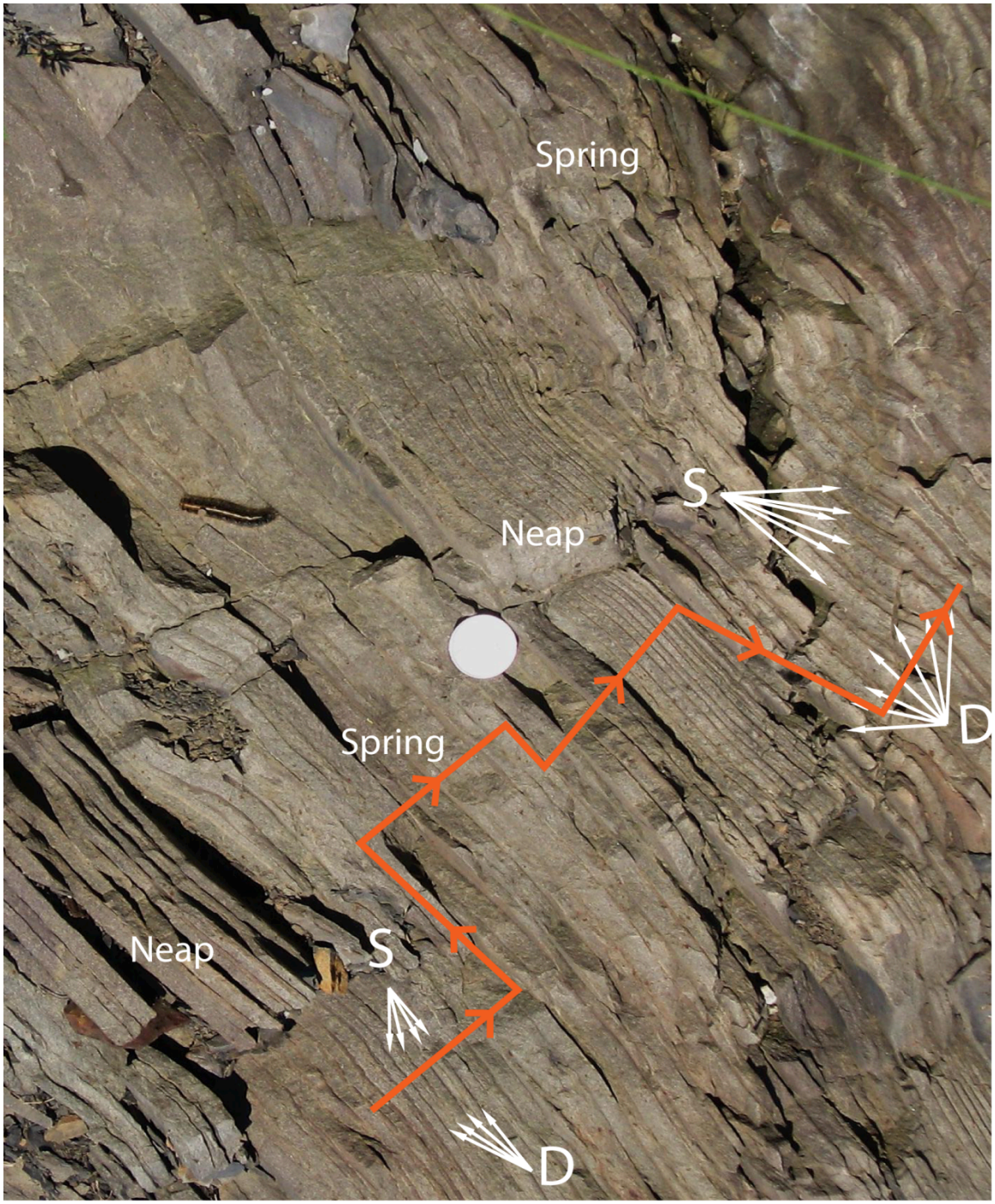
Spring
S
Neap
Spring
D
Neap
S
D

Figure 1.12: Laminae counts for the Princeton estuarine tidal rhythmites. Note the overall thickening and thinning trends indicate neap-spring cyclicity. Also apparent are thick-thin pairs of laminae representing diurnal dominant and subordinate tides.

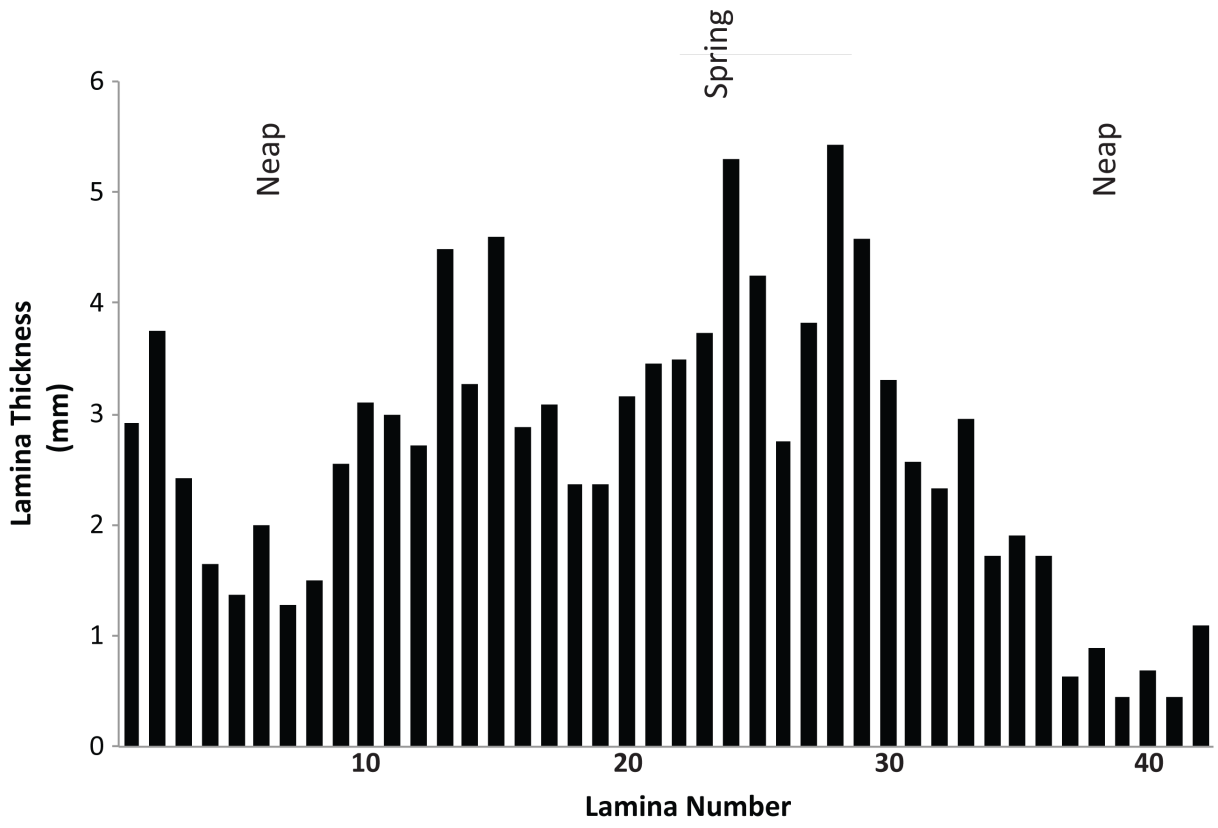
Spring
Neap
Neap
Lamina Thickness (mm)
0
1
2
3
4
5
6
10
20
30
40
Lamina Number

Figure 1.13: Incised-valley-fill model showing facies relationships within the Princeton Formation in the eastern part of the study area (adapted from Miller & Eriksson, 2000). Conglomeratic fluvial facies are overlain by estuarine sand-flat, marsh, and tidal-creek facies. Tidally influenced estuarine deposits are truncated along a regional, flat ravinement surface that is capped by a marine condensed section at the base of the Pride Shale.

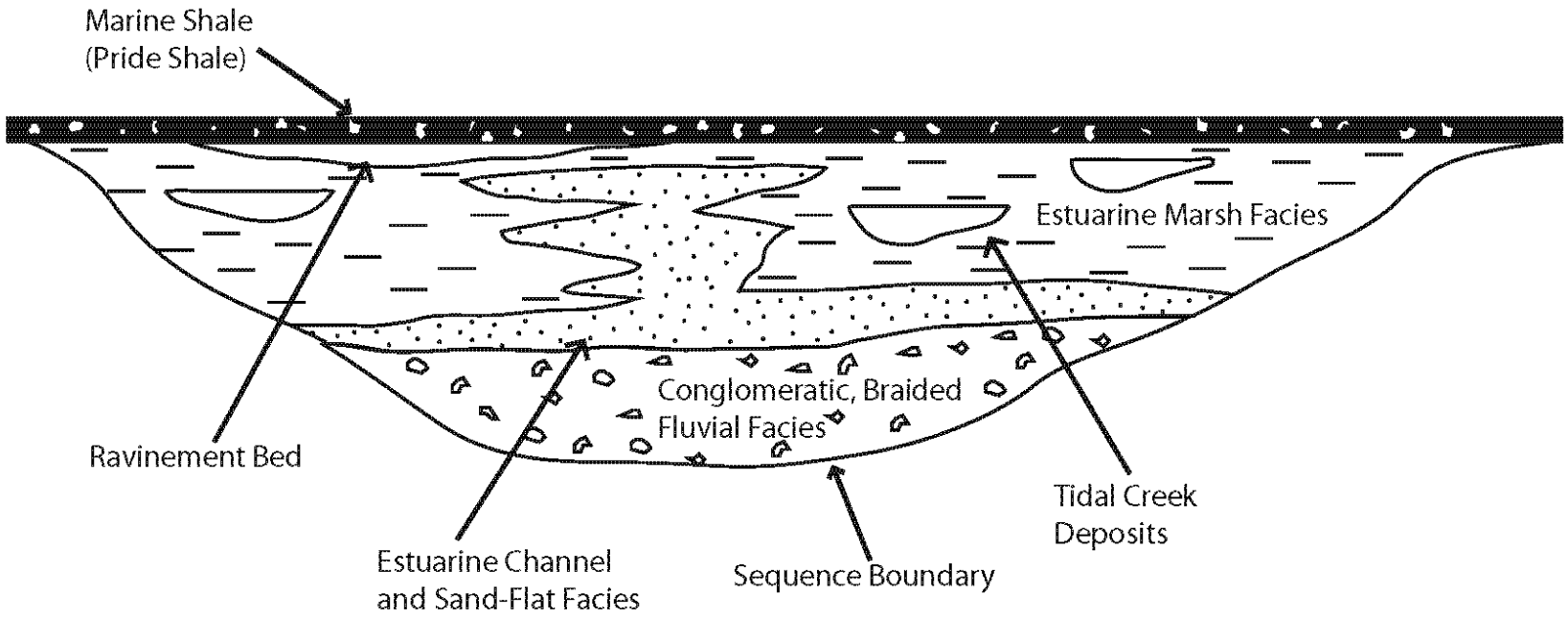
Marine Shale
(Pride Shale)
Estuarine Marsh Facies
Conglomeratic, Braided
Fluvial Facies
Ravinement Bed
Tidal Creek
Deposits
Estuarine Channel
and Sand-Flat Facies
Sequence Boundary

Figure 1.14: Detrital zircon age spectra for: a) the Stony Gap Sandstone and b) the Princeton Formation (data from Park *et al*., 2010).

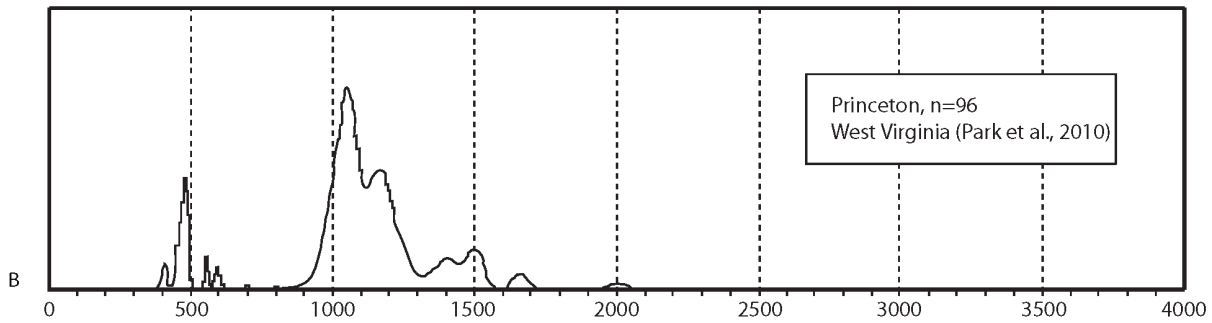
B
Princeton, n=96
West Virginia (Park et al., 2010)
0
500
1000
1500
2000
2500
3000
3500
4000

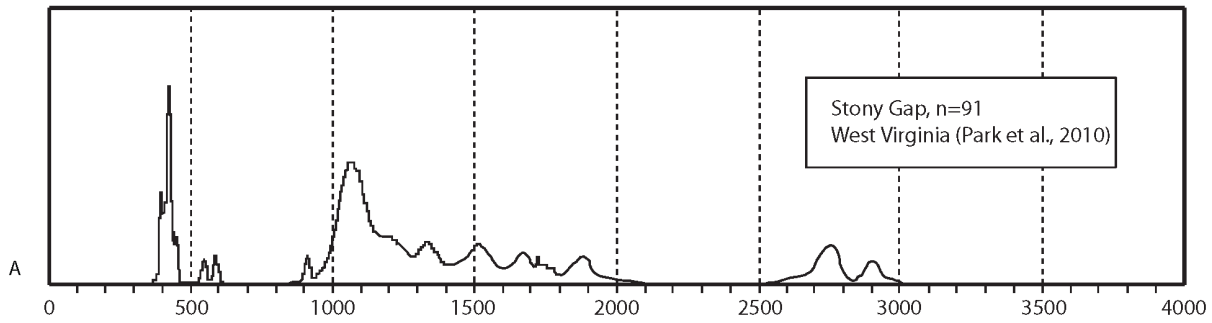
A
Stony Gap, n=91
West Virginia (Park et al., 2010)
0
500
1000
1500
2000
2500
3000
3500
4000

Figure 1.15: Width: thickness plots for incised-valley fills ranging in age from Carboniferous to Mesozoic (adapted from Gibling, 2006). Note that the Stony Gap, Ravencliff and Princeton incised valleys are plotted as stars and are consistent in scale with other Carboniferous incised-valley fills.

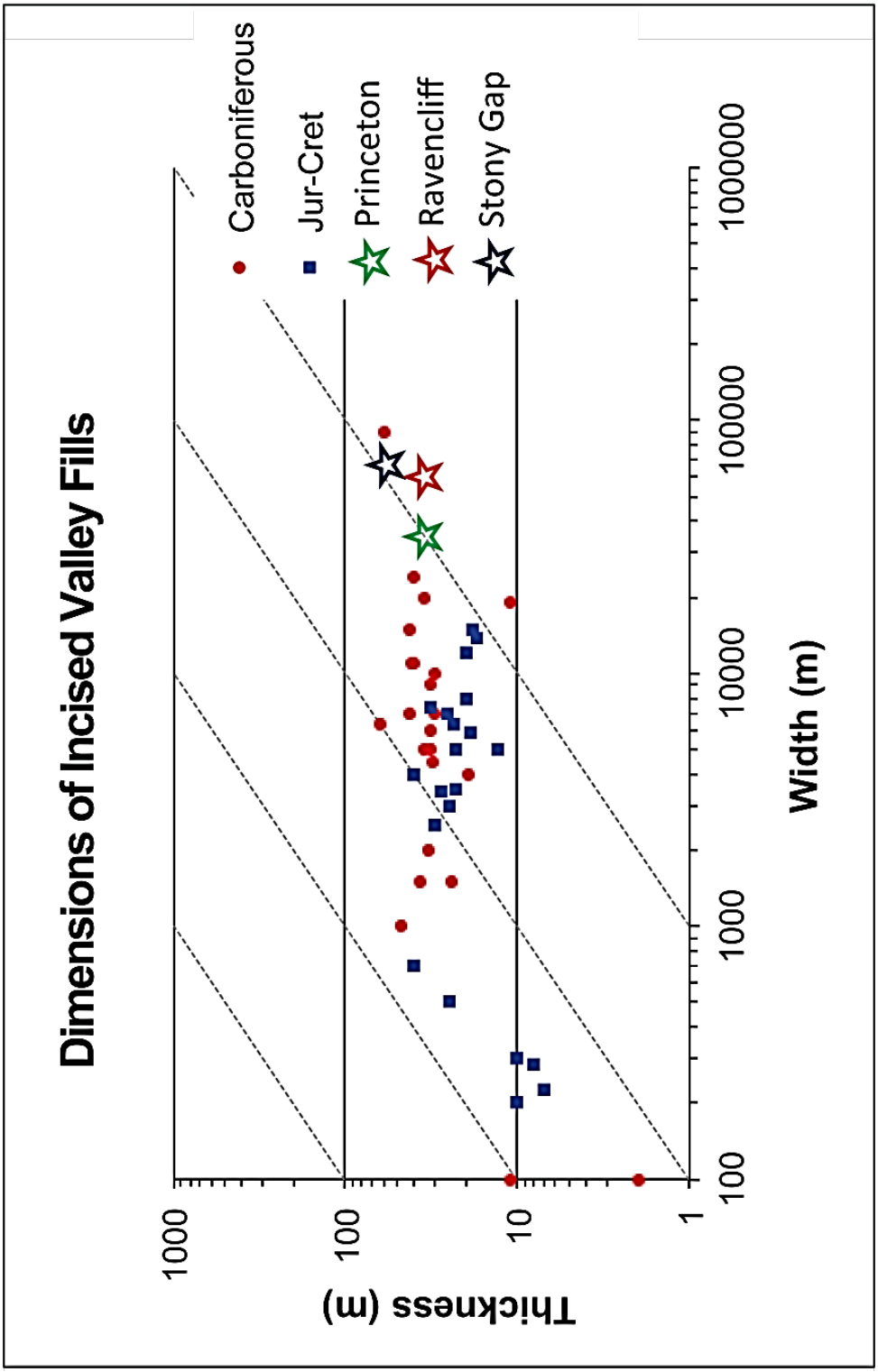
Dimensions of Incised Valley Fills
Carboniferous
Jur-Cret
Princeton
Ravencliff
Stony Gap
Thickness (m)
1000
100
10
1
Width (m)
100
1000
10000
100000
1000000

Figure 1.16: Paleogeographic reconstruction of estimated drainage basin areas systems for the Stony Gap Sandstone, Ravencliff sandstone and Princeton Formation incised-valleys superimposed on a map of North American basement provinces of Karlstrom *et al*. (2001). The estimated Stony Gap incised-valley drainage basin area (black outline) is one-half to one order-of-magnitude greater than the estimated Ravencliff (orange outline) and Princeton (blue outline) incised-valley drainage basin areas.

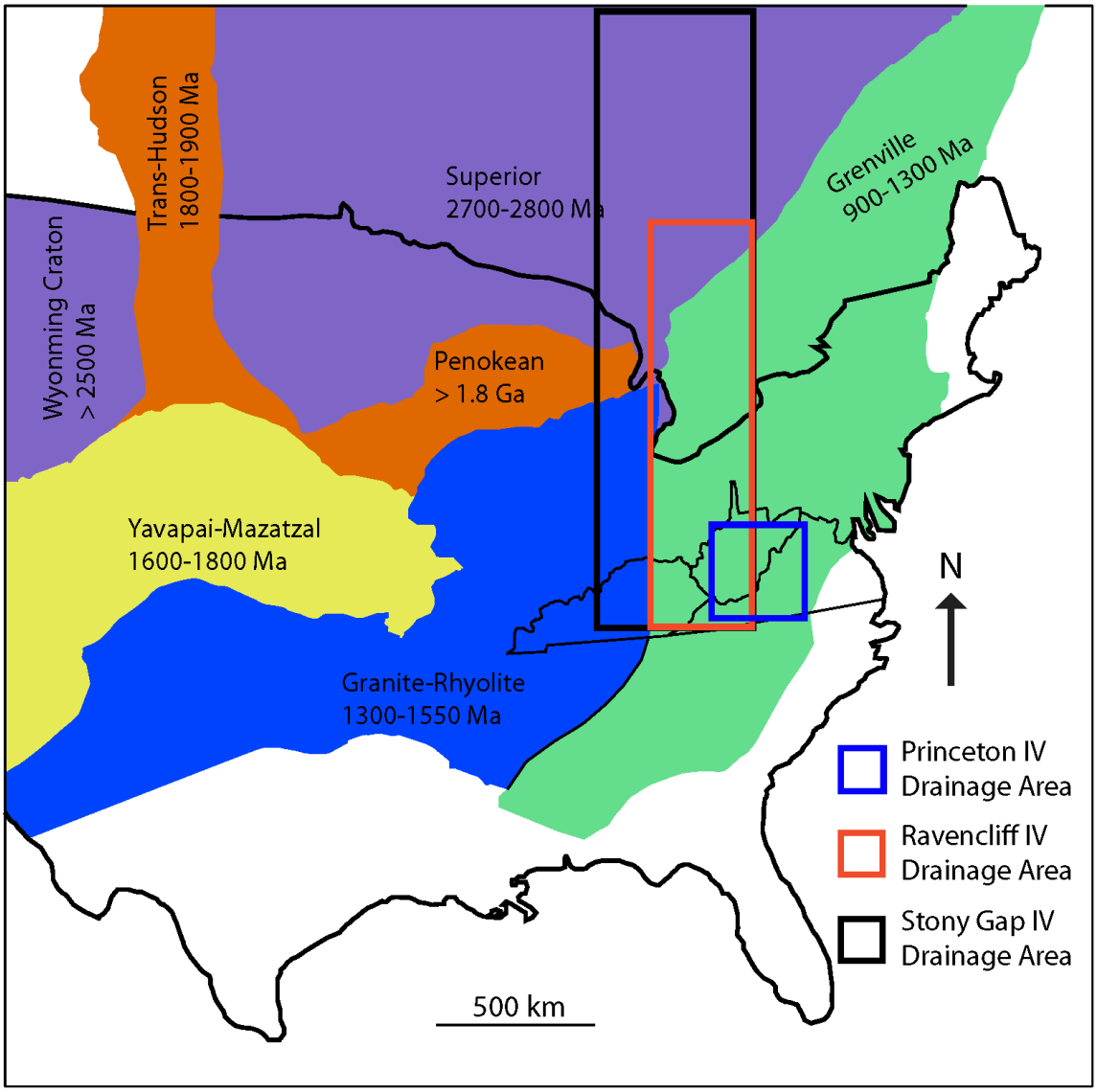
Trans-Hudson
1800-1900 Ma
Superior
2700-2800 Ma
Grenville
900-1300 Ma
Wyonming Craton
> 2500 Ma
Penokean
> 1.8 Ga
Yavapai-Mazatzal
1600-1800 Ma
Granite-Rhyolite
1300-1550 Ma
N
Princeton IV
Drainage Area
Ravencliff IV
Drainage Area
Stony Gap IV
Drainage Area
500 km

Figure 1.17: Generalized block model for co-existing, Early Pennsylvanian longitudinal and transverse fluvial systems within the foredeep of the Pocahontas Basin (adapted from Grimm *et al*., 2013).

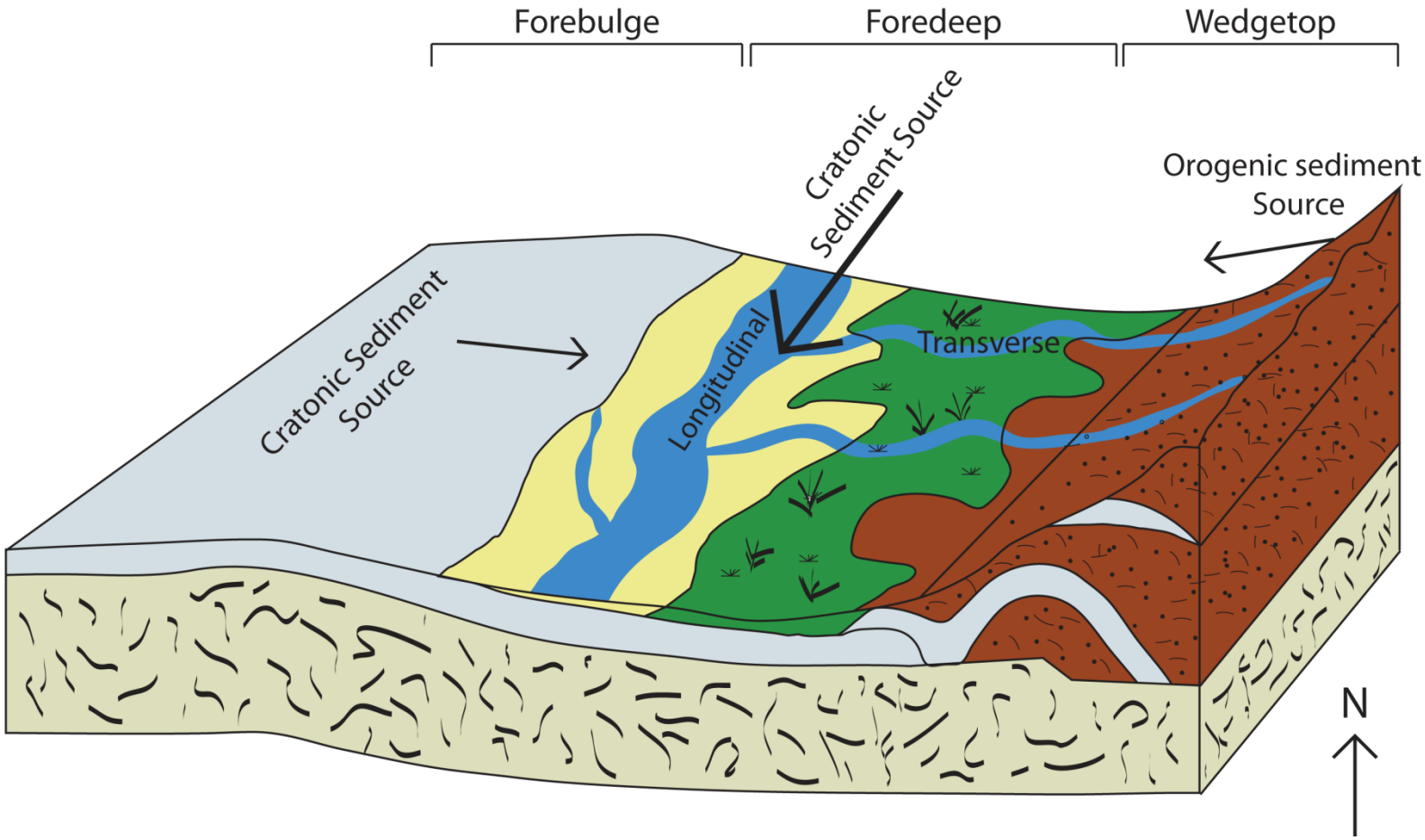
Forebulge
Foredeep
Wedgetop
Cratonic Sediment Source
Orogenic sediment Source
Cratonic Sediment Source
Longitudinal
Transverse
N

Table 1.1: Characteristics of studied incised-valleys based on identified facies in outcrop, lithology of fluvial sandstones, measurements of overall dimensions and internal architectural elements, detrital zircon ages of fluvial sandstones, and calculated estimates of bankfull depths and drainage basin area.

Attribute	Stony Gap	Ravencliff	Princeton
Facies:	Fluvial, Estuarine	Fluvial, Estuarine	Fluvial, Estuarine
Max Thickness (m):	~ 60 m	~ 40 m	~ 40 m
Max Width (km):	~ 70 km	~ 60 km	> 35 km
Lithology:	Quartzarenite	Quartzarenite	Sublitharenite
Detrital Zircon Age Populations:	Acadian and Taconic peaks (350-500 Ma), Grenvillian peaks (0.95-1.5 Ga), Yavapai-Mazatal (1.6-1.8 Ga), Archean (2.5-3.0 Ga)	N/A	Acadian and Taconic (350-500 Ma), Grenvillian (0.95-1.5 Ga)
Architectural Element Thickness (m):	7-9 m n=31	~6 m n=1	.25-3.6 m n=5
Bankfull Depth (m):	11.2 - 14.4 m	9.59 m	.40 – 5.76 m
Calculated Drainage Basin Area (km^2):	640,996 – 1,372,764 km^2	401,775 km^2	27.36 – 85,384 km^2

Chapter Two:

STABLE CARBON ISOTOPES AS PROXIES FOR ANNUAL CLIMATIC CYCLES IN THE UPPER MISSISSIPPIAN PRIDE SHALE, APPALACHIAN BASIN

Ty B. Buller

Department of Geosciences, Virginia Polytechnic Institute and State University, Blacksburg, Virginia 24061, U.S.A

ABSTRACT

The Upper Mississippian Pride Shale developed following a regional transgression and is an extensive prodeltaic deposit, which, in places, records hundreds of years of nearly continuous sedimentation. It represents the most extensive tidal rhythmite succession identified in the geologic record. The submillimeter- to meter-scale cycles in the Pride Shale record a hierarchical bundling of tidal- and climate-forced processes. Sandstone/siltstone-shale couplets between 0.01 and 1 mm thick are interpreted as suspension fallout deposits related to semi-diurnal, ebb-tidal flows associated with the dominant tide of the day. Rare thick-thin pairs record diurnal dominant and subordinate tides. Up to 17 couplets display a progressive upward thickening and thinning in 0.1 to 3 cm thick neap-spring (semimonthly) tidal cycles. Successive neap-spring cycles are thicker and thinner, and are interpreted to reflect unequal perigean and apogean tides. Up to 18 neap-spring cycles are arranged in upward thickening and thinning bundles that range from 2 to 50 cm thick and reflect annual cyclicity. Annual cyclicity is interpreted to reflect climatic (seasonal) driven cycles related to monsoonal and intermonsoonal periods. Thicker, coarser-grained neap-spring cycles are interpreted to reflect the monsoonal season and thinner, finer-grained cycles record the intermonsoonal period. Previously recognized and recently mapped, concave-up discontinuities in laterally extensive

(100s of meters) outcrops along Interstate 77 at Camp Creek, West Virginia are interpreted as slump scar features related to over steepening of the depositional interface. Uncompacted thicknesses of annual cycles indicate that accumulation rates for the Pride Shale typically ranged between 3 and 20 cm per year, but reached over 60 cm per year where sandy rhythmites developed as marginal infills of slump scars. Total organic carbon (TOC %) values are higher within intermonsoonal and lower within monsoonal components of annual cycles reflecting, respectively, lesser and greater dilution by terrestrial flux. Stable isotope data ($\delta^{13}C$) reveal a strong marine signal at the base and a prominent terrestrial signal through the remainder of the Pride Shale. Ongoing research aims to investigate whether stable isotope variations can be used as a proxy for annual cyclicity.

1. Introduction

Tidal cycles in both modern and ancient sedimentary systems have been well documented (e.g. Kuecher *et al*., 1990; Kvale & Archer, 1991; Archer *et a*l., 1994; Chan *et al*., 1994; Miller & Eriksson, 1997; Greb & Archer, 1998). Preserved within flat-laminated, fine-grained sediments, tidal cycles preserved as tidal rhythmites have been examined in with a variety of intents such as investigating ancient Earth-Moon dynamics encoded within ancient tidal deposits (Archer, 1991; Kvale, 2006), reconstructing paleoenvironments (Miller & Eriksson, 1997) and inferring past sedimentation rates (Archer, 1991*;* Frouin *et al*., 2006). Previous studies have invoked a number of different methods including sedimentologic and stratigraphic analysis (Hovikski *et al*., 2005; Miller & Eriksson, 1997), as well as numerical modeling (Wells *et al.,* 2007).

One of the previously studied rhythmite successions is the Upper Mississippian Pride Shale in the Appalachian basin of southern West Virginia, which preserves a unique record of hundreds of years of nearly continuous prodeltaic sedimentation (Miller & Eriksson, 1997). Detailed thin-section to outcrop-scale analysis indicated that the Pride Shale preserves a hierarchy of tidally- and climatically-forced periodicities. One of these periodicities is interpreted to reflect annual (seasonal), climatic cyclicity defining the portion of the paleoyear when fluvial discharge was elevated during times of increased precipitation due to the annual monsoon (Miller & Eriksson, 1997). Tidal currents and surface waves play an important role in sedimentation in tide-dominated systems (Harris *et al.,* 1993), but seasonal variation in discharge may also play an important role.

The annual monsoon occurs when the land is hot relative to the cooler ocean; low air pressure over the land results in precipitation on land. During this time sediment flux to the basin is enhanced due to an increase in terrestrial runoff (Rudiman, 2001). The large landmass present during the late Mississippian may have allowed for a heightened monsoonal signal resulting in increased precipitation and detrital runoff during the monsoonal season, and more biogenic sedimentation for the rest of the year (Larkins, 2009). Previous carbon isotope studies on modern sediments revealed that $\delta^{13}C$ values of marine organic matter typically range from -22‰ to -18‰ (Peters *et al*., 1978; Wada *et al.,* 1987; Middelburg & Nieuwenhuize, 1998). The $\delta^{13}C$ value of fluvial organic carbon depends of vegetation, climate, and riverine primary productivity and falls roughly between -24.0‰ and -28‰ (Raymond & Bauer, 2001; Lamb *et al.*, 2006).

In this study, we discuss the stable carbon isotope analysis and total organic carbon content of Pride Shale's annual cycles with intent to further strengthen the interpretation that observed decimeter-scale bundles represent annual cycles driven by the seasonal monsoon when fluvial discharge was heightened allowing for increased detrital sediment to be supplied to the subaqueous delta. Stable carbon isotope analysis from samples of the Pride Shale will reveal if annual cyclicity can be confirmed based on carbon isotopes; variations in carbon isotope ratios may reflect different fluxes of sedimentation correlating to monsoonal versus intermonsoonal periods. Monsoonal conditions are predicted to be represented by thicker, coarser-grained, bundles depleted in $\delta^{13}C$ resulting from more terrestrial-derived detritus mixed with marine-derived sediment. Intermonsoonal conditions are predicted to be represented by thinner, finer-grained bundles with elevated $\delta^{13}C$ values resulting from weakened terrestrial input due to decreased precipitation and thus a higher proportion of marine derived organic carbon. Total organic carbon (TOC %) values are predicted to be higher within intermonsoonal and lower within monsoonal components of annual cycles reflecting, respectively, lesser and greater dilution by terrestrial flux. Stable carbon isotope data will also give insight to the Prides Shale's potential as a shale gas based upon its total organic carbon values (TOC %) which, if promising, could spur further analysis.

2. General Geologic Setting

The Upper Mississippian Pride Shale outcrops in a northeast-southwest trending foreland trough along the east margin of the Appalachian Basin, and extends southwest into the subsurface of West Virginia, Virginia, Kentucky, and Tennessee (Fig. 2.1). Covering approximately 15,000 km^2 and averaging 60 m in thickness throughout the basin (Englund &

Thomas, 1990) the Pride Shale may possess potential as a shale gas play. The Pride Shale is the basal member of the Upper Mississippian Bluestone Formation. In West Virginia the Bluestone Formation is the uppermost formation of the Mauch Chunk Group and in adjacent parts of southwest Virginia, eastern Kentucky and northeast Tennessee is the upper member of the Pennington Group (Fig. 2.2). Chesterian in age, Mauch Chunk strata represent approximately seven million years of deposition of a thick (up to 1000 m), predominantly siliciclastic wedge sourced from the Alleghanian fold-and-thrust belt to the east along the eastern margin of the Appalachian Basin. Sediments of the Mauch Chunk Group were deposited in a number of terrestrial and shallow marine settings (Englund & Thomas, 1990). Accommodation was created through subsidence due to thrust loading in the central basin (Ettensohn, 1994; Rice & Schwietering, 1998). Mauch Chunk/Pennington strata thin westward and are truncated by the Mississippian-Pennsylvanian unconformity (Fig. 2.3; Miller & Eriksson, 1997).

Based on both outcrop and subsurface studies, the Mauch Chunk Group has been subdivided into three, third-order composite sequences of ca. 3 Myr duration that consist of fourth-order sequences of ca. 400 k.y. duration (Miller & Eriksson, 2000). In West Virginia the Princeton Formation, Pride Shale and Glady Fork Sandstone comprise one unconformity-bounded, fourth-order depositional sequence. Incised-valley fill deposits of the Princeton Formation define lowstand and transgressive systems tracts and the Pride Shale and Glady Fork Sandstone define the highstand systems tract (Fig. 2.4; Miller & Eriksson, 2000).

2.1 Princeton Formation

Trending southwest to-northeast, the Princeton paleovalley dispersed sediment southwest towards open-marine settings in the Black Warrior Basin (Miller & Eriksson, 2000). The base of the Princeton Formation defines a third-order, as well as, a fourth-order sequence boundary. The Princeton Formation is ~60 feet thick in its type area in Mercer County, West Virginia (Henry & Gordon, 1992). Typifying the lower Princeton Formation are braided-fluvial multistory channel sandstones and conglomerates eroding into older Hinton Formation strata (Fig. 2.5). Carbonaceous mudstones with a well-developed coal define the top of the Hinton Formation (Miller & Eriksson, 2000). Clasts within conglomerate facies consist of rounded quartz pebbles, shale, sandstone, limestone, metamorphic lithics, and nodules of caliche and siderite. Conglomerates and nested channels are interpreted to mark initial fluvial aggradation within the incised-valley related to a base level rise (Miller & Eriksson, 2000).

Upper Princeton Formation facies in West Virginia include laterally variable packages of tabular sandstones, heterolithic channel-fills, and dark mudstones with siderite concretions marking a transgressive shift from tidal-estuarine to deeper-water sedimentation (Miller & Eriksson, 2000). Tabular sandstone bodies outcropping in Mercer County, WV display crude bundling of mm-thick laminae or cm-thick bedding interpreted to be tidal-estuarine sand-flat deposits. Adjacent to sand-flat deposits are 1-2 m thick, tidal channel/creek-fill deposits within dark mudstones and displays cyclic rhythmites. Tidal rhythmites of the Princeton Formation estuarine deposits are characterized by systematic thickness variations of millimeter-to-centimeter-scale sandstone/mudstone couplets that represent fortnightly, neap-spring cycles. Also apparent are thick-thin pairs of laminae representing the deposits of diurnal dominant and subordinate tides. These cyclic rhythmites record a spectrum of tidal periodicities including

sand-mud semi-diurnal couplets, diurnal thick-thin pairs, semi-monthly neap-spring cycles, and anomalistic monthly perigee-apogee cyclicity (Miller & Eriksson, 2000). Neap-spring (semimonthly) cycles display progressive thinning and thickening of semi-diurnal couplets in which thicker couplets record spring tide deposition when the earth, moon, and sun were aligned (syzygy) and thinner couplets record neap tide deposition. Laminae bundling counts show that neap-spring cycles consist of fewer than 15 sand-mud couplets that were deposited during unequal semidiurnal tidal flows recording only the strongest ebb tidal flows (Miller & Eriksson, 2000). Some of these tidal rhythmites preserve an uninterrupted short -term (<0.5 yr) record of deposition that in some places can be resolved into individual flood and ebb tidal flows (cf. Archer *et al*., 1994).

The Princeton Formation-Pride Shale contact (Fig. 2.6) is commonly recognized as a thin (<1m) fossiliferous and conglomeratic bed containing quartz pebbles, marine bivalves, gastropods, and brachiopods. This surface is prominent across much of the study area and is interpreted as a lag surface that developed during tidal ravinement via scouring (sensu Dalrymple, 1992) as the Princeton estuary was transgressed (Miller and Eriksson, 1997).

2.2 Pride Shale

The base of the Pride Shale is marked by a few-meter-thick, fissile black shale containing carbonate concretions and is characterized in geophysical well logs by high gamma ray values (Fig 2.4). This high gamma ray signature is interpreted in both outcrop and subsurface as a condensed section that defines the maximum flooding surface (Miller & Eriksson, 2000). This condensed section deposit contains carbonate concretions bearing marine invertebrate

(foraminifera and bivalves) and vertebrate (fish) fossils (Weems & Winddolph, 1986). The remainder and bulk of the upward-coarsening Pride Shale (Fig. 2.7) consists of rhythmically interlaminated dark shales and fine-grained sandstones that record a hierarchy of tidal periodicities ranging in thicknesses from submillimeter- to meter-scale (Miller & Eriksson, 1997). In West Virginia the Pride Shale grades upwards into the Glady Fork Member, a wavy-bedded, fine-grained sandstone (Larkins, 2009) representing delta front/distributary bar deposits (Miller & Eriksson, 2000).

Other than small vertical-escape structures in sandy intervals and circular features that are in-filled with fine grained sand and interpreted to be horizontal feeding burrows (Larkins, 2009), laminae of the Pride Shale show minimal disruption from bioturbation (Miller & Eriksson, 2000). Plant fossils (*Stigmaria stellate*) and bivalves (*Sanguinolites, Modiolus sp.*) are locally present, as well as shrimp-like arthropods preserved as delicate carbonized impressions towards the top of the Pride Shale (Miller & Eriksson, 1997). The near absence of bioturbation suggests a paleoenvironment with frequent salinity fluctuations and/or anoxic conditions that deterred benthic fauna (Miller & Eriksson, 1997). A semi-arid, monsoonal climate that would have promoted fluctuating salinities is suggested by the presence of paleo-vertisols in the underlying Hinton and overlying red beds of the Bluestone formation (Cecil & Englund, 1989) and in age-equivalent strata in Tennessee (Caudill *et al*., 1996).

Previous researchers have suggested a range of depositional environments for the Pride Shale, including a low-energy tidal environment (Cecil & Englund, 1989), a shallow-marine lagoonal or estuarine environment (Miller, 1974), and a deltaic environment (Englund &

Thomas, 1990). Based on stratigraphic and grain size relationships, the Pride Shale is interpreted as a highstand, prodeltaic deposit of a prograding tide-dominated delta with the basal condensed section resting upon the fluvial to tidal deposits of the Princeton Formation. Bedding in the Pride Shale is inclined at a few degrees steeper than regional dip and is interpreted to represent prograding clinoforms toward the southwest (Miller & Eriksson, 2000). This interpretation is consistent with the general upward-coarsening of the Pride Shale into Glady Fork Member facies (Miller & Eriksson, 1997). Recording a hierarchy of tidal periodicities with unrivaled preservation, the Pride Shale likely records the most extensive tidal rhythmite succession identified thus far in the geologic record.

2.3 Discontinuity Surfaces in the Pride Shale

Large, concave-up discontinuities are present within the laterally extensive outcrops along Interstate 77 at Camp Creek, West Virginia (Figures 2.8 and 2.9). In general, the discontinuity surfaces dip southwest and reveal several meters of relief (Fig. 2.10a). Discontinuities commonly separate finer-grained rhythmites from overlying sand-dominated rhythmites (Miller & Eriksson, 1997). Where subhorizontal, the disconformities appear conformable with underlying beds. Meter-scale rotated blocks are present locally along discontinuities (Fig. 2.10b). Infills above surfaces lack a sandy or conglomeratic basal lag yet drape the rotated blocks. Rhythmite infills predominate and are coarsest along the trough shoulders and pinch out into finer-grained beds within the troughs. Sand-dominated neap-spring cycles thin from 50 cm at the discontinuity surface to less than 1 cm over a distance of

several-to-tens of meters. These sandy intervals are commonly restricted to one side of the trough, and are clearly progradational towards the trough axes (Miller & Eriksson, 1997).

Interpretations of the discontinuities include slump and channel scouring origins, but neither interpretation adequately explains the irregular geometry and sedimentary fill. Similar discontinuity-bounded sedimentary packages in slope carbonates of the Sverdrup Basin were interpreted by Davies (1977) as the infills of large slump scars. A slump scar interpretation explains the features associated with the trough-like discontinuities in the Pride Shale, and provides an autogenic explanation for the inconstancy in accumulation rate recorded by rhythmites (Miller & Eriksson, 2000). This interpretation invokes gravity sliding of thick (up to 15 meters) of semi-coherent sediment packages basinward. Blocks derived from the scar-margins or from the trailing edge settled within the scar interior to later undergo rapid rhythmite fill via tidal currents. Rhythmites draped the blocks and filled the scar. Sandier rhythmites reflect proximity to the source, where sands cannibalized from the underlying sediments were confined to an area of high current velocities along the topographically high scar margins. The irregular and asymmetrical distribution of sands along scar margins likely represents local erosion/ deposition via tidal currents oblique to the slump direction (Miller & Eriksson, 1997).

3. Cyclicity in the Pride Shale

The Pride Shale preserves a hierarchy of submillimeter-to decimeter-scale cycles that record an array of tidal and climatic periodicities (Fig. 2.11; Miller & Eriksson, 1997). Five orders of cyclicity are observable in outcrop and in thin section. Tidally forced cyclicity in the Pride

Shale includes: semidiurnal and diurnal cycles, neap-spring (semi-monthly) cycles, monthly perigee-apogee cycles, and multiyear cycles. Annual cyclicity is also observed, but is interpreted to reflect seasonal, climatic forcing. All levels of cyclicity can be recognized in thin section (semidiurnal and diurnal) and in well-preserved outcrops (neap-spring, annual and multiyear); multiyear cyclicity also is apparent in subsurface gamma-ray and bulk density logs (Miller & Eriksson, 2000).

Sandstone-shale or siltstone-shale couplets ranging from 0.01 and 1 mm thick are interpreted as deposits from individual ebb tidal flows that reworked sediment of the prodeltaic environment (Figs. 2.12a and b). Each microlaminated couplet is interpreted as the product of suspension fallout, where silt/sand was deposited during peak tidal flows and clay during the slackwater period. Up to 17 of the microlaminated couplets define neap-spring cycles are systematically bundled into thickening and thinning couplets ranging from 0.1-3 cm thick (Figs. 2.12a and b). Thickets couplets were deposited by spring tides (Earth, Sun, and Moon alignment) and make up the semimonthly cycles. The abbreviated nature of the neap-spring cycles reflects the distal setting of deposition where the subordinate daily and weakest ebb flows were too weak to transport sediment.

Up to 18 neap-spring cycles are arranged in an upward thickening and thinning centimeter-to decimeter-scale bundles ranging 2-50 cm thick reflecting annual cyclicity (Fig. 2.12c). Each decimeter-scale annual bundle consists of 6-13 relatively well-developed neap-spring cycles that are bounded by or interspersed with several thin, finer-grained neap-spring cycles. Annual cyclicity is easily recognized in outcrop from its distinctive rib and furrow like

weathering profile. More resistant ribs are composed of sand-dominated neap-spring cycles, where less resistant furrows are finer grained (Miller & Eriksson, 1997). Unlike tidally forced cycles, annual cyclicity is interpreted to reflect climatic (seasonal) driven cycles relating to monsoonal and intermonsoonal climates. During monsoonal conditions, the terrestrial realm is hot relative to the cooler ocean; low pressure over the land results in precipitation on land, causing increased fluvial discharge able to carry coarser sediments to the basin. The thicker, coarser neap-spring cycles are interpreted to reflect the monsoonal season, and thinner cycles recording the intermonsoon when sediment supply was diminished. The best preserved annual cycles can be observed in Spanishburg, WV (Figs. 2.12a and b). While still visible on I-77 outcrops, the Spanishburg outcrop records more distal deeper water sedimentation. Being further basinward, sediments are subjected to less frequent bottom water currents and bioturbation allowing for great preservation. Thus, it can be concluded that more distal prodeltaic sub-environments should preserve a more pristine record of annual cyclicity.

Larkins (2009) conducted a study on a boulder from Spanishburg, WV and a slabbed succession of Pride Shale from along I-77 Camp Creek outcrop, Mercer County, WV using X-ray fluorescence scanning (XRF), Evolutive Harmonic analysis and Ti, Ca/Ti and Si/Ti proxies, to demonstrate that the Pride Shale preserves multiple paleoenvironmental signals (detrital, biogenic, and authigenic). Analysis revealed a dominant cycle with a period of approximately 27 mm. The 27 mm cycle recorded elevated detrital Ti values in dark, coarse-grained Pride Shale laminations suggested periods of increased precipitation producing greater terrigenous sediment flux, and greater Si/Ti values in lighter, fine-grained laminations suggested periods of

seasonally increased biogenic silica productivity when sedimentation rates were low (Larkins, 2009).

A weakly developed, multiyear cyclicity is recognized in outcrop by differential weathering, and progressive thickening and thinning of 17-21 annual beds within meter-scale bundles (Fig. 2.12d). This multiyear cyclicity with an average of 19 years of deposition is interpreted to reflect tidal amplitude modulation at the lunar nodal period, presently at 18.6 yr. duration (Miller & Eriksson, 1997). Nodal cycles relate to the slow rotation of the Moon's nodes such that the inclination of the lunar orbital plane varies between 18° and 28° from the Earth's equator. This shift in the attitude of the lunar orbital plane is known to weakly modulate tidal systems and can have a significant effect on sediment transport capacity in tidal environments (Wood, 1986; Oost *et al*., 1993)

4. Methods (C-isotopes and TOC)

Samples for carbon isotopic analysis, and TOC contents were collected from exposures of Pride Shale from a large roadcut along Interstate 77, immediately northwest of Exit 20 at Camp Creek, West Virginia. Sampling location was determined by ease of monsoonal and intermonsoonal bundle recognition. This exposure of Pride Shale, in sections, weathers out to form a rib and furrow profile reflecting decimeter thick annual cycles. The rib and furrow profile allows for best possible sampling of individual intermonsoonal and monsoonal periods. Using a rock hammer and chisel, twenty-three hand sample sized samples were excavated from outcrop. Ten samples are interpreted to correspond to the intermonsoonal season and the

other ten of the annual monsoonal season. Samples were excavated from a continuous interval of annual rhythmites interpreted to record ten years of prodeltaic sedimentation.

All twenty-three samples were ground into a fine powder using a handheld dremel tool. Approximately 0.1 grams of powder was derived from each sample. Powders were then decarbonated by acidification with 2N hydrochloric acid for approximately 48 hours. The solutions were neutralized by repeated rinsing of the sample with 18.2 mΩ deionized water and siphoning out the supernatant after centrifugation. Upon neutralization, samples were dried in an oven for approximately 72 hours at 32°C. Samples were subsequently homogenized to a powder using an agate mortar and pestle, and then their masses were recorded.

Carbon isotopic analysis was performed with a Vario ISOTOPE Cube elemental analyzer connected to an Isoprime 100 isotope ratio mass spectrometer. Results are expressed in the conventional delta notation (δ):

$$\delta^{13}C = (R_{sample}/R_{standard} - 1) \times 1000$$

where *"R"* represents the ^{13}C / ^{12}C ratio of the sample and VPDB or the Vienna Pee Dee Belemnite standard. Samples where calibrated to the VPBD scale using the International Atomic Energy Agency IAEA-CH-6 and IAEA-CH-7 standards as well as commercial standards. Percent total organic carbon and nitrogen was then calculated using percent carbon generated from the Vario ISOTOPE Cube elemental analyzer software. Replicate analysis of standards indicated a precision of ± < 0.1‰.

5. Analytical Results

$\delta^{13}C$ and TOC data are presented in Table 2.1. Samples interpreted to represent periods of monsoonal deposition have an average $\delta^{13}C$ value of -22.794‰ and an average TOC% of 1% whereas inferred intermonsoonal samples have an average $\delta^{13}C$ value of -23.025‰ and an average TOC% of 1.3% (Figs. 2.13 a and b). TOC% values for monsoonal and intermonsoonal deposits fluctuate between 0.8 to 1.3% and 1.0 to 1.7% (Fig. 2.13 a). Samples from the basal condensed section of the Pride Shale (PR-1, PR-4 and PR-4-2) have $\delta^{13}C$ values that range from 22.76‰ to 28.22 ‰ and TOC% values that range from 1.0 - 2.3% (Table 2.1). TOC% concentrations in both intermonsoonal and monsoonal deposits display a systematic decrease upwards within the sampled interval (Fig. 2.13a). Overall, $\delta^{13}C$ values for intermonsoonal and monsoonal deposits display a slight increasing trend within the sampled interval (Fig 2.13b). For all samples, a negative correlation between $\delta^{13}C$ and TOC% is observed (Fig 2.13c).

6. Discussion

Numerous studies have noted a positive correlation between TOC weight percentages and terrestrial flux (Stein, 1990; Ricken, 1996; Hansell & Peltzer, 1998; Kim *et al*., 2000; Yu *et al*., 2012). Stein (1990) noted that this correlation does not exist in settings of characterized by extremely high sedimentations rates (e.g. Mississippian fan where sedimentation rates reach more than 1,000 cm/ 1,000 yr. (Bouma & Coleman, 1985) where, rather, a negative correlation exists. Ibach (1982) observed that highest TOC weight percentages in black shales are associated with sedimentation rates of less than 41 m/m.y. Lower TOC weight percentages are associated with sedimentation rates greater than 41 m/m.y., which Ibach (1982) attributed to dilution by clastic material. Similarly, Ricken (1996) observed lower concentrations of organic

carbon within rhythmically bedded deposits associated with high sediment yields and, conversely, elevated concentrations of organic carbon associated with low sediment yields.

TOC variations within the Pride Shale support the findings of Ibach (1982) and Ricken (1996). Highest TOC contents in the basal condensed section (sample PR1) are consistent with lowest sedimentation rates associated with maximum flooding (cf. Creaney & Passey, 1993). Within annual cycles, higher TOC values are associated with deposits of the intermonsoon at which times sedimentation rates are inferred to have been lowest resulting in higher concentration of organic carbon. In contrast, lowest values are associated with deposits of the monsoon at which times sedimentation rates are considered to have been highest resulting in dilution of organic carbon. The systematic decrease in TOC values for both monsoonal and intermonsoonal deposits within the ten year-long sampled interval (Fig. 2.13a) is attributed to progradation of the Pride delta that resulted in an increase in terrestrial sources and thus siliciclastic dilution through time.

The highly depleted $\delta^{13}C$ value of sample PR-1 for the Pride Shale in the study area (Fig. 2.13b) records a marine signature, which is consistent with maximum flooding.Other samples have $\delta^{13}C$ values more consistent with a mixed terrestrial-marine signature which is explored with reference to a previous study on the Pride Shale from Pound Gap, KY which report similar $\delta^{13}C$ and TOC values to those in this study (2.13b; Kahmann-Robinson, 2008). Samples from Pound Gap have average $\delta^{13}C$ values of -22.94‰ and average TOC% of 1.197% (Kahmann-Robinson, 2008). In her thesis, Kahmann-Robinson (2008) plotted $\delta^{13}C$ vs C/N and concluded that organic carbon was derived from both from both terrestrial C3 land plants and marine

algae. Kahmann-Robinson (2008) also noted a steady increase in C/N ratios up section, which were interpreted to be the product of nitrogen-bearing compounds degrading at higher rates than pure carbon compounds. Degradation resulted in elevated %C vs %N skewing $\delta^{13}C$ vs. C/N ratios toward C3 land plant organic carbon source values. Factoring in the interpreted skewed $\delta^{13}C$ vs. C/N values, Kahmann-Robinson (2008) concluded that organic carbon sources for the Pride Shale were derived from marine algae.

The Pride Shale in WV represents a more proximal deltaic setting than at Pound Gap and yet the $\delta^{13}C$ values, except for sample PR-1, are similar at both localities. On a cross plot of $\delta^{13}C$ vs. TOC% (Fig. 2.13c), samples from the present study show considerably more scatter than samples from Pound Gap. This scatter is interpreted to be related to fluctuations in terrestrial runoff in the more proximal deltaic setting in WV. The more distal deltaic setting at Pound Gap will have been less susceptible to fluctuations of terrestrial runoff and records a more consistent flux of organic carbon derived from terrestrial and marine sources as exhibited by the clustering of $\delta^{13}C$ vs. TOC% values (Fig. 2.13c).

The greater variation in $\delta^{13}C$ vs. TOC% and the systematic variation in TOC% in decimeter-scale cycles in the Pride Shale from Camp Creek, WV (Figs. 13a, c) are consistent with the interpretation that decimeter-scale cycles record a climatic (monsoonal) signal. Systematic TOC% variations support the observations of Larkins (2009). The lower concentration of organic carbon in annual cycles associated with monsoonal conditions corresponds to the elevated Ti signal interpreted by Larkins (2009) to be the product of enhanced terrestrial runoff and sedimentation resulting in the dilution of organic carbon. Greater Si/Ti values in finer-grained

intervals and interpreted by Larkins (2009) to be the product of increased silica productivity when sedimentation rates were lower, correlate to higher TOC values within annual cycles associated with deposits of the intermonsoon.

7. Conclusions

• Systematic variations in TOC% in decimeter-scale cycles in the Pride Shale in WV record an annual climatic signal associated with the seasonal monsoon.

• Higher TOC values are associated with deposits of the intermonsoon at which times sedimentation rates are inferred to have been lowest resulting in higher concentration of organic carbon.

• Lower values are associated with deposits of the monsoon at which times sedimentation rates are considered to have been highest resulting in dilution of organic carbon.

• $\delta^{13}C$ vs. TOC % values of annual cycles recorded in intermonsoonal and monsoonal deposits suggest that organic matter was derived from both marine and terrestrial sources.

• Highest TOC contents and $\delta^{13}C$ values in the basal condensed section (sample PR1) are consistent with lowest sedimentation rates associated with maximum flooding consistent with the sequence stratigraphic interpretation of the Pride Shale.

The interpreted ten-year succession of annual cycles sampled in this study represents only a short increment of time but reveal interesting differences in TOC in particular. These preliminary results call for a detailed study of the entire Pride Shale that may give insight to large- scale climate trends and, specifically, whether the intensity of the annual monsoon was

affected by the northward latitudinal drift of the Appalachian Basin out of the paleomonsoonal belt.

8. References

ARCHER, A.W. (1991) Modeling of tidal rhythmites using modern tidal periodicities and implications for short-term sedimentation rates. Kansas Geological Survey Bulletin, 233 185-194.

ARCHER, A.W., HOWARD, R., FELDMAN, E.P. KVALE & LANIER, W.P. (1994) Comparison of drier-to wetter-interval estuarine roof facies in the Eastern and Western Interior coal basins, USA. Palaeogeography, Palaeoclimatology, Palaeoecology, 106, 171-185.

BOUMA, A. H., & COLEMAN, J. M. (1985) Mississippi Fan: Leg 96 program and principal results. In: Submarine fans and related turbidite systems. Springer New York, 247-252.

CAUDILL, M.R., DRIESE, S.G., & MORA, C.I. (1996) Preservation of a paleo-vertisol and an estimate of Late Mississippian paleoprecipitation. Journal of Sedimentary Research, 66, 58-70.

CECIL, C.B., & ENGLUND, K.J., (1989) Origin of coal deposits and associated rocks in the Carboniferous of the Appalachian basin. In: Carboniferous Geology of the Eastern United States (Eds. by C.B. Cecil and C. Eble), 28th International Geological Congress, Field Trip Guidebook, 143, 84-88.

CHAN, M.A., KVALE. E.P, ARCHER, A.W. & SONETT. C.P. (1994) Oldest direct evidence of lunar-solar tidal forcing encoded in sedimentary rhythmites, Proterozoic Big Cottonwood Formation, central Utah. Geology 22, 791-794.

CREANEY, S. & PASSEY, Q. R. (1993) Recurring patterns of total organic carbon and source rock quality within a sequence stratigraphic framework. AAPG Bulletin, 77, 386-401.

DALRYMPLE, R.W. (1992) Tidal depositional systems. In:Facies Models, Response to Sea Level Change (Eds. by R. Walker, and N. James), Geological Association of Canada, 195-218.

DAVIES, G.R. (1977) Turbidites, debris sheets, and truncation structures in upper Paleozoic deep-water carbonates of the Sverdrup basin, Arctic Archipelago. In: Deep Water Carbonate Environments (Eds. by H. Cook and P. Enos), Society of Economic Paleontologists and Mineralogists, Special Publication 25, 221-247.

ENGLUND, K.J. & THOMAS, R.E. (1990) Late Paleozoic depositional trends in the Central Appalachian Basin. U.S. Geleological Survey,1839, 19.

ETTENSOHN., F.R. (1994) Tectonic control on formation and cyclicity of major Appalachian unconformities and associated stratigraphic sequences. In: Tectonic and Eustatic Controls on Sedimentary Cycles: Concepts in Sedimentology and Paleontology (Eds. by J.M. Dennison and F. R. Ettensohn), SEPM Special Publication 4, 217-242.

GREB, S. F. & ARCHER, A.W. (1998) Annual sedimentation cycles in rhythmites of Carboniferous tidal channels. In: Tidalites-Processes and Products (Eds. by R.A. Davies, C.R. Alexander and V.J. Henry), Society of Economic Paleontologists and Mineralogists, Special Publication 61, 75-83.

HANSELL, D. A., & PELTZER, E. T. (1998) Spatial and temporal variations of total organic carbon in the Arabian Sea. Deep Sea Research Part II: Topical Studies in Oceanography, *45*, 2171-2193.

HARRIS, P.T., E.K. BAKER, COLE, A.R. & SHORT, S.A. (1993) A preliminary study of sedimentation in the tidally dominated Fly River Delta, Gulf of Papua. Continental Shelf Research, 13, 441-472.

HENRY, T.W., & GORDON, M. (1992). Middle and upper Chesterian brachiopod biostratigraphy, eastern Appalachians, Virginia and West Virginia. In: Recent advances in Middle Carboniferous biostratigraphy—a symposium. Oklahoma Geological Survey Circular, 94, 1-21.

HOVIKOSKI, J., RASANEN, M., GINGRAS, M., RODDAZ, M., BRUSSET, S., HERMOZA, W., PITTMAN, L. & LERTOLA, K. (2005) Miocene semidiurnal tidal rhythmites in Madre de Dios, Peru. Geology, 33, 117-180.

IBACH, L. E. J. (1982) Relationship between sedimentation rate and total organic carbon content in ancient marine sediments. AAPG Bulletin, 66, 170-188.

Kahmann-Robinson, J. A. (2008). Late Mississippian (Chesterian) High-frequency Climate Change in the Pennington Formation at Pound Gap, KY, USA. Unpublished dissertation. University Libraries, Baylor University, Texas, Waco, 134.

KAHMANN, J.A. & DRIESE, S.G. (2008) Paleopedology and geochemistry of Late Mississippian (Chesterian) Pennington Formation paleosols at Pound Gap, Kentucky, USA: Implications for high-frequency climate variations. Palaeogeography, Palaeoclimatology, Palaeoecology, 259, 357-381.

KIM, B., CHOI, K., KIM, C., LEE, U. H., & KIM, Y. H. (2000) Effects of the summer monsoon on the distribution and loading of organic carbon in a deep reservoir, Lake Soyang, Korea. Water Research, 34, 3495-3504.

KVALE, .E P. (2006) "The origin of neap–spring tidal cycles." Marine geology 235, 5-18.

KVALE, E.P., & ARCHER, A.W. (1991) Characteristics of two, Pennsylvanian-age semidiurnal tidal deposits in the Illinois Basin, U.S.A. In: Clastic Tidal Sedimentology (Eds. by D., Smith, G. Reinson, B.A. Zaitlin, and R.A. Rahmani), Canadian Society of Petroleum Geologists, Memoir 16, 179-188.

KUECHER, G. J., WOODLAND, G. & BROADHURST, F.M. (1990) Evidence of deposition from individual tides and of tidal cycles from the Francis Creek Shale (host rock to the Mazon Creek Biota), Westphalian D (Pennsylvanian), northeastern Illinois. Sedimentary Geology 68, 211-221.

LAMB, A. L., WILSON, G. P., & LENG, M. J. (2006) A review of coastal palaeoclimate and relative sea-level reconstructions using $\delta^{13}C$ and C/N ratios in organic material. Earth-Science Reviews, 75, 29-57.

LARKINS, K. (2009) Cyclic Sedimentation in the Mississippian Pride Shale: Quantitative Geochemical Analysis of Tidal Rhythmites Using X-Ray Fluorescence Scanning and Advanced Spectral Methods. Unpublished Master's thesis.University of North Carolina at Chapel Hill Library, North Carolina, University of North Carolina, Chapel Hill, 69.

MIDDELBURG, J. J., NIEUWENHUIZE, J., & VAN BREUGEL, J. (1999) Black carbon in marine sediments. Marine Chemistry, 65, 245-252.

MILLENA, F., SEBAG, D., LAIGNEL, B., OGIER, S., VERRECCHIA, E.P & DURAND, A. (2006) Tidal rhythmites of the Marais Vernier Seine estuary, France and their implications for relative sea-level. Marine Geology, 235, 165-175.

MILLER, M.S. (1974) Stratigraphy and coal beds of upper Mississippian and lower Pennsylvanian rocks in southwestern Virginia: Virginia Division of Minerals Bulletin, 84, 211.

MILLER, D.J. & ERIKSSON, K.A. (1997) Late Mississippian prodeltaic rhythmites in the Appalachian basin: a hierarchical record of tidal and climatic periodicities. Journal of Sedimentary Research, 67, 653-660.

MILLER, D.J. & ERIKSSON, K.A. (2000) Sequence stratigraphy of Upper Mississippian strata in the central Appalachians: A record of glacioeustasy and tectonoeustasy in a foreland basin setting. AAPG Bulletin, 84, 210-233.

OOST, A.P., DE HAAS, H., IJNSEN, F., VAN DEN BOOGERT J.M. & DE BOER, P.L. (1993) The 18.6 yr nodal cycle and its impact on tidal sedimentation. Sedimentary Geology 87, 1-11.

PETERS, K. E., SWEENEY, R. E. & KAPLAN, I. R. (1978) Correlation of carbon and nitrogen stable Isotope ratios in sedimentary organic matter. Oceanography, 23, 598-604.

RAYMOND, P. A., & BAUER, J. E. (2001)Use of C14 and d13C natural abundances for evaluating riverine, estuarine, and coastal DOC and POC sources and cycling: a review and synthesis. Organic Geochemistry, 32, 469-485.

RICE, C.L. & SCHWIETERING, J.F. (1988) Fluvial deposition in the central Appalachians during the Early Pennsylvanian, Evolution of sedimentary basins - Appalachian Basin. Washington, D.C.. United States Geological Survey Bulletin 1839, B1-B10.

RICKEN, W. (1996) Bedding rhythms and cyclic sequences as documented in organic carbon-carbonate patterns, Upper Cretaceous, Western Interior, US. Sedimentary Geology, 102, 131-154.

RUDDIMAN, W. F. (2001) Earth's Climate Past and Future. New York, W.H. Freeman & Co., 33-35.

STEIN, R. (1990) Organic carbon content/sedimentation rate relationship and its paleoenvironmental significance for marine sediments. Geo-Marine Letters, 10, 37-44.

WADA, E., MINAGAWA, M., MIZUTANI, H., TSUJI, T., IMAIZUMI, R. & KARASAWA, K. (1987) Biogeochemical studies on the transport of organic matter along the Otsuchi River watershed, Japan. Estuarine Coastal and Shelf Science, 25, 321-336.

WEEMS, R.E., & WINDOLPH, J.F., JR. (1986) A new actinopterigian fish (paleonisciformes) from the upper Mississippian Bluestone Formation of West Virginia. Biological Society of Washington, Proceedings, 99, 584-601.

WELLS, J.T. & J. M. COLEMAN (1981) Periodic mudflat progradation, northeastern coast of South America; a hypothesis. Journal of Sedimentary Research, 51, 1069-1075.

WOOD, F.J. (1986) Tidal Dynamics, Coastal Flooding, and Cycles of Gravitational Force. Boston, Reidel, 558.

YU, F., ZONG, Y., LLOYD, J. M., LENG, M. J., SWITZER, A. D., YIM, W. W., & HUANG, G. (2012) Mid-Holocene variability of the East Asian monsoon based on bulk organic δ13C and C/N records from the Pearl River estuary, southern China. The Holocene, 22, 705-715.

Figure 2.1: Map showing the regional mapped extent of the Pride Shale and the study area in southern West Virginia and southwestern Virginia. The Pride Shale crops out in the eastern part of the study area (gray shading) and is particularly well exposed in the central part of Mercer County, WV. Preserved in the NE-SW-oriented foreland trough (dashed lines), the Pride Shale extends from southern West Virginia to northeastern Tennessee and eastern Kentucky.

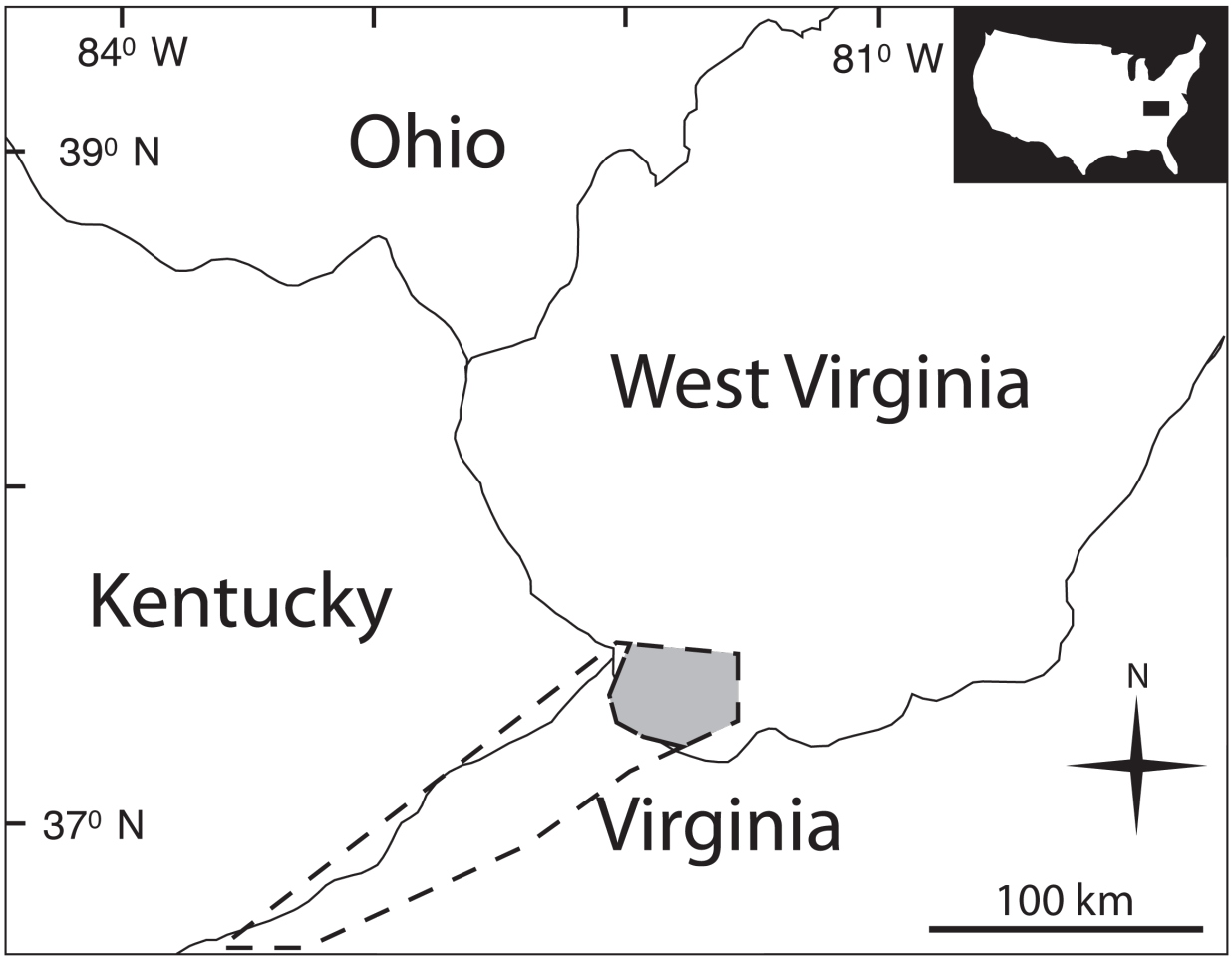
84⁰ W
81⁰ W
39⁰ N
37⁰ N
Ohio
West Virginia
Kentucky
Virginia
N
100 km

Figure 2.2: Stratigraphic column of the Mauch Chunk Group. Heavy black lines demarcate third-order sequence boundaries; blue highlights are third-order maximum flood deposits and green defines the Pride Shale.

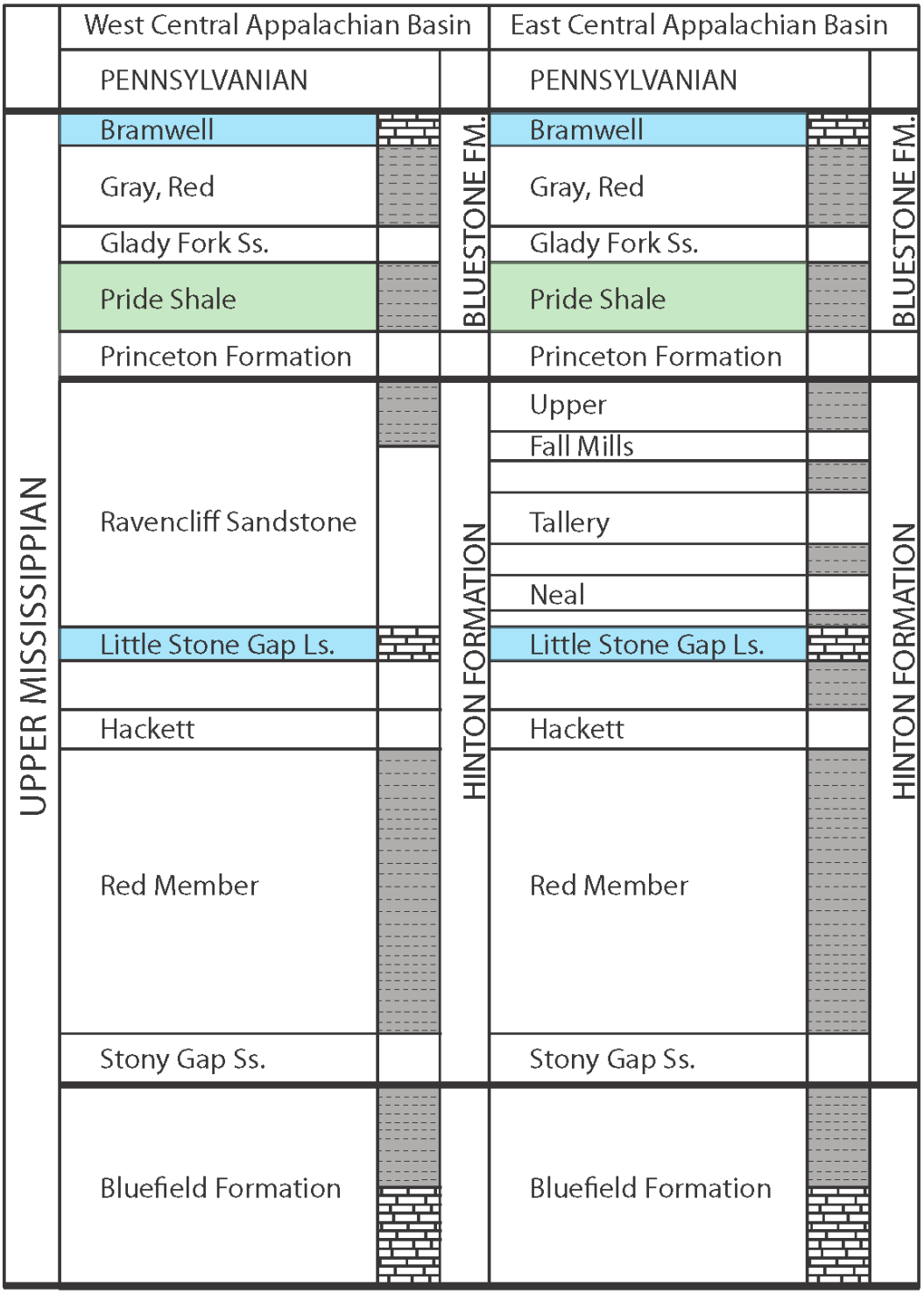
West Central Appalachian Basin
East Central Appalachian Basin
PENNSYLVANIAN
PENNSYLVANIAN
UPPER MISSISSIPPIAN
Bramwell
Gray, Red
Glady Fork Ss.
Pride Shale
Princeton Formation
Ravencliff Sandstone
Little Stone Gap Ls.
Hackett
Red Member
Stony Gap Ss.
Bluefield Formation
BLUESTONE FM.
HINTON FORMATION
Upper
Fall Mills
Tallery
Neal

Figure 2.3: Regional NW-trending, gamma-ray log cross-section showing regional thinning of Mauch Chunk strata in southwestern Virginia. The Pride Shale is a distinctive stratigraphic unit-both in the subsurface and 100 km northeast where exposed in outcrop in southern West Virginia. Basal Pennsylvanian sandstone (erosional unconformity) is used as a datum.

NORTHWEST
A
SOUTHEAST
A'
DI-50504
DI-1633
DI-1313
DI-1535
DI-1540
218-v-530117
RU-0413
RU-0379
PENNSYLVANIAN
MISSISSIPPIAN
MAUCH CHUNK GROUP
Bluestone
Pride Shale
Princeton
Hinton
Bluefield
Greenbrier
100 m
1000 ft
5 km
5 Miles
West Virginia
Kentucky
Virginia
A
A'
Buchanan
Tazewell
Dickenson
Russell
Wise
Scott
Lee
N
55 km

Figure 2.4: Stratigraphic section of the Princeton Formation, Pride Shale, and Glady Fork Sandstone from central Mercer County, WV. The Pride Shale rests upon estuarine facies of the Princeton Formation incised valley-fill, and is overlain by the Glady Fork Sandstone (adapted from Miller & Eriksson, 1997).

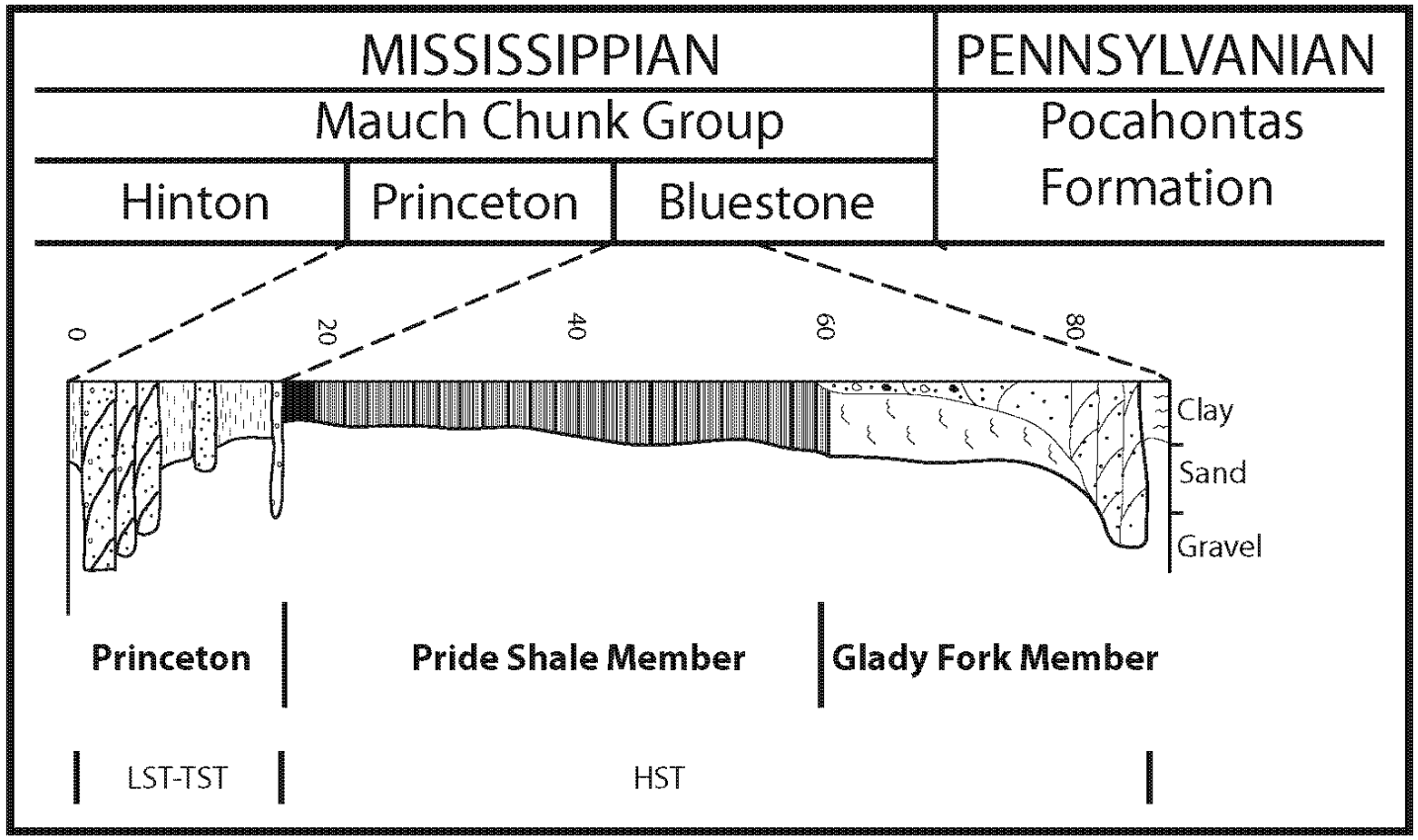
MISSISSIPPIAN
PENNSYLVANIAN
Mauch Chunk Group
Pocahontas Formation
Hinton
Princeton
Bluestone
0
20
40
60
80
Clay
Sand
Gravel
Princeton
Pride Shale Member
Glady Fork Member
LST-TST
HST

Figure 2.5: Multistory, channel architectural elements of the Princeton Formation at the Athens turnoff from I-77, WV. Person is shown for scale. This sandstone is erosional into the Hinton Formation and overlies an inferred third-order sequence boundary.

Figure 2.6: Photomosaic of condensed section at the base of the Pride Shale overlying estuarine facies of the Princeton Formation at Camp Creek, WV.

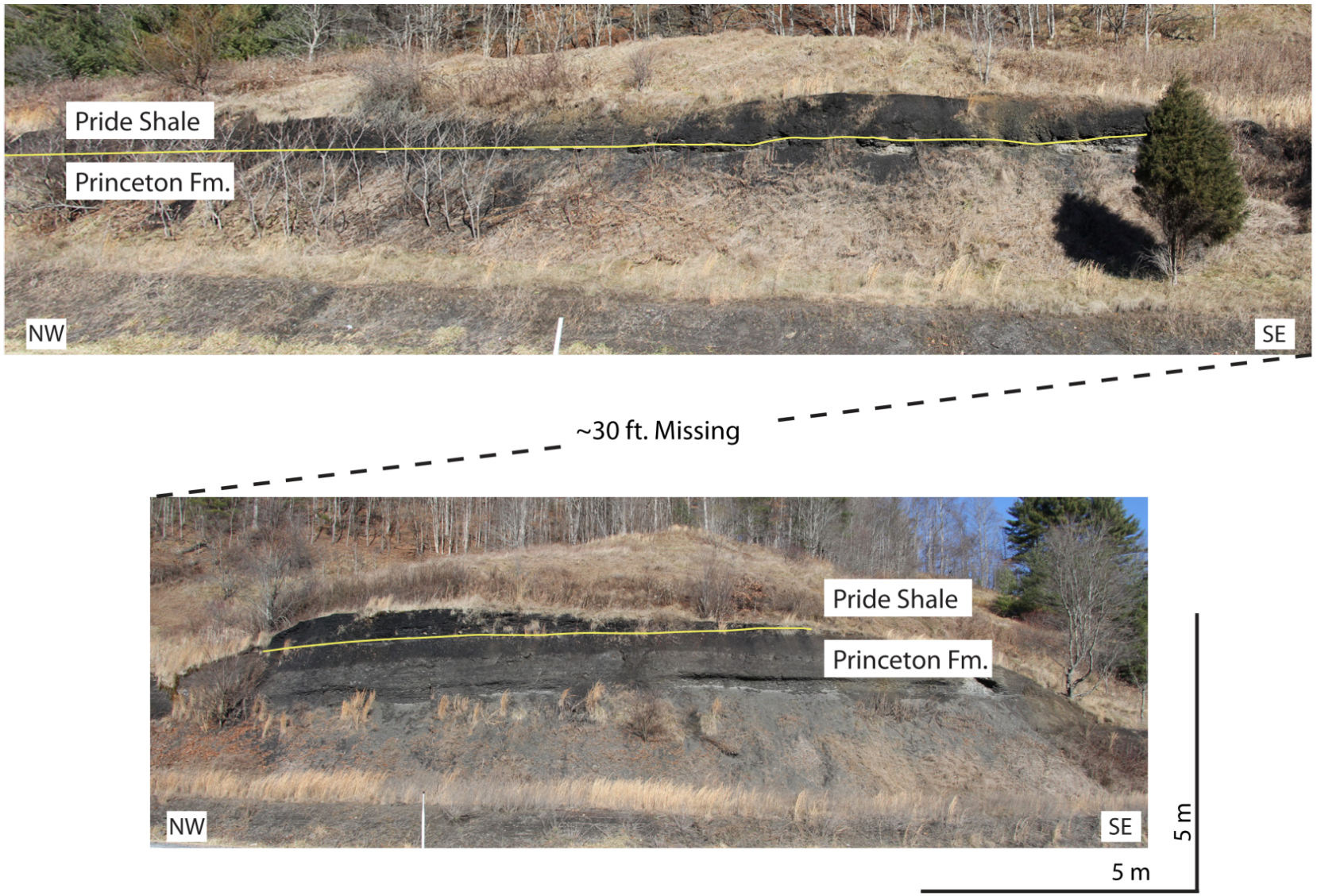
Pride Shale
Princeton Fm.
NW
SE
~30 ft. Missing
Pride Shale
Princeton Fm.
NW
SE
5 m
5 m

Figure 2.7: Upward increase in thickness of annual cycles related to an increase in proportion of sand at Camp Creek, WV (scale shown is 2 m).

Increasing Sand Content
LEFT LANE
NO TRUCKS
½ MI
2 m

Figure 2.8: Photomosaic of Pride Shale and overlying Glady Fork Sandstone at the eastern road cut near Camp Creek, WV (vertical exaggeration 2:1). Discontinuities are annotated in red and are interpreted as slump scars produced by basinward-sliding of semi-coherent packages of strata.

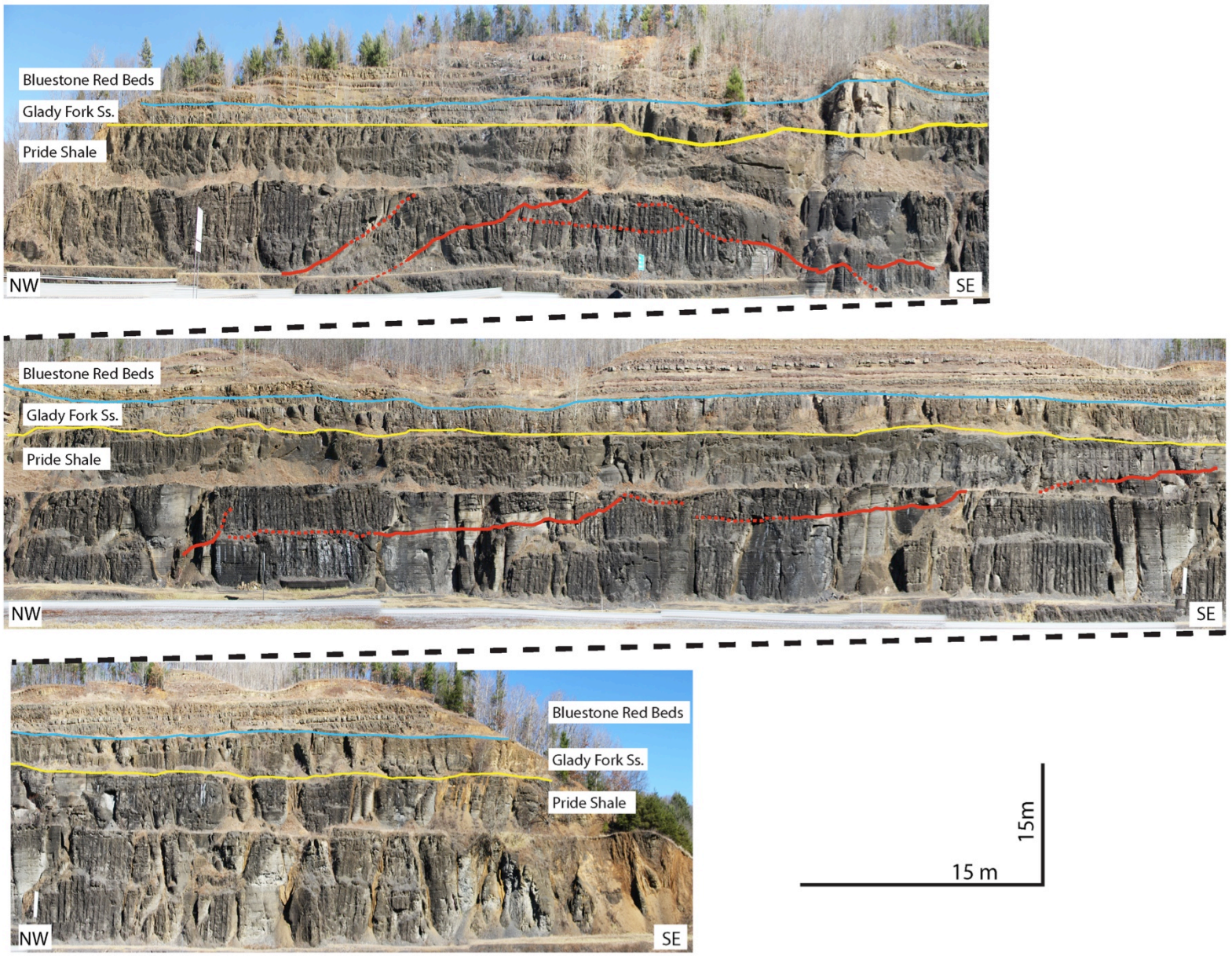
Bluestone Red Beds
Glady Fork Ss.
Pride Shale
NW
SE
Bluestone Red Beds
Glady Fork Ss.
Pride Shale
NW
SE
Bluestone Red Beds
Glady Fork Ss.
Pride Shale
NW
SE
15m
15 m

Figure 2.9: Photomosaic of Pride Shale and overlying Glady Fork Sandstone at the western road cut near Camp Creek, WV (vertical exaggeration 2:1). One major discontinuity is preserved and is projected to extend below road level. Rotated blocks are developed along the discontinuity.

30 m
SE
30 m
Bluestone Red Beds
Glady Fork Ss.
Pride Shale
NW

Figure 2.10: a) Discontinuity preserved at Camp Creek, WV outcrop. Person is shown for scale; b) Rotated block along discontinuity (scale is 20 cm long).

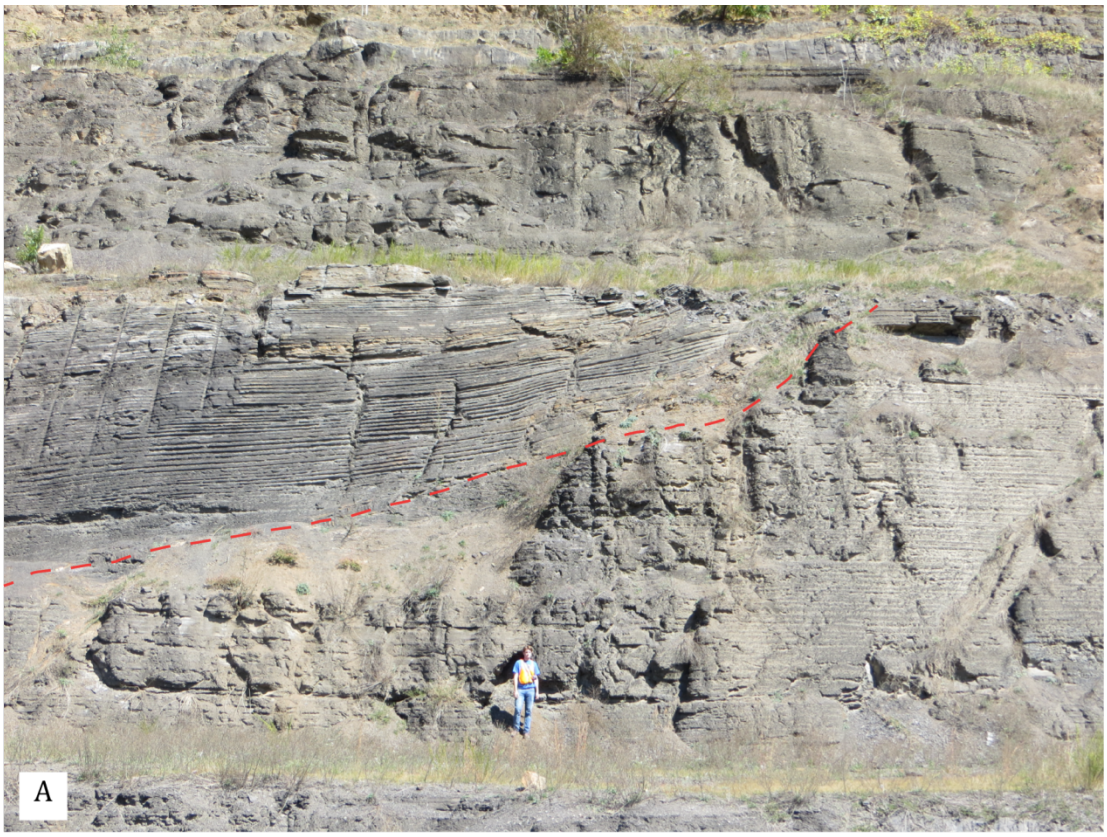
A


B

Figure 2.11: Hierarchy of tidal cycles in the Pride Shale. Five orders of laminae bundling are interpreted to reflect tidal and climatic controls on prodeltaic sedimentation (adapted from Miller & Eriksson 1997).

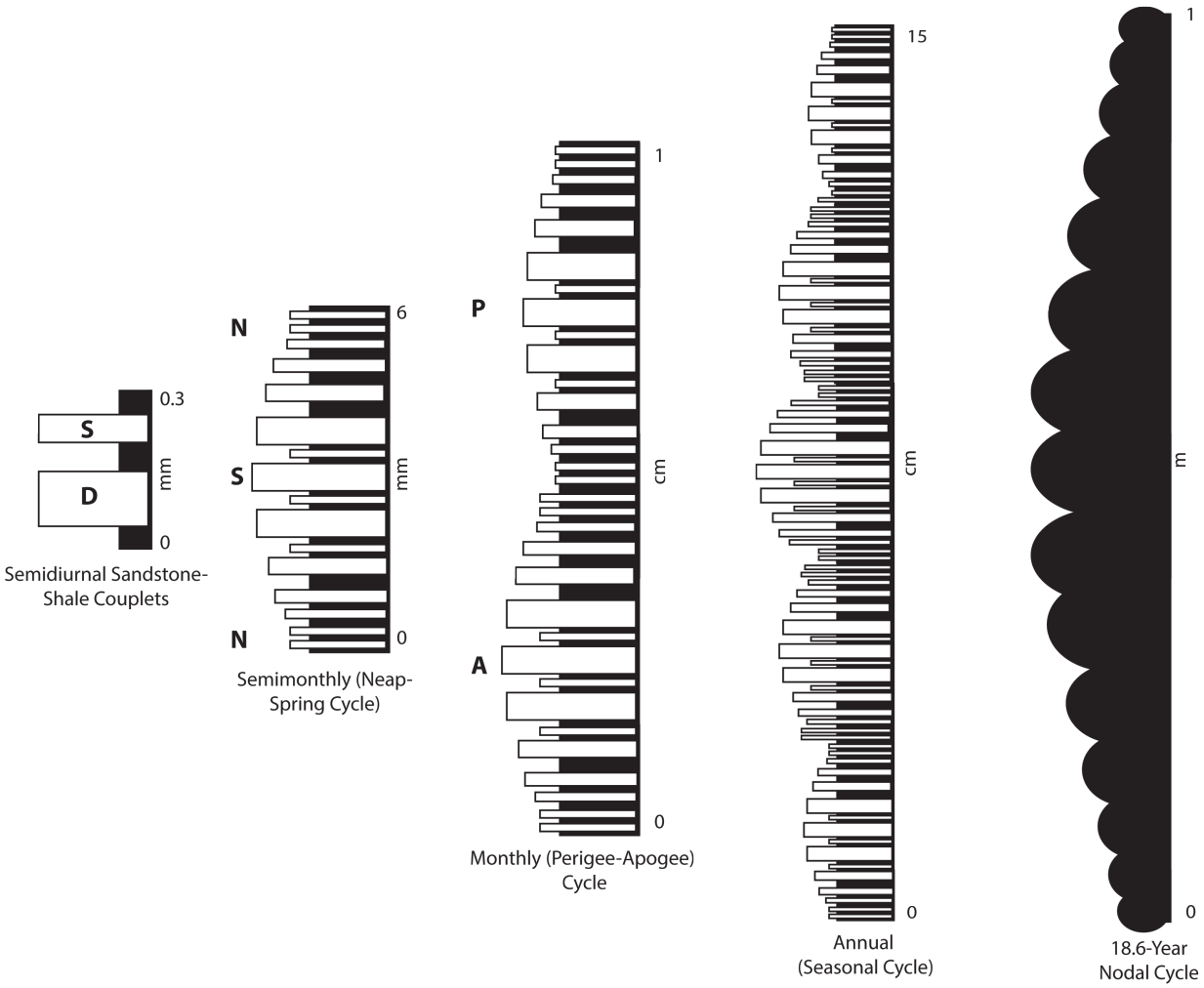
S
D
0.3
mm
0
Semidiurnal Sandstone-Shale Couplets
N
S
N
6
mm
0
Semimonthly (Neap-Spring Cycle)
P
A
1
cm
0
Monthly (Perigee-Apogee) Cycle
15
cm
0
Annual (Seasonal Cycle)
1
m
0
18.6-Year Nodal Cycle

Figure 2.12: a) Photomicrograph of dominant semi-diurnal sandstone-siltstone/shale couplets with one example of a thick-thin diurnal pair representing the dominant and subordinate tides of the day; b) Photomicrograph of microlaminated, neap-spring-neap cycles from Spanishburg, WV outcrop. Cycles typically consist of 15 or fewer distinct sandstone-siltstone/shale couplets. Each sandstone-siltstone lamination represents a semidiurnal deposit of the dominant tide of each day. Rarely preserved are the deposits of the subordinate tide of the day. Annual cycles consist of systematic thickening and thinning of between 11 and 18 neap-spring-neap cycles; c) Decimeter-scale annual cycles at Camp Creek, WV. Each furrow-rib-furrow contains up to 18 neap-spring-neap cycles. Annual cycles reflect climatic changes in which thicker, coarser laminae record seasonal monsoonal conditions when fluvial input was enhanced because of increased terrestrial runoff and thinner, finer-grained laminae record intermonsoonal conditions when sediment flux was less (scale is 20 cm long); d) Decimeter-scale multiyear cycles from Spanishburg, WV interpreted by Miller & Eriksson (1997) to represent 18.6 year nodal cycles (scale is 100 cm long).

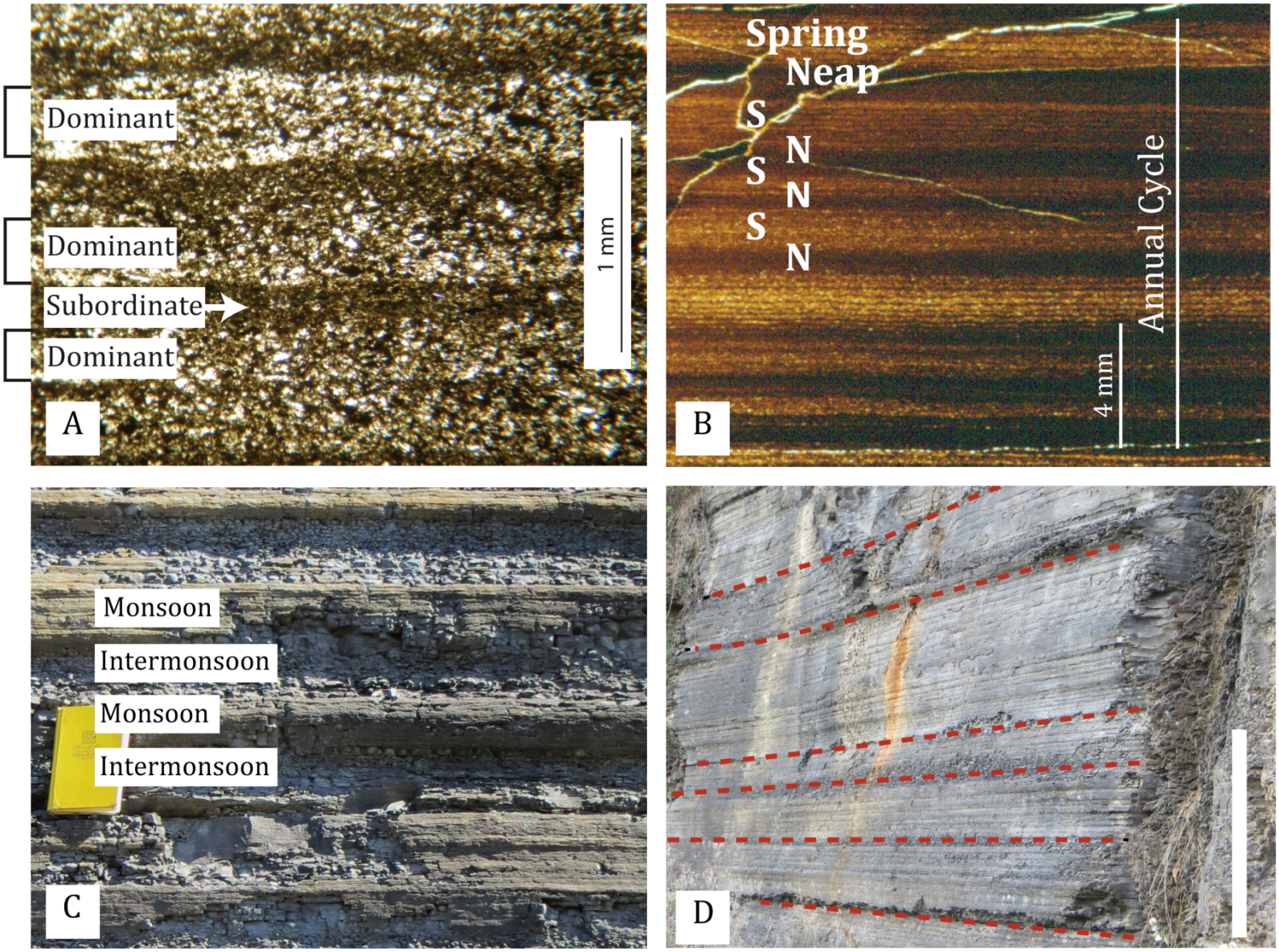
Dominant
Dominant
Subordinate
Dominant
1 mm
A
Spring
Neap
S
S
S
S
N
N
N
4 mm
Annual Cycle
B
Monsoon
Intermonsoon
Monsoon
Intermonsoon
C
D

Figure 2.13: a) TOC weight percentages of the basal condensed section (PR) and of monsoonal (M) and intermonsoonal (IM) deposits in the Pride Shale. The IM and M samples together are interpreted to represent ten years of prodeltaic deposition; b) $\delta^{13}C$ values of the basal condensed section and of monsoonal (M) and intermonsoonal (IM) samples in the Pride Shale. Also plotted for comparison are data for the Pride Shale from Pound Gap, KY (Kahmann-Robinson, 2008); c) $\delta^{13}C$ vs TOC cross plot values of monsoonal (M) and intermonsoonal (IM) deposits from Camp Creek, WV. Also plotted for comparison are data for the Pride Shale from Pound Gap, KY (Kahmann-Robinson, 2008).

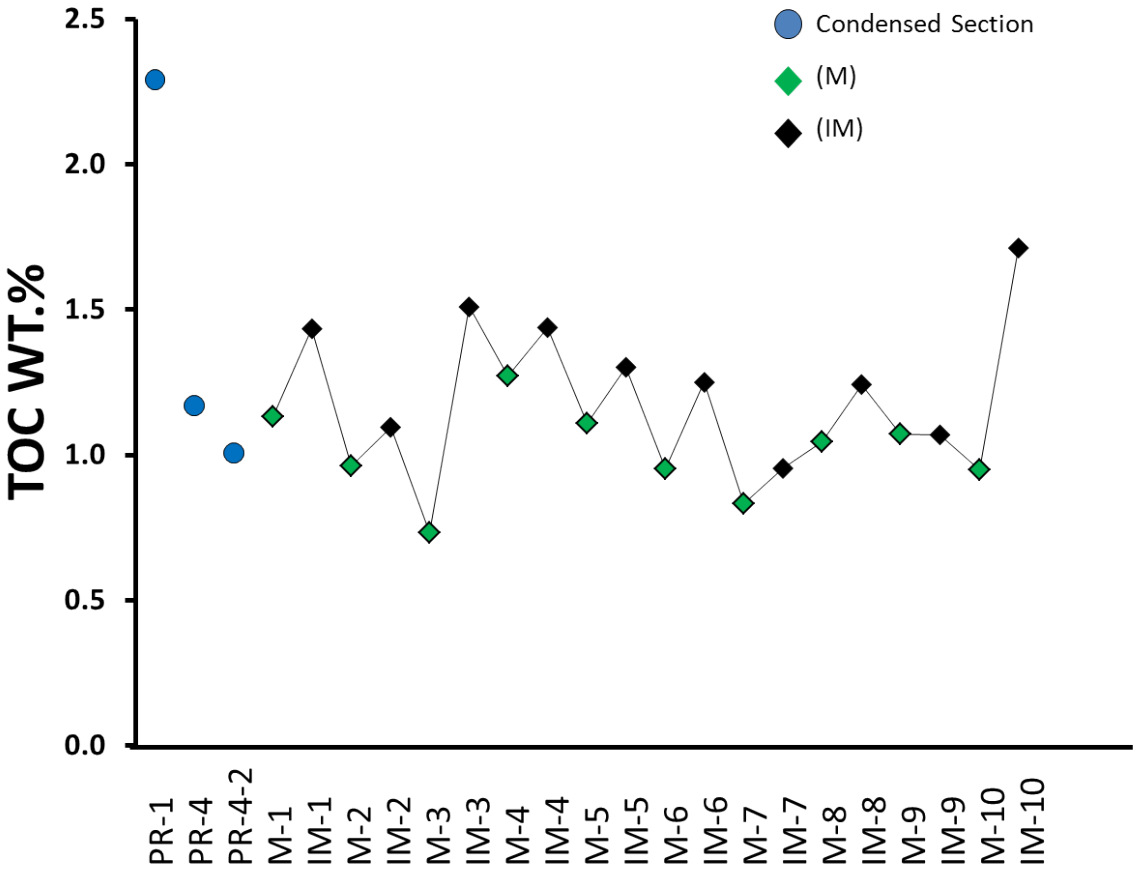
Condensed Section
(M)
(IM)
TOC WT.%
2.5
2.0
1.5
1.0
0.5
0.0
PR-1
PR-4
PR-4-2
M-1
IM-1
M-2
IM-2
M-3
IM-3
M-4
IM-4
M-5
IM-5
M-6
IM-6
M-7
IM-7
M-8
IM-8
M-9
IM-9
M-10
IM-10

A

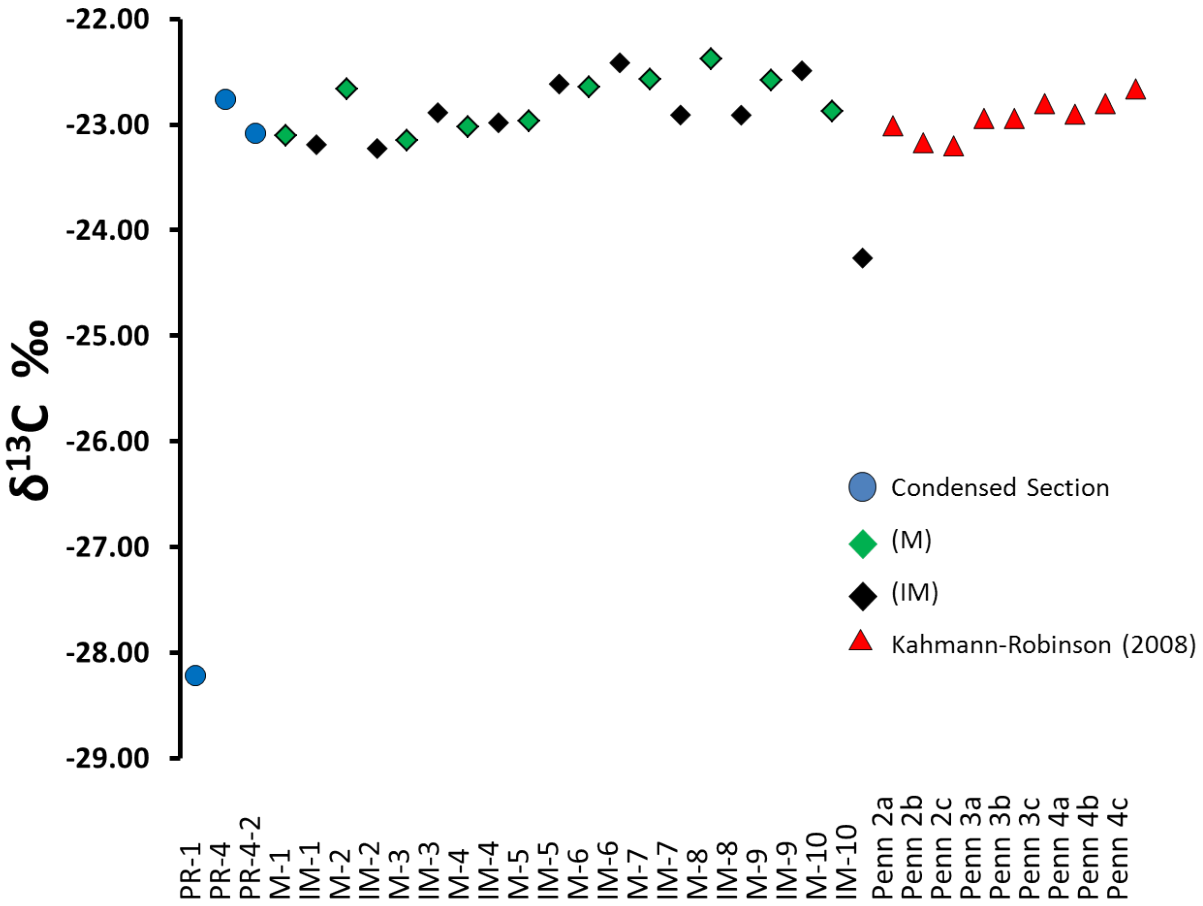
-22.00
-23.00
-24.00
-25.00
-26.00
-27.00
-28.00
-29.00
δ13C ‰
PR-1
PR-4
PR-4-2
M-1
IM-1
M-2
IM-2
M-3
IM-3
M-4
IM-4
M-5
IM-5
M-6
IM-6
M-7
IM-7
M-8
IM-8
M-9
IM-9
M-10
IM-10
Penn 2a
Penn 2b
Penn 2c
Penn 3a
Penn 3b
Penn 3c
Penn 4a
Penn 4b
Penn 4c
Condensed Section
(M)
(IM)
Kahmann-Robinson (2008)

B

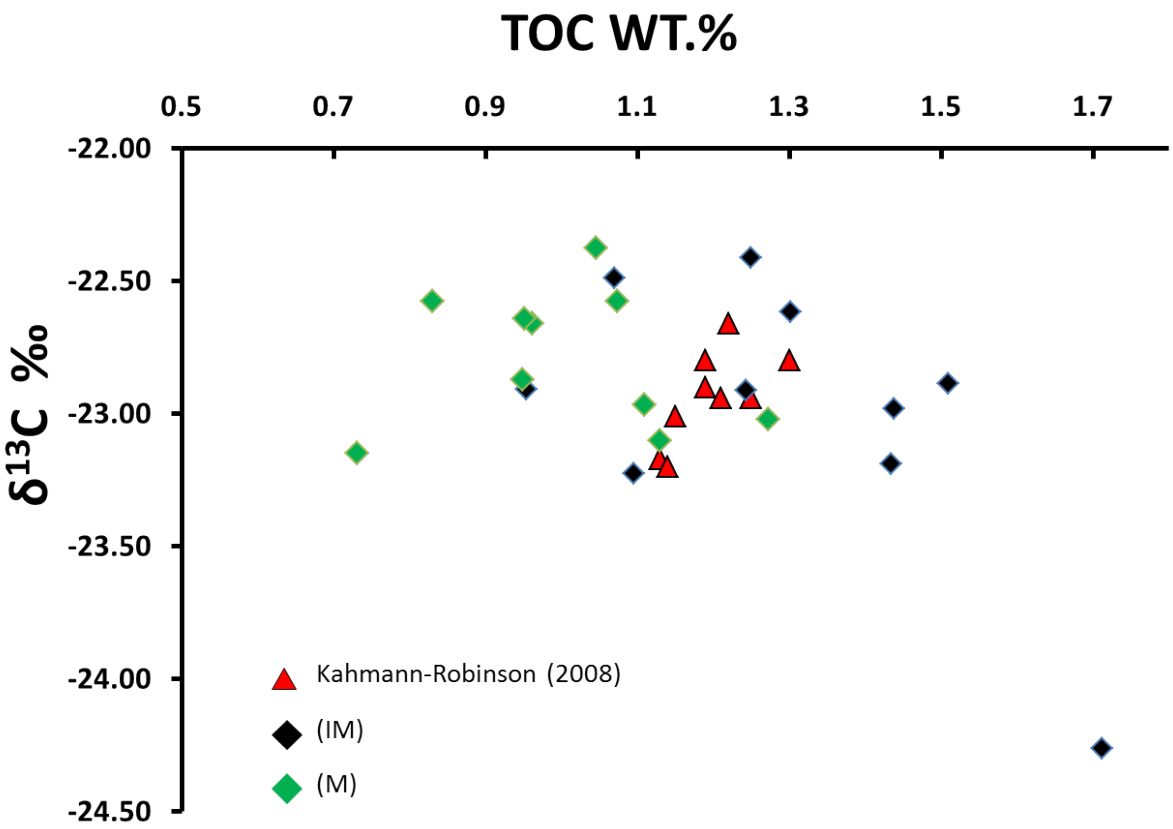
TOC WT.%
0.5
0.7
0.9
1.1
1.3
1.5
1.7
-22.00
-22.50
-23.00
-23.50
-24.00
-24.50
δ13C ‰
Kahmann-Robinson (2008)
(IM)
(M)

C

Table 2.1: Measured carbon data for the Pride Shale's basal condensed section (PR-1, PR-4 and PR-4-2) and annual cycles associated with the monsoon (M) and intermonsoon (IM) from Camp Creek, WV.

Sample	$\delta^{13}C$ ‰	Bed Thickness (cm)	TOC (%)
PR-1	-28.22	NA	2.3
PR-4	-22.76	NA	1.2
PR-4-2	-23.08	NA	1.0
M-1	-23.10	7.5	1.1
IM-1	-23.19	3	1.4
M-2	-22.66	7	1.0
IM-2	-23.23	3	1.1
M-3	-23.15	7	0.7
IM-3	-22.89	2.5	1.5
M-4	-23.02	7	1.3
IM-4	-22.98	3.5	1.4
M-5	-22.97	7	1.1
IM-5	-22.62	2	1.3
M-6	-22.64	8	1.0
IM-6	-22.41	3	1.3
M-7	-22.57	4.5	0.8
IM-7	-22.91	2	1.0
M-8	-22.38	9	1.0
IM-8	-22.91	5.5	1.2
M-9	-22.58	6	1.1
IM-9	-22.49	2.5	1.1
M-10	-22.87	11	0.9
IM-10	-24.26	9	1.7

Appendix: Supplementary Cross Sections

Refer to Figure 1.1 for locations of cross-sections.

Cross-section A-A’

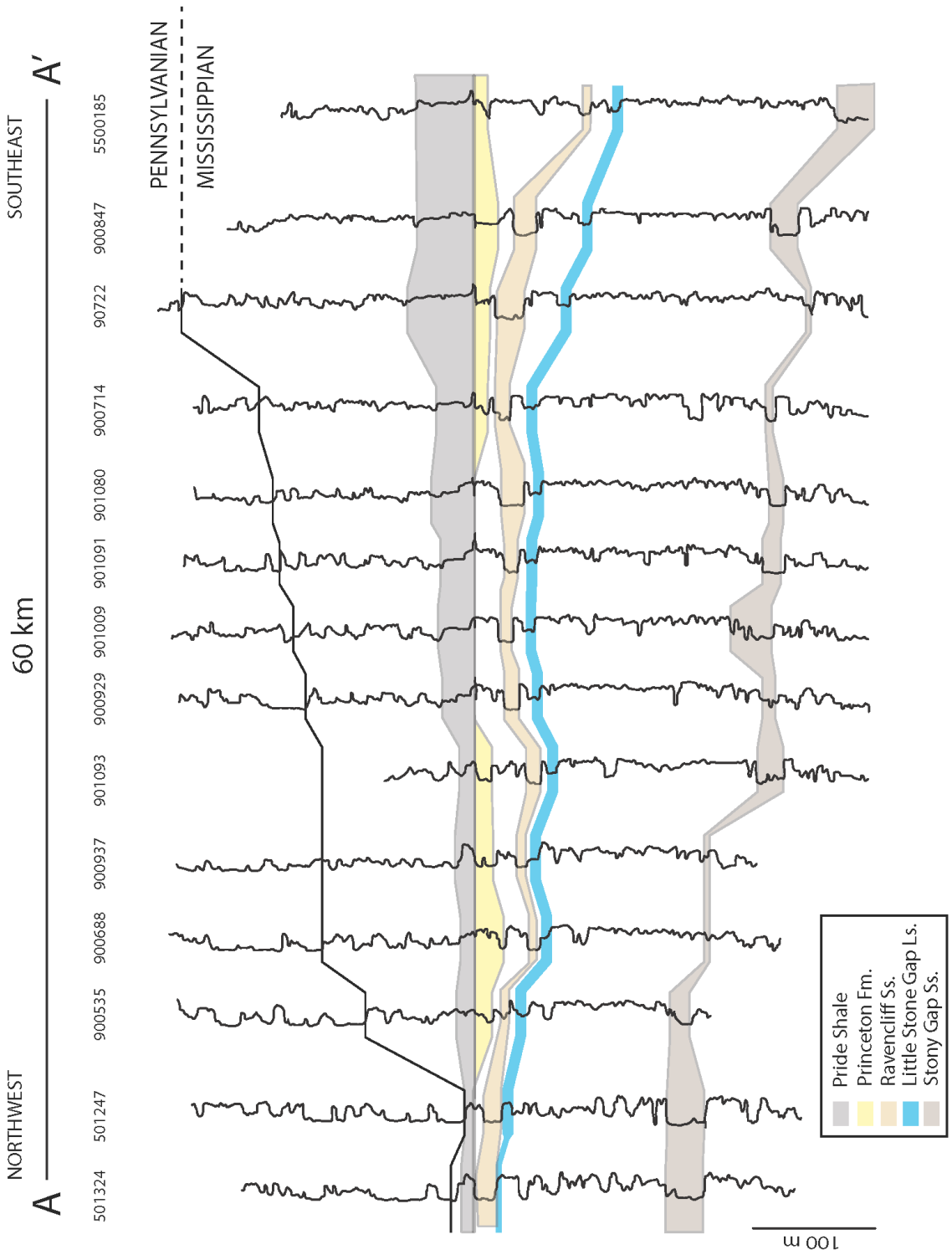

Cross-section C-C’

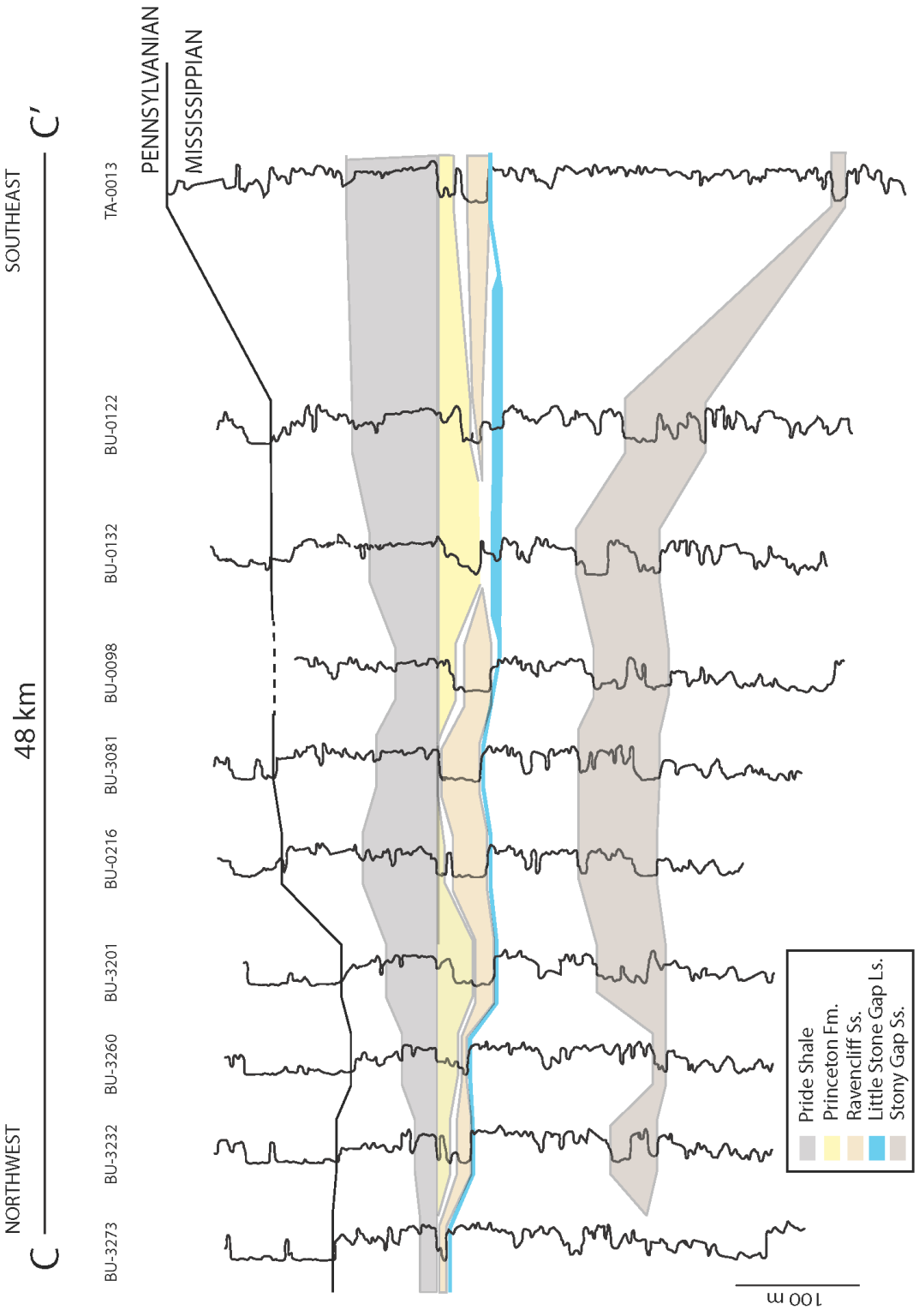

Cross-section D-D’

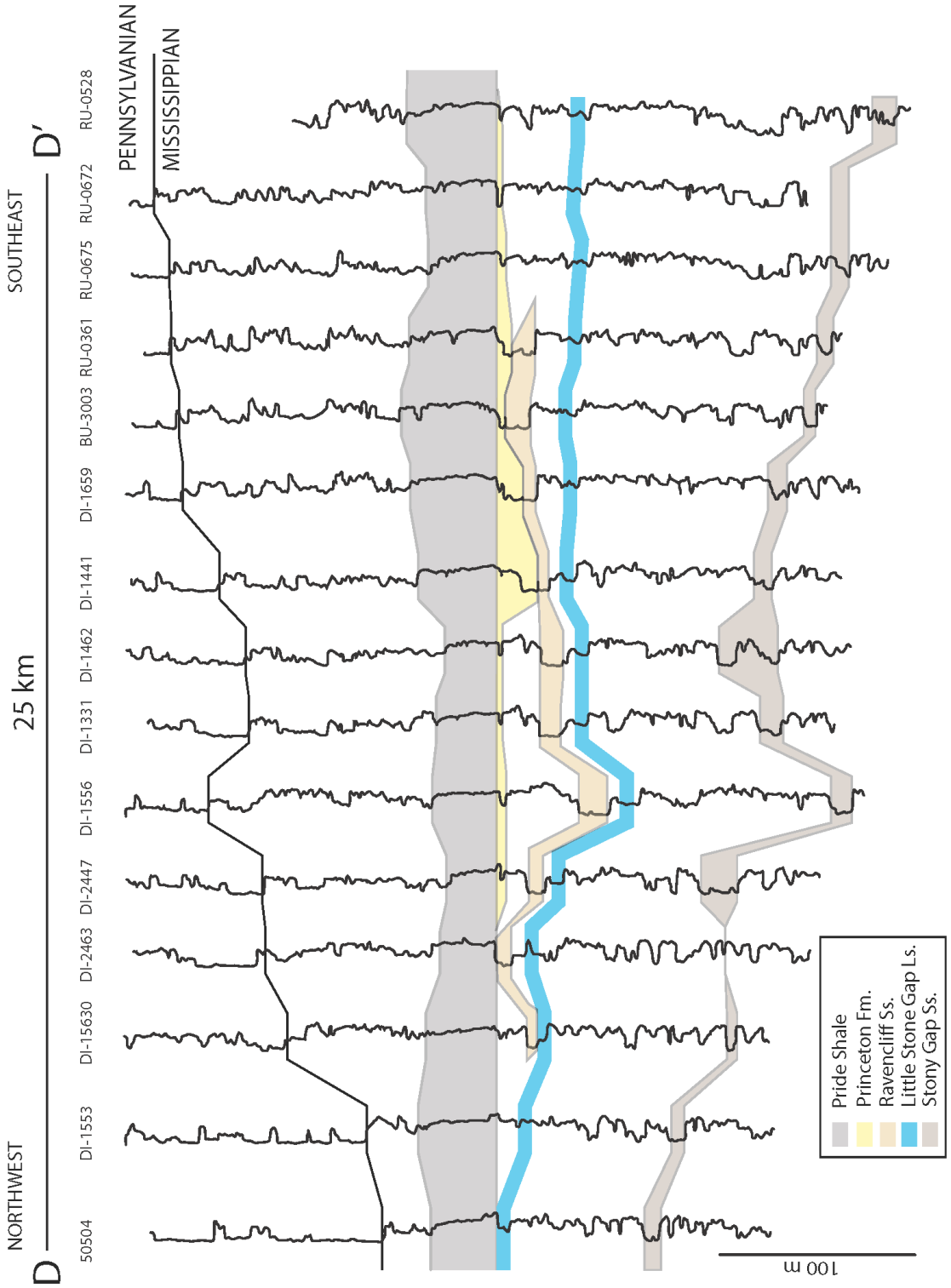

Cross-section E-E’

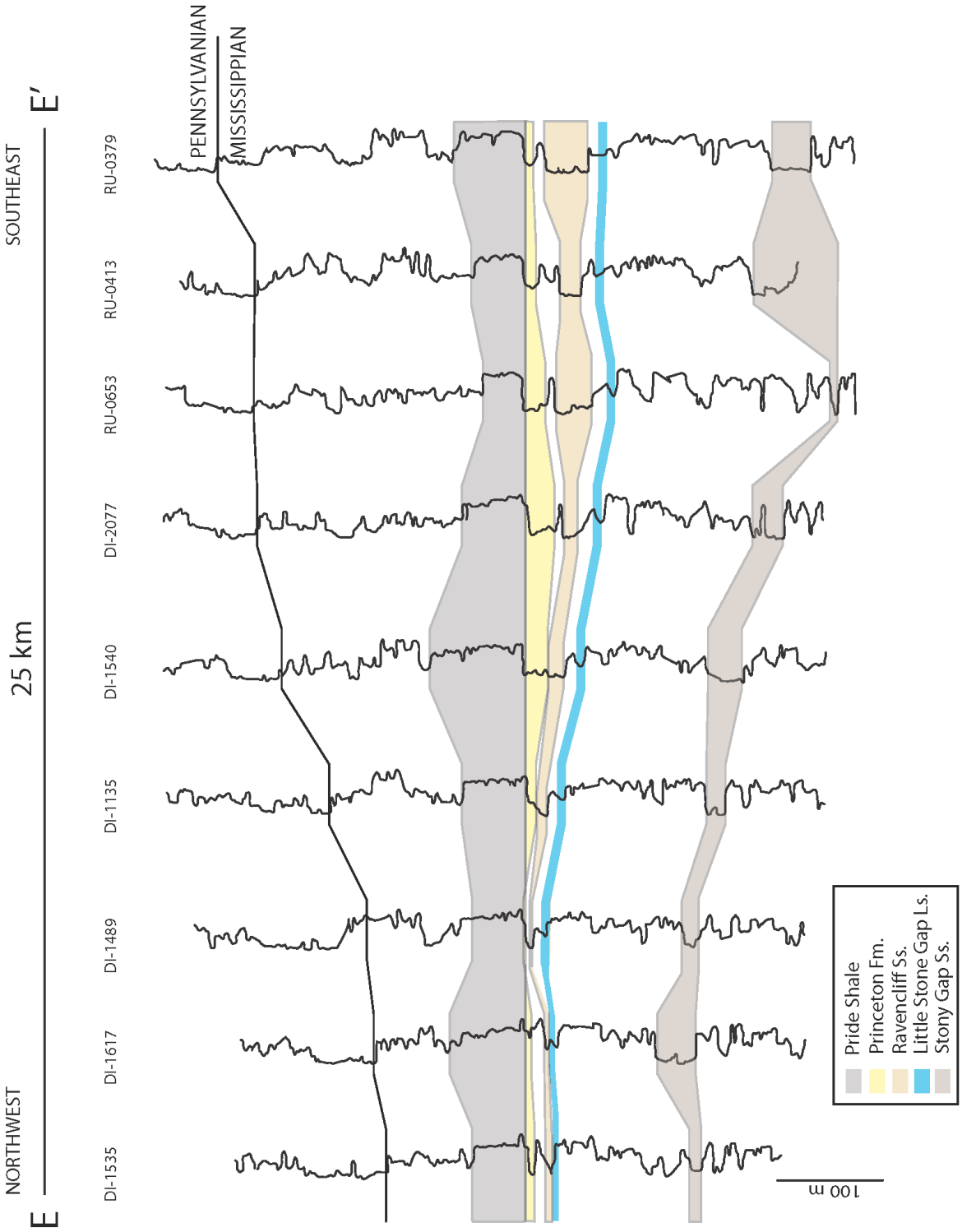

Cross-section G-G’